ALMA MATER STUDIORUM UNIVERSITA' DI BOLOGNA

FACOLTA' DI SCIENZE MATEMATICHE FISICHE E NATURALI

Corso di laurea magistrale in

SCIENCE FOR THE CONSERVATION-RESTORATION
OF CULTURAL HERITAGE

"The roman nails of Zwammerdam ships: a proposal for provenance, conservation and technological level"

Tesi di laurea in "Ancient metallurgy"

Relatore
Prof. Rocco Mazzeo

Presentata da
Mauri Marco

Correlatore
Dr. Ineke Joosten

II sessione

Anno Accademico 2011-2012

INDEX:

ACKNOWLEDGMENTS:

After six months of work it is necessary, also for me, to write down the “acknowledgments” section, but it is something really difficult because I do not think that this few lines are able to really describe my sincere gratitude to all the people that have support and help me in this period. The first two people that I really want to cite and give them particular thanks are my supervisor and my tutor, respectively Ineke Joosten and Janneke Nienhuis. They have given me the possibility to work independently and responsibly, leaving always the final decision to me, but in the background they were always present to help, correct and give me a hand, and the words are really not enough to express my most sincere thanks for all this. The second people that need to be cite are all the people that have made possible this project. So another special thanks to Anna-Katrien Mol and to Yardeni Vorst, because without them I probably never had the possibility to work at the RCE on a so wide and interesting project. Now I want to give a special thanks to all the people of the RCE and of the Rijksmuseum in particular to Luc Megens, Bertil van Os, Arie Pappot and Han Neevel, they have always given me a hand and have create an amazing working environment.
Other big thanks go to the entire helpful technician and scientist of the University of Delft and of the University of Utrecht, in particular Erick Peestock, Mehdi Lalpoor and Helen de Waard, without them the use of the instrumentation and the collection of the data were simply not possible.

The last big thank you goes to all the friends that I have met in Amsterdam, in particular to the intern of the RCE. Thank you for all for have support me during all this long months together.

THE ZWAMMERDAM SHIPS

1.1 *Archaeological background* *(Edited by Yardeni Vorst[1])*

Between 1971 and 1974 six vessels of Roman date were found along the former Roman border in the Dutch town of Zwammerdam. The vessels, three river barges and three dugout canoes, had ended up close together in front of the Roman fort of *Nigrum Pullum* in a silted-up former channel of the river Rhine (*fig.* 1). The layout of the fort and its phases of occupation had been studied extensively by archaeologists from the *University of Amsterdam* some years prior to the discovery of the vessels. [i]

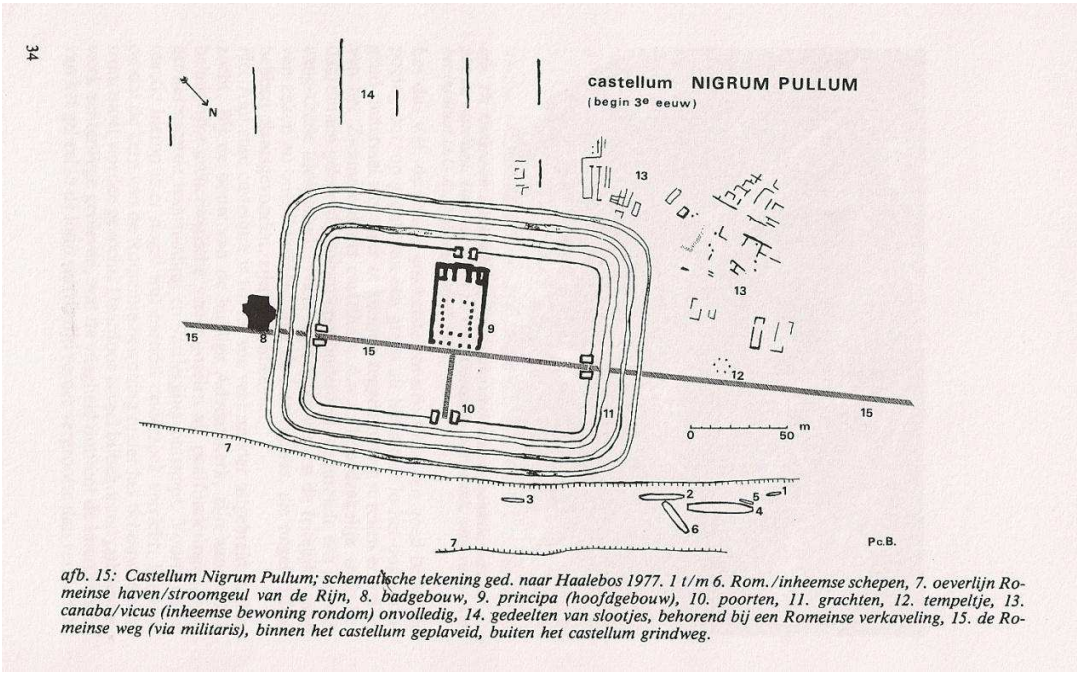

afb. 15: Castellum Nigrum Pullum; schematische tekening ged. naar Haalebos 1977. 1 t/m 6. Rom./inheemse schepen, 7. oeverlijn Romeinse haven/stroomgeul van de Rijn, 8. badgebouw, 9. principa (hoofdgebouw), 10. poorten, 11. grachten, 12. tempeltje, 13. canaba/vicus (inheemse bewoning rondom) onvolledig, 14. gedeelten van slootjes, behorend bij een Romeinse verkaveling, 15. de Romeinse weg (via militaris), binnen het castellum geplaveid, buiten het castellum grindweg.

Figure 1 Vessels 1 to 6 in front of he Roman fort Nigrum Pullum (Beunders 1986, 34, fig. 15).

[1] Yardeni Vorst is a PhD student of the University of Leiden. The Doctorate research that she is developing is about the ships of Zwammerdam and Woerden and their dating by the used of the technique of the dendrochronology. It is within this research that was done this thesis project.

The subsequent research focus was directed towards the vessels themselves. It presented the archaeologists not only with a large number of vessels, but also with three examples of a new type of vessel, the river barge, relatively unknown in Roman ship archaeology. Collectively the ships were named the "Zwammerdam type", after the name of the town in which they were found. They have the following characteristics (see *fig*. 2):

- Long, narrow ships with a length to beam ratio between 6:1 and 8:1;
- A flat bottom without a keel;
- Low vertical sides with L-shaped planks (chines) forming the transition between the bottom and the sides;
- Single or paired floor timbers with a vertical knee in the form of a branch at one end of each floor timber and placed alternately to port and starboard. For extra support some vessels have an additional futtock placed in the knee-less end;
- Floor timbers attached to the hull- and bottom planks with iron nails; and
- The mast step, positioned in a heavy frame or in the form of a separate mast step with a keelson sitting across the frames, placed well forward at c. a quarter of the ship's length.

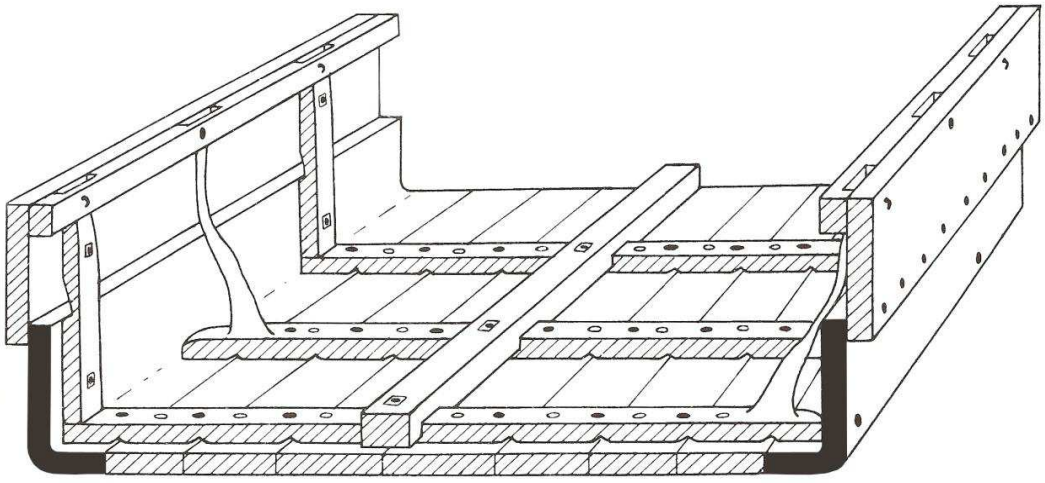

Figure 1 A cross section of Zwammerdam 2 with the L-shaped chines in black (De Weerd 1988, 297, fig. 172).

The Zwammerdam ships were numbered in order of discovery and measured: [ii]

Zwammerdam 2: 22.75 m x 2.95 m x 0.95 m

Zwammerdam 4: 34 m x 4.40 m x 1.20 m

Zwammerdam 6: 20.30 m x 3.55 m x 0.90 m

The ships date to the end of the first century (Zwammerdam 4), the middle of the second century (Zwammerdam 6) and the beginning of the third century AD (Zwammerdam 2). The excavations were each carried out in a very short amount of time. The recording of the vessels was under the direction of the *University of Amsterdam* (UvA)[2] and the lifting and subsequent conservation was undertaken by the *Rijksdienst voor de IJsselmeerpolders* (RIJP). Canoes numbers 3 and 5 from Zwammerdam were fully documented before and after conservation[iii]. They are currently on display at the *National Depot for Ship Archaeology of the Cultural Heritage Agency of the Netherlands* (RCE) in Lelystad. The three ships of Zwammerdam and canoe number 1 took much longer than the others ships to conserve due to differences in hardness of the wood[3]. These vessels still await reconstruction.

1.1.1 New research and the ship Woerden 7

A report from 1988 on the excavations of the Zwammerdam vessels is based only on the information that was recorded during the rescue excavations[iv]. The report only describes Zwammerdam 2 in detail. New research on the timbers after conservation will provide extra information on all of the ships. This research is currently being carried out as part of a research project into the management of raw materials, construction technology, use and disposal of barges in the Lower Rhine region during the Roman period.[4] Supplementing the data of the Zwammerdam ships is important in order to make comparisons with other Zwammerdam type ships.[5] The comparison between the Zwammerdam 6 and the Woerden 7 is especially relevant. Woerden 7 was discovered in

---

[2] The University department of archaeology was then called the Institute for Pre- and Protohistory, IPP.

[3] Some of the timbers were initially too hard for conservation with polyethylenglycol and were only treated after further degradation of the wood, years later. Some timbers still await conservation.

[4] NWO Humanities programme *Arts and crafts in Roman ship building: raw materials management, construction technology, use and disposal of barges in the Lower Rhine region in the Roman period*. (RCE, VU).

[5] For example the excavations of the ships De Meern-1 (Jansma & Morel 2007), Woerden 7 (Blom et al. 2008), both excavated in 2003, and ship De Meern 4(De Groot & Morel 2007), excavated in 2005.

Woerden in 2003 and the ship resembles the Zwammerdam 6 very closely in construction. Some of their shared characteristics are (see fig. 3):

Figure 2 Zwammerdam 6 (left) and Woerden 7 (right) (photo's IPP and Y.Vorst).

Alongside these visible similarities, both ships date to the same year (163 AD) and both their timber provenance[6] and the way oak timbers originating from different areas are used within the vessels are very similar. A hypothesis within the ship research project[7] is that these vessels were built (possibly together) at the same shipyard.

[6] The ship timber was partly imported and part-locally felled.
[7] NWO Humanities programme *Arts and crafts in Roman ship building: raw materials management, construction technology, use and disposal of barges in the Lower Rhine region in the Roman period*. (RCE, VU).

1.2 Current research outline

Inside these ships were found hundreds of iron nails and some of them were still in situ during the excavation. This gave the possibility to start this research. A previous study on these objects was conducted by Anna-Katrien Mol[v]. That study has tried to find a correlation between the nails, of the different ships, on the base of the metal composition, with the use of the X-Ray Fluorescence (XRF), and on the microscopic examination. At the end of that research however was not possible to arrive to a precise conclusion. The nails have shown differences and similarities, but nothing definitive. Therefore this research is focused on the characterization of the nails from a different point of view: i.e. technological level and provenance and production.

1.2.1 Technological level

The technological level is based on the quality of the iron. The characteristics that will be discovered and compared with the same data in literature, to see if this iron is comparable to the level of the iron production inside the Roman Empire or not.

The examination under the optical microscope will provide us information about the microstructure of the alloy, which is an indication of the production history of the object (combination of iron production, reheating and smithing process). The chemical composition of the metal and slag inclusions will be studied with a Scanning Electron Microscope with Energy Dispersive Spectroscopy (SEM-EDS). The second parameter used to characterize the technological level is the hardness, measured with Vickers's hardness tests. The results from all of these analyses will be matched together for a better evaluation of the intrinsic features of the nails and of correspondences between the nails of the various ships. The data obtained will be also compared to that from the literature[vi]

1.2.2 Provenance and production

One of the main aims of this research is to outline the possibility that the iron used to create the nails from Zwammerdam and Woerden ships comes from the same production site or from several ones and secondly if there is the possibility that they come from the important iron production site of Heeten, dating to the Roman period[vii]. This aspect gives

also the possibility to understand whether there are differences inside the same ship and between different ships.

The chance to make this correlation between the production site and the object is given by the presence inside the metal of slag inclusions. During the bloomery process the charcoal and the ores were heated below the iron melting temperature, thus mean that a part of the slag coming from the non reduced part of the ore can be entrapped in the metal and form the above cited slag inclusion. On the base of this assume the chemical features of the bloom are related to the ore used, ore that is unique for a production site. This correlation gives the opportunity to try to link the slag of the production site with the slag of the object. This common thread will be analysed on two different levels. The first one identifies and quantifies the major and minor elements inside the slag with the use of the SEM-EDS. The second level gives more detailed information about the provenance, because with the use of the Laser Ablation- Inductively coupled plasma-mass spectrometry (LA-ICP-MS) the trace elements will be analysed, which allow a differentiation between the different possible sites. The data will be compared with the data from literature[viii] and with samples of nails from Heeten.

A second aspect of the production of the nails will be achieved by the study of the so called “fingerprints” under the head of the nails. The “fingerprints” are the impressions left from the forging applied to create the head. To do that, the nails were hammered inside a metal block, the leaving unique signs on the nails. These marks are always the same and allow correlating the nails to the block, and at least to the place of production. Thus the nails with same signs are probably made in the same block[ix]. A simple test to evaluate this possibility is the macroscopic view under the head, after a soft cleaning of the surface with brushes, scalpel with a small cutting edge or, at least, with an abrasive blasting at a pressure of about 2 bar. This test helps to correlate the nails of the different ships, or at least to say if some nails come from the same blacksmith.

---

[i] See Haalebos 1977 for a report on the excavations of this fort.

[ii] De Weerd 1988, 93-95, 148 & 156; the canoes were numbered 1, 3 and 5.

[iii] De Weerd 1988 and Koehler 1997

[iv] De Weerd 1988.

[v] This study: Anna-Katrien Mol, 2012, *Romeinse scheepsspijkers Een onderzoeknaar de materiaaleigenschappen van de spijkers uit de Zwammerdamschepen.* Archeological thesis project for the UvA performed at the RCE under the supervision of dr. Ineke Joosten. From now and onwards when referred to previous studies or previous analyses this one is referred to.

[vi] N.S. Angus, G.T. Brown, H.F. Cleere, 1962, 957-986 and M. Boniardi, E. Gariboldi, M. Vedani, 1992, and P. Dillman, P.fluzin, L. Long, G. Pages, 2010, 1234-1252.

[vii] Groenwoudt & van Nie 1993, Joosten 2004

[viii] I. Joosten, 2004.

[ix] A. Beat, 1992, 6270 and A. Beat, 1999, 76-81.

TECHNICAL INSTRUMENTATION AND ANALYSES:

In this chapter all the technical instruments will be shown and the related analyses which have been performed during this thesis work. The theoretical and procedural aspect of all these different tests will also be highlighted. For clarity of writing and explanation it was been decided to present the various techniques from the most general one to the most detailed one. However, for technical reasons the optical microscopy is the last analysis performed since the etching process could affect the results of all the other tests.

1. Samples:

1.1. The nail Types:

- Type I
- Type II
- Type III
- Type IV
- Type V
- Type VI
- Location of the nails

1.2. Samples preparation:

- The nomenclature of the nails
- The cut
- The new embedding
- The polishing

2. Optical Microscopy (OM):

2.1. Theory

2.2. The microscope

2.3. The procedures

3. Scanning electron microscope (SEM) with dispersive X-ray spectroscopy (EDS):

3.1. Theory

3.2. The microscope

3.3. The procedures

4. Vickers's hardness test:

4.1. Theory

4.2. The instrument

4.3. The procedures

5. Laser Ablation - Inductively Coupled Plasma - Mass Spectrometry (LA-ICP-MS):

5.1. Theory

5.2. The instrument

5.3. The procedures

1.1 THE NAILS' TYPES:

This study will focus on the nails that have been found in the Zwammerdam and Woerden vessels. The nails were divided into different types, like in literature studies of the site of the fortress of Inchtuthil, on the basis of the function. This function was obtained either from the position of the nail itself inside the wooden structure, where possible, or on the external characteristics (like length, head dimension, thickness of the nail keg, position of the keg in stead of the head). From these elements it was possible to create six typologies and one sub-typology.

The classification made in the previous study (Mol 2012) will be used also for this research.

Figure 4: Schematic overview of the entire nail types (taken from A Mol 2012).

Type I

The first type of nail is long in comparison with the others. The length varies from nearly 22,0 to 44,0 centimetres. Their primary function is to vertically connect two planks. In fact, the nails pass through the entire length of the two planks. These nails are probably created especially to link two planks. To accommodate the nails inside the wooden structure, holes are specifically drilled. On the top part of the holes a cavity is dug to accommodate the head of the nails. On some of the nail heads a wooden cap to close completely the socket is found.

Type II

These nails are the so-called standard type. They are used for practically all the common employment. These nails are used to join the different planks and they are also employed to strengthen the link between the horizontal boards that form the bottom of the ships and the boards that form the vertical sides of the ship. The second type can be found in different shapes (the form of the head can be round and flat, round and convex or look like a mushroom, etc), sizes and lengths, which has an average of 14,8 centimetres. These nails can present a curve, which can be of 90° in some particular cases[1]. For this reason they were grouped in the subtype IIb, in order to be able to distinguish their study. In some cases it is possible to notice a drilled hole in the planks, to accommodate the straight nails. However, if no hole is visible, this does not mean that this is not present. In fact the drilled hole could have been smaller than the nail itself, leaving in the wood only its impression instead of the signs of the drilling process. The hundreds of nails founded in the ships, the ordinary use in other different fields, like in the construction of military buildings (N.S. Angus, G. T. Brown, and H. F. Cleere 1962) and the possibility to a wide comparison with the literature have made this nail type the one chosen for this research.

Type III

The nails that belong to this type have an average length of 16,3 centimetres. This feature is due to the dovetail that they have inside the timber. In fact these nails are not placed in

[1] An example of that is the nail ZW7-7 analysed in the previous study (A. Mol 2012).

a hole, but in a triangular recess. They are used mostly on the sides of the boards; hammered obliquely from the upper side to the lower side of the plank, until they reach the new board and create a link between these two. These nails are all placed vertically from top to bottom and are partially embedded inside the caulking material[2].

Type IV

The nails belonging to this group were found only in the Zwammerdam 4 ship. The head can have a diameter that goes from 1,5 to 5,0 cm and beneath it can still be found some grams of caulking material. These nails are employed as aid to waterproofing. For this reason the heads have undergone to a huge level of degradation, in the majority of the cases only the stem is found inside the wood planks. Only in some boards of the Zwammerdam 6 these nails are found in their original position.

Type V

The nails of this type are relatively small, the average length is 62,5 millimetres, and very different both in shape as well as in thickness and length and are only found outside of the hull in a long line one after the other. A possible function of these spikes could be the blockage of a metal plate on the topside of the ship.

Type VI

This is the last type of nail present in the Zwammerdam ships. They are relatively small, with a maximum length of 4 centimetres and a maximum thickness of 5 millimetres with a needle-like shape. The use of this particular nail is to place it inside cracks or the little space between the planks and the caulking material.

Location of the nails:

The sampled nails of Zwammerdam 6 are from a section of the ship's side on portside. During the excavation of ship number 4, a section was cut out of the ship by the

[2] The materials used for this operation are typically vegetables fibres, like cotton and hemp, hairs mixed with tar or resins. All these elements were pressed inside the voids between the planks to make the boat perfectly waterproof.

cofferdam placed around ship 4. Consequently ship 6 was discovered. The section of several timber elements (connected by nails) was put in conservation without taking it apart. Therefore, after conservation it was still possible to study these nails in terms of their function within the construction. This direct link between the place and the function in the planks from Zwammerdam 6 was subsequently used as a comparison for the nails of the other Zwammerdam ships. It has also been possible to recognize similar types of nails from the ship Woerden 7, from which nails were collected without recording information on their context. The typology has enabled the comparison of the nails from the ships Zwammerdam 2, 4, 6 and Woerden 7. Nail type II was chosen for further research, because it is the most frequent type of nail in all the vessels.

After the conservation process, when the ships were deconstructed, the nails were removed and stored, separately from the timbers, in the depot of RCE in Lelystad.

Figure 5 Zwammerdam 6 during excavation. The red arrows mark the cut-out section on portside (photo IPP)

1.2 SAMPLE PREPARATION:

The selected nails were already embedded in an epoxy resin, but during the preliminary studies it turned out that the embedding medium was not suitable for performing most of the analyses since it was inhomogeneous so as to be in some zone too soft and in some other too few, i.e. around the tip, fact that compromise the stability of the sample itself. The big size of the sample as also affected the analysis, because was difficult to handle, stabilize and give an optimal polishing. Therefore it has been decided to redo the embedding with a different resin.

The nomenclature of the samples:

The selection of the specimens taken from the nails was done on the base of the precedent study. Each nail was cut into parts of 2 cm length each. To limit the amount of samples it was found that three to six samples per nail would be suitable to represent the most relevant features of the nail. To every "new" sample a new name was given: first of all the name of the ship, then the number of the nail taken from the previous study and finally a letter from *a* to *h* ranging from the head of the nail until the tip.

The cut:

The preparation of the samples started with cutting all the nails in smaller parts. The cutting was performed at the laboratories of the RCE in Amersfoort[3] with the use of a hydraulic circular saw with a diamond blade. To avoid the possible overheating, produced by the cutting action, water has been allowed to flow on the blade. Nevertheless during this operation some sparks were still produced, first proof of the excellent mechanical resistance of Roman iron. The samples before the cutting consisted of the entire nail embedded in a soft epoxy resin cut vertically to allow the examination of the

[3] The operations were done with the help of Bertil van Os, senior scientist inorganic materials and degradation at the Rijksdienst voor het Cultureel Erfgoed.

core of the metal. This compact block has been cut horizontally to obtain the needed smaller samples. The specimens obtained in this way a length of about 2 centimetres[4] .

The new embedding:

A selection of 51 samples has undergone the new embedding process. Most of the samples needed a pre-polishing to eliminate the old resin excess that surrounded them. For this first polishing a Struers LABOPOL-21 was used, with the use of an abrasive cloth with the CAMI[5] grit designation of 320, which has an average particle diameter of 36 µm. The resin chosen to embed in is Struers SpeciFix-20®.

The polishing:

The polishing process was performed with the help of the Laboratory of Conservation and restoration of metals of the Rijksmuseum. For the polishing an EcoMet® 250 Grinder-Polisher, membrane controlled base with AutoMet® 250 Power head was used. Firstly, the excess of resin and rust was abraded from the upper surface of the samples using a BuhelerMaet® II. After this initial step the sample and the stage holder have been put in an ultrasonic bath to remove all the residuals of the iron dust created during the polishing from the surface.

The second polishing step was performed with the use of a Buehler Verdutex® abrasive cloth in combination with Buehler MetaDi monocrystalline Diamond suspension® lubricant with a particle size of 6 µm. After this action the samples and the stage holder were again put into the ultrasonic bath to clean the surfaces.

The third and final step was performed with a Buehler Ultrapad® abrasive cloth. During the performance the spray lubricant DP-Spray Polycrystalline diamond® with a particle size of 3 µm was added. The samples were put inside the ultrasonic bath and to be sure that the entire water residue was taken out, they were cleaned with acetone and immediately dried with compressed air. The final result of the surface was a mirror surface without any visible scratches.

[4] This length was chosen after viewing a standard metallographic sample, which was provide by the laboratories of conservation and restoration of the Rijksmuseum.

[5] United States CAMI (Coated Abrasive Manufacturers Institute, now part of the Unified Abrasives Manufacturers' Association

2 OPTICAL MICROSCOPY (OM):

2.1 Theory:

Optical microscopy[6] is an investigation of the structure of a material under the microscope. To perform this type of analysis on iron and alloys it might be necessary to reveal this structure by etching. Metallographic etching is the process of revealing micro structural details that would otherwise not be evident on the polished sample. A properly prepared specimen will reveal properties such as grain size, segregation, shape, size, and distribution of the phases and inclusions that are present, while other aspects such as mechanical deformation and thermal treatments may also be determined. Two different solutions are used for etching nital[7] and picral[8]. The choice of the nital was made on the basis of the possibility to have more reference in literature.

2.2 The microscope:

The microscope used for this research is an AXIOPLAN 2 Imaging® developed by Carl Zeiss s.p.a®. This microscope is connected to a personal computer to collect the images with the use of the AXIO Vision® software. This microscope is able to perform analyses on different types of samples from metal to biological tissues. There is the possibility to work in reflection, in transmission, with crossed polarizers and with UV-radiation.

2.3 Procedures:

For the metallographic observation nital was used as etchant to obtain data comparable to that in literature. The nital solution is particularly suitable because it is sensitive to crystal orientation, so as to reveal ferrite grain boundaries and for the study of martensitic structures. After the etching process the sample was rinsed with ethanol and dried by blowing hot air on the surface. To navigate over the sample and collect the data it was

[6] In this fields it is also know as metallography. From now and onwards it will be called in this way.
[7] Solution of 2% in volume of Nitric acid in Ethanol; it is suitable for revealing ferrite grain boundaries, pearlite, martensite, trostite.
[8] Solution of 4 grams of picric acid in 96 cm^3 of ethanol; it is suitable for revealing the pearlite and bainite.

decided to divide the surface in 9 sections, 3 for the right side, 3 for the middle and 3 for the left side.

3 SCANNING ELECTRON MICROSCOPE (SEM) WITH DISPERSIVE X-RAY SPECTROSCOPY (EDS):

3.1 Theory:

With the use of the Scanning electron microscope (SEM) in combination with the Energy Dispersive X-ray spectroscopy (EDS) it is possible to achieve information about the composition of specimen and about the morphology of the surface[9]. The information is generated by the interaction of the X-ray beam with the surface of the sample. This interaction causes the release of different types of radiations that can be collected and processed by different types of detector. Two important aspects that have to be kept in mind are the interaction volume between the X-ray beam and the sample and the spatial resolution.

For what concern interaction volume, the X-rays are able to excite only a small volume of the matter under examination, thus the data achieved are related only to that volume and they can not totally describe the real composition of the entire sample. For what concern the spatial resolution, so the smallest length that can be achieved without distortion, is about 1 μm.

3.2 The microscope:

The microscope used for this work is a JSM-5910LV® made by Jeol Ltd. The enlargement is 10x to 300.000x. The source of the electrons is a tungsten filament with a maximum acceleration voltage of 30 keV. This microscope is a variable pressure SEM able to work in low vacuum conditions, 1 to 230 Pa, to analyze non-conductive specimens without coating them with a conductive layer. The software directly linked to the EDS detector, a Noran UltraDry X-ray detector, for the identification of the elements

[9] The composition will be given by in terms of Wt%.

inside the specimens is the NORAN System Seven microanalysis system® developed by the Thermo Scientific®.

3.3 Procedure:

To avoid the charging of the specimen, a conductive bridge is created with carbon strips, which allows the electrons to flow away from the surface to the metal holder. A copper arrow is attached to the surface of the sample for orientation purposes and to dissipate the excess charge. To perform the analysis, it is necessary to reach high vacuum (approximately $10^{-}5$ Pa) inside the chamber.. The ideal working distance between the pole piece and the surface of the sample is about 10 mm. An acceleration voltage of 15 keV was used. To navigate over the sample and collect the data, the division already used for the metallographic investigation was used to be able to match the data.

4 VICKERS'S HARDNESS TEST:

4.1 Theory:

The Vickers hardness test is an easy way to evaluate the hardness of practically every material. The important aspect of this technique is the possibility to perform a microtest, in combination with an optical microscope. In this case the load's range is limited and goes from a minimum of 10g to a maximum of 1000g. The shape of the diamond indenter was developed on mathematical law and represent to the ideal condition for performing these measurements.

4.2 The instrument:

The tests were performed at the Delft University of Technology in the laboratory of the faculty of Material Science and Engineering[10]. After the new embedding the samples are totally suitable to be tested with the DuroScan 70®, an automatic tester distributed by the Strauers® Ltd. The use of this instrument is linked with the dedicated software the ecos

[10] The analyses were done with the help of Erick Peestock and dr. Medhi Lalpoor of the Material and innovation institute of the Delft University of Technology.

workflow. The indenter is diamond pyramid suitable for microanalysis with a test head resolution of 5 nm[11].

4.3 The procedures:

The sample is clamped in a holder that stabilizes the sample and creates a flat surface. In this a load of 100 grams with an application time of about 10-12 seconds was used (N.S. Angus, G. T. Brown and H. F. Cleere, 1962; M. Boniardi, E. Gariboldi, M. Vedani, 1992; C. Mapelli, W. Nicodemi, R. F. Riva, M. Vedani, E. Gariboldi, 2009).

The number of measurements goes from 5, in a homogeneous specimen, these characteristics have been evaluated in base of the data achieved by the SEM-EDS analyses already performed, up to 12 in case of a very layered and stratified one.

5 LASER ABLATION INDUCTIVELY COUPLED PLASMA MASS SPECTROMETRY (LA-ICP-MS):

5.1 Theory:

Laser ablation-inductively coupled plasma-mass spectrometry (LA-ICP-MS) is a particular type of mass spectrometry that is able to detect elements in concentrations as low as one part per trillion. The material volatized by the action of the laser is taken inside a gas flow, typically formed by helium, argon, a mixture of the two or a noble gas plus a halide. This mixture is canalized into the plasma torch and from there inside the mass spectrometer where the elements are detected. The laser used for the ablation are typically high power laser like an nd:YAG laser or an exciplex laser. As said in the introduction chapter the material that will be analyzed is the one of the slag inclusion to try to make a correlation between the nails of the different ships and the production site of Heeten.

[11] Value stated by the manufacturer.

5.2 The instruments

The instrumentation necessary for this analysis is form by four parts that work together. The head of the system is a computer interface, which control the cycles of the analysis and all the parameters of the laser and of the mass spectrometer.

The instrument[12] is composed of an exciplex laser; the sample holder with a camera and the mass spectrometer. The laser is an exciplex of the COMPex® series by the Coherent® Lambda physik Inc. The pulse rate to ablate the material of the slag is of 10 Hz with fluence of 5 J/cm² for the glassbeats and of 9 J/cm² for the nails. The microscope used for investigate the surface of the sample is a Zeiss® Axioplan2®, the linked camera is a Zeiss® axiocam ERC5s®. The mass spectrometer used is the Thermo Scientific® Element 2®. The mass spectrometer itself has a high sensitivity of1 x 10^9 counts per second, and a high detection power of < 1 ppb for non-interfered nuclides, but the measurements are effected by an instrumental error around 10% wt%, thus this analysis results to be a semi-quantitative ones.

5.3 The Procedures:

The measurement time is divided into three sections to interpret the data and the concentration of detected elements. In the first 30 seconds, the signal without the ablation of the surface is registered to create a reference. In the next 80 seconds, the signal with the ablated particles is collected and in the last 10 seconds again the signal without the ablation. As a reference, a glass N610 is used.

Since the maximum width of the slag inclusions is around 60 micrometer, a spotsize of 60 micrometer was used.

[12] The apparatus used for these analyses is the one owned by the University of Utrecht, under the supervision of the Ing. Helen de Waard, Technical support for the Petrology group and for the LA-ICP-MS laboratory of the University.

ANALYTICAL RESULTS:

In this section will be described the analytical results obtained from the instruments. The result will be dived in sections on the basis of the techniques and on the samples. The data obtained will be presented already with an order and some averaging, all the further discussion and comment about the interpretation and the management of this information will be discussed in the next chapter. As it was done in the previous chapter the presentation of the results will start with the most general feature (optical microscopy) go on till the most detailed one (LA-ICP-MS).

1 OPTICAL MICROSCOPY (OM):

In this section the will be introduced the main characteristics of the metallographic investigation. For a better selection of the images all the references to the grain size are related to the ASTM number, which is a standardized value that represents a range of grains dimension. This value has been created and normalized by American Society for Testing and Materials, which is an international association that provides standards for the industrial and technical field. In the figure 6 is shown the monograph for the grain size, estimated on the basis of the Hilliard's method. In the figure below is also possible to notice that lower is the dimension of the grain, higher is the value of the ASTM number.

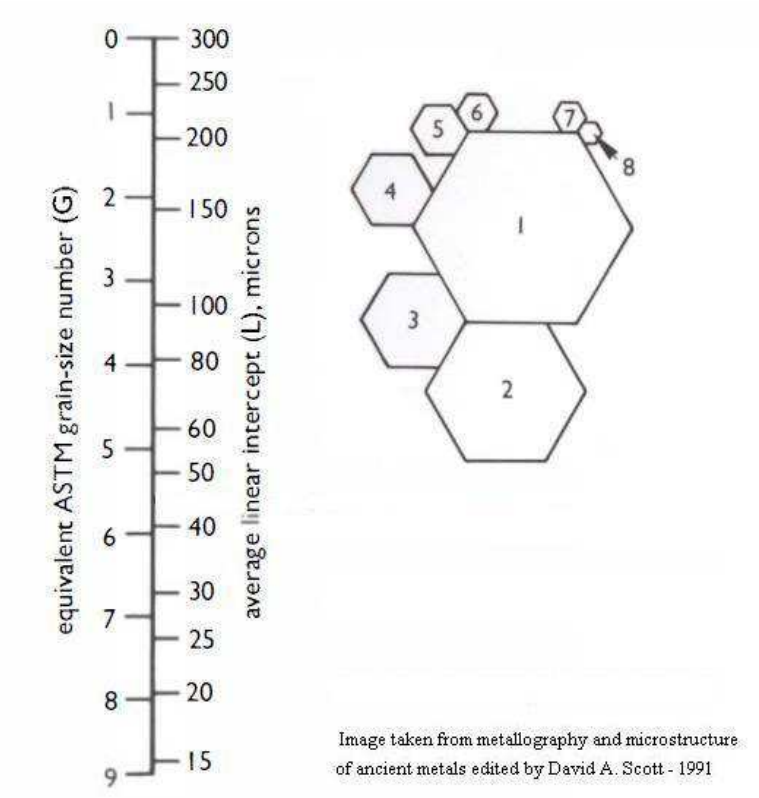

Figure 6: monograph for the grain size, estimated on the basis of the Hilliard's method- photo taken form David A. Scott -1991

1.1 Zwammerdam 2:

1.1.1 Nail ZW2-2 (samples ZW2-2a, ZW2-2c, ZW2-2d and ZW2-2g)

The selected samples consists of the head of the nail (*sample a*), the stem part (*samples c* and *d*) and the tip (*sample g*). This selection allows the investigation of the changes in the texture of the metal over the entire length of the nail. What was observed is a difference in the size and in the arrangement of the metal's grains. In the head were identified areas with different grain sizes, i.e. in the inner area of the head, grains with a size between 3 and 5 (fig. 9) are found. On the sides the grain size decreases until 8 (fig 7) and in some cases, i.e. inter-granular crystals, it can decrease till 9. The situation along the stem is characterised by a relatively homogeneous grain size around 4 or 5 (fig 9). In some particular areas are present small grains with a size around 7-8. The situation is quite different in the tip. In fact there are three different layers, two in the external sides where the grains size is around 8 and one in the central core, where the grains remain with size around 4 or 5, like in the stem (fig. 10).

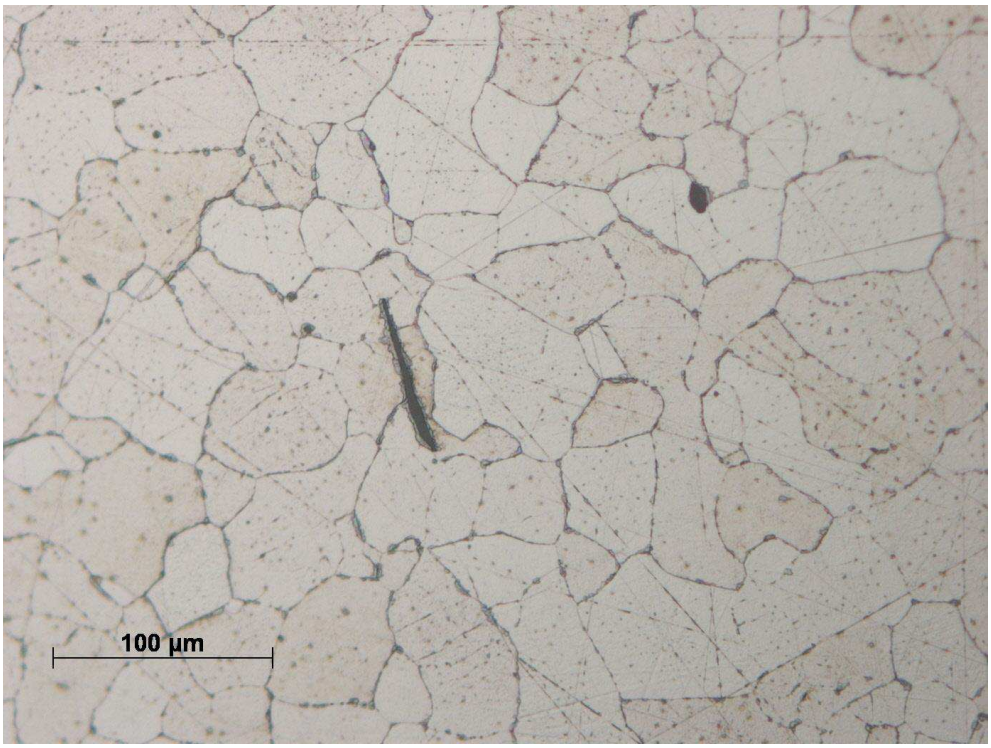

Figure 7: Sample ZW2-2a x200 difference of the grain sizes in the head of the nail.

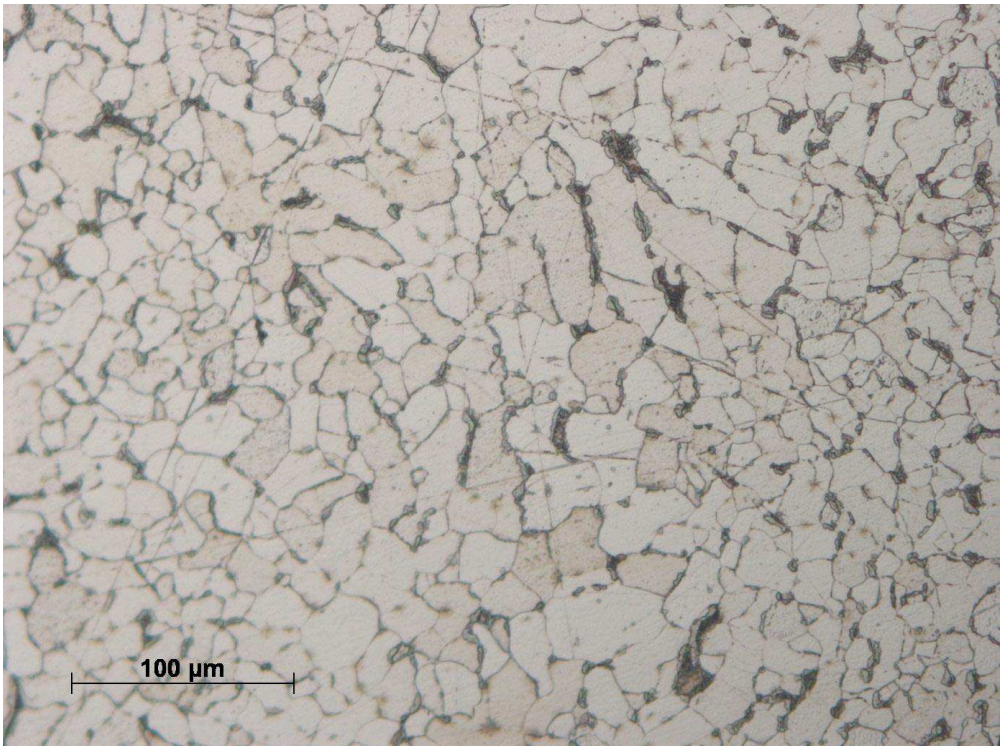

Figure 8: Sample ZW2-2a x200 right side with grain size around 8

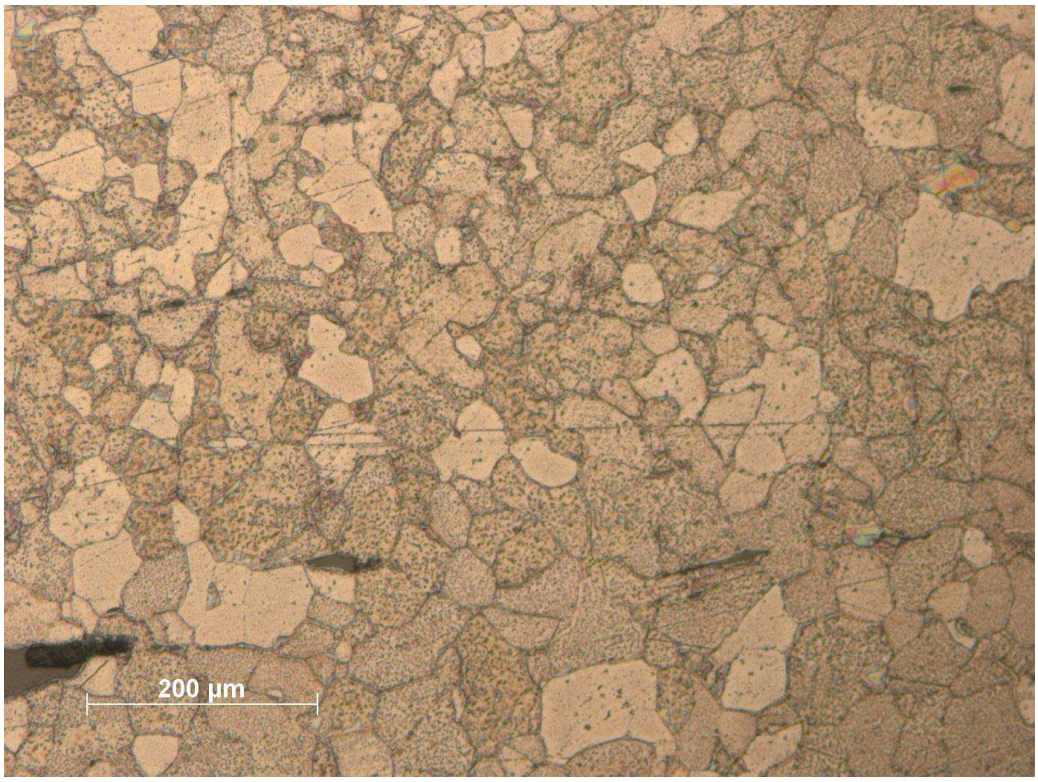

Figure 9: Sample ZW2-2d x100 grain structure of the stem

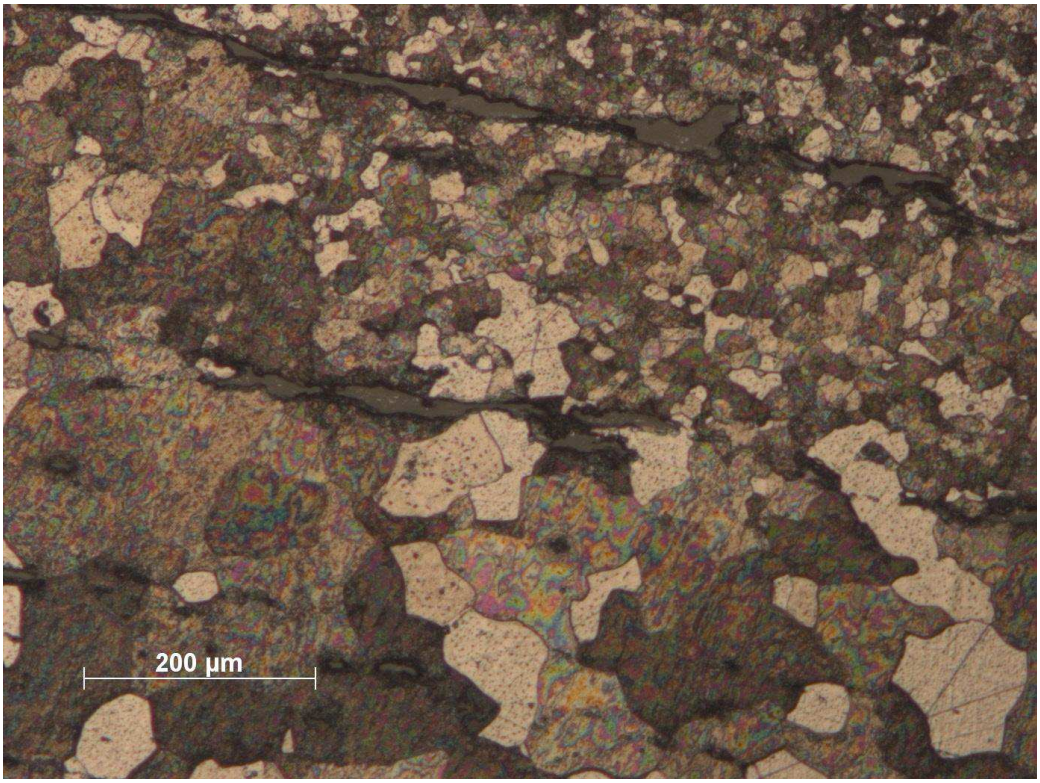

Figure 10: Sample ZW2-2g different grain size zone between the centre and the external area. The internal area is the one with big grains, the external one (in the upper part of the image) have little grains. The rainbow effect is an undesired effects created during the etching process.

1.1.2 Nail ZW2-3 (samples ZW2-3d and ZW2-3e)

The stem of this nail (*sample d*) is characterized by a homogeneous grain size. The ASTM number is around 4. A particular situation is visible in the left side of this sample. It is possible to see grains of the same size but with an elongated and flattened shape instead of the normal crystal structure. In the tip the situation observed is different, because are present grains with a size around 3 and inside the space between these big grains were grown small grains with a size around 7. The amount of these grains is greater in the two external sides of the tip.

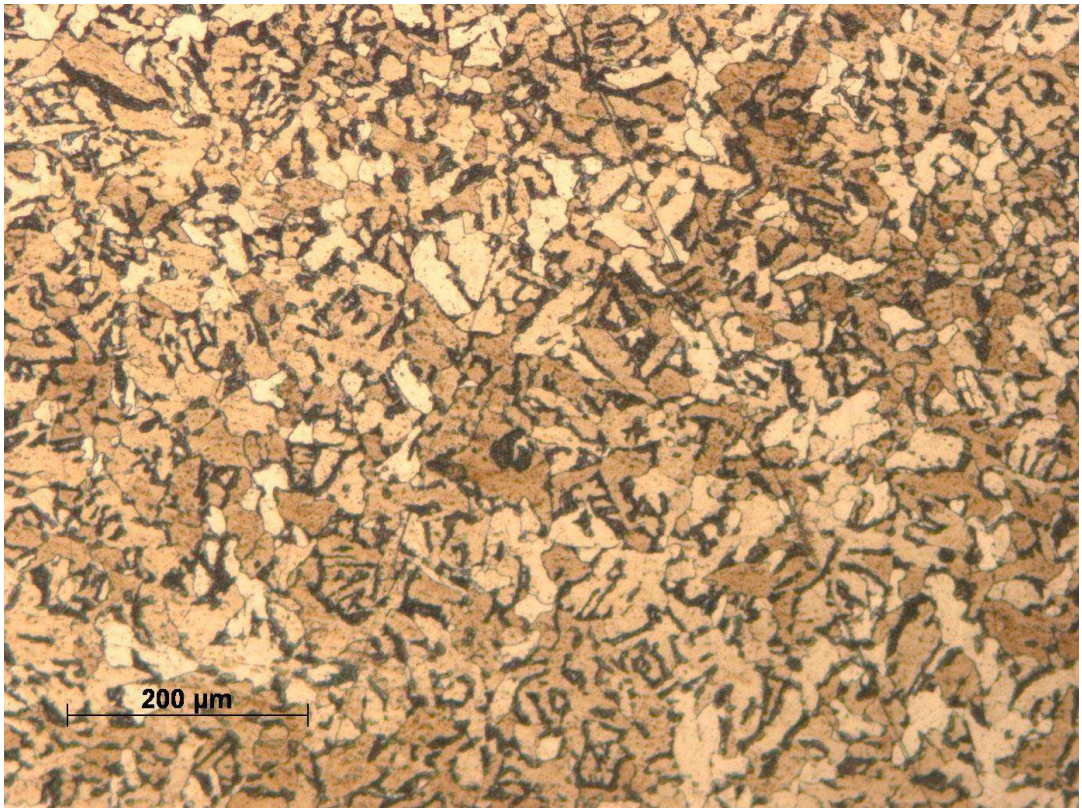

Figure 11: Sample ZW2-3d x100 elongated grains

1.1.3 Nail ZW2-GE2K (samples ZW2-GE2Kb, ZW2-GE2Ke, and ZW2-GE2Kf)

The upper part of the stem is characterized by the presence of big grains with a size around 2. At a certain point (*sample b*) can be appreciate a radical change in the grains size that goes from 2 down until 6-7 (fig 12). This situation starts in the very first section of the stem and last until the tip of the nail. From the upper part of the stem to the tip are also clearly visible areas in which it is possible to recognize the presence of the phosphorus inside the metal, the presence of this element = inside the metal is evident by a shadow or watery effect over the metal's grains. This particular effect is well describe in literature by E.G. Godfrey, 2007 (fig. 12). The figure 13 exemplifies a particular effect due to the cold working of the object: the twinning of the grains. The twinning is the structure rearrangement in a metal artefact subjected to the combined effect of cold working and re-crystallization. Twinning induces the formation of typical features evidenced by parallel-sided forms within a grain.

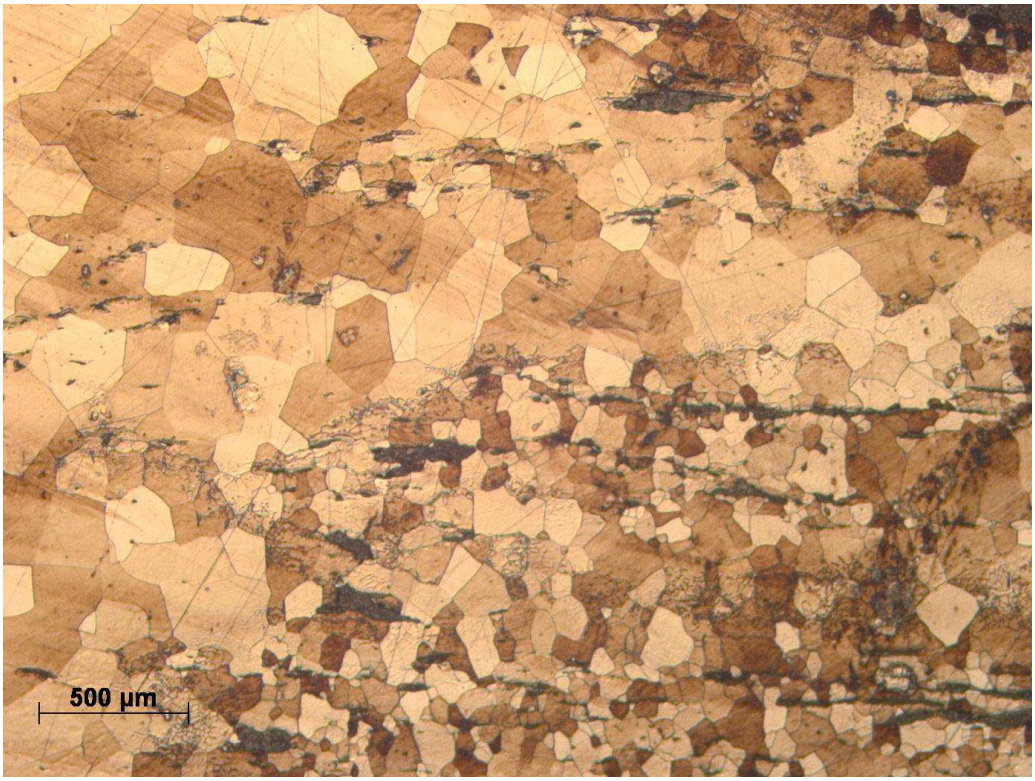

Figure 12: Sample ZW2-GE2Kbx25 division site in the grain size

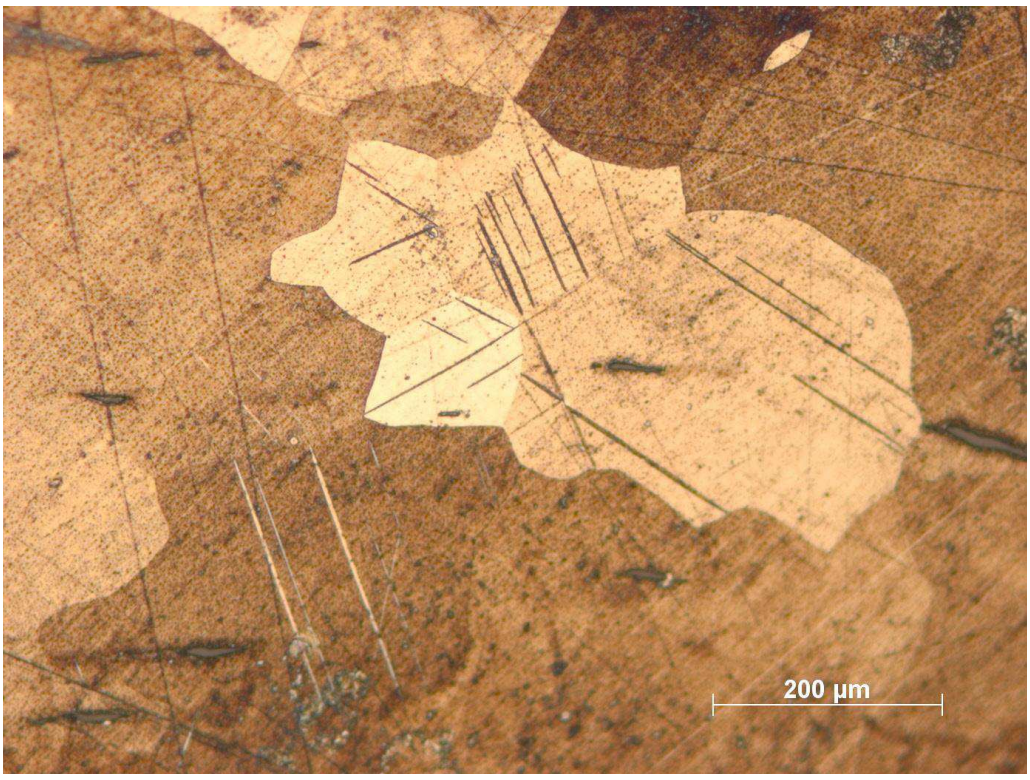

Figure 13: Sample ZW2-GE2Kb x100 twinned grains

1.1.4 Nail ZW2-GE2R (samples ZW2-GE2b, ZW2-GE2Rd, ZW2-GE2Re and ZW2-GE2Rg)

The first sample selected from this nail is characterized by the clearly presence of the phosphorus shadow effect spread all over the surface. The grain size is variable and can go from dimension of 1-2 to 6-7 in some particular areas. *Sample d* presents a variable structure with different layers and features. In the macro[13] photograph (fig. 14) are clearly visible four different layers and again the Phosphorus shadow effect. In one of the external sides was registered the presence of a combination structure of ferrite, the lighter grains, and probably pearlite, the darker areas. This layered aspect lasts also in the structure of the tip.

[13] In this context with the word macro means an enlargement of x25 in which it is possible to have an overview of the layered structures of the different specimen.

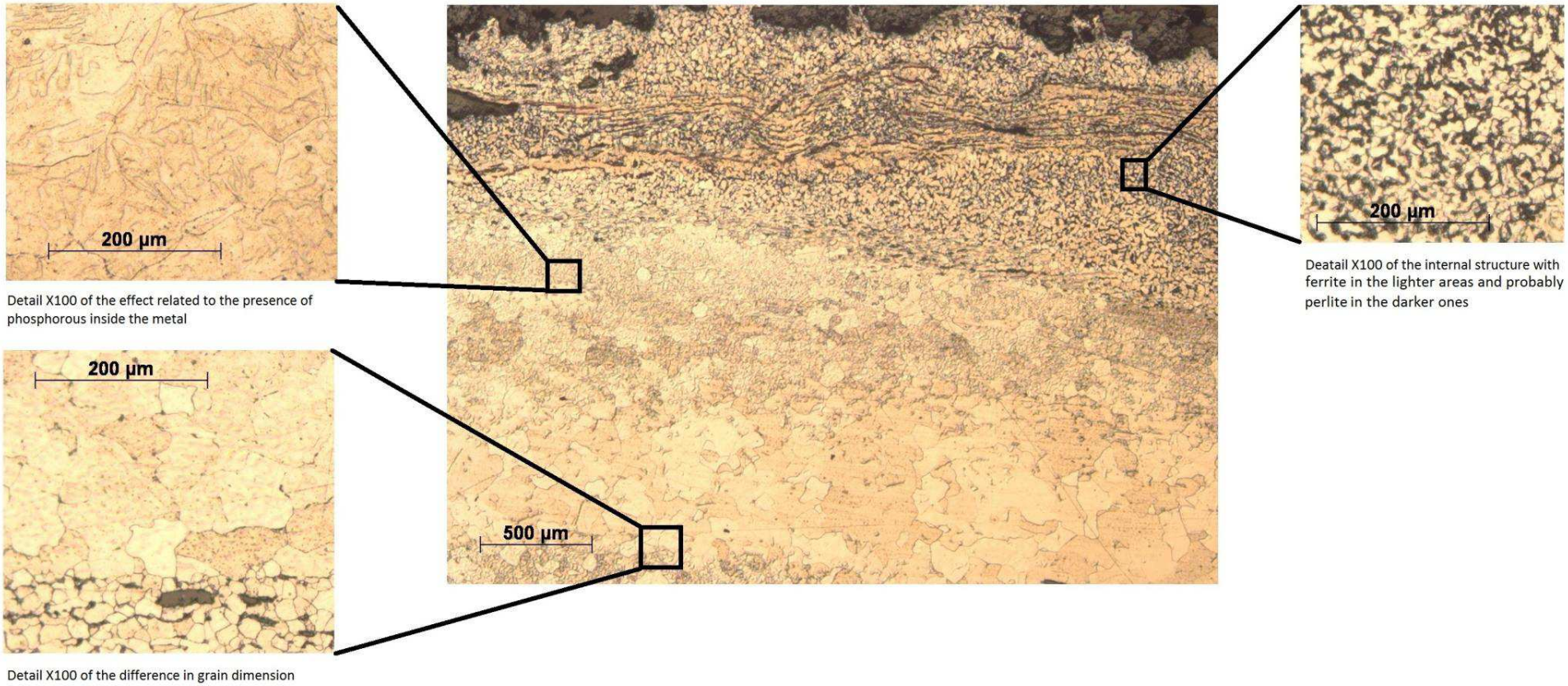

Figure 14: Sample ZW2-GE2Rd macro x25 with details of the different layers. The detail images are not directly related to the position show in the image.

1.1.5 Nail ZW2-GG2K (sample ZWGG2Kb, ZW2-GG2Kd, ZW2-GG2Ke and ZW2-GG2Kg)

The upper part of the stem (*sample b*) shows a layered structure. Inside the layers a structure with two different arrangements is visible. The first layer is situated in the one of the external sides of the specimen, is characterized by the presence of small grains with a size around 7(fig. 15). The other layer has grains with a greater size, between 3 and 4. This situation disappears along the length of the nail, in tip's direction. It is possible to notice that the grains size inside the *sample d* is quite homogeneous and is maintained around 3-4, with few variations, till the tip (*sample g*).In this last specimen is possible to appreciate a decreasing of size from around 3 to around 6, along the length of the tip itself.

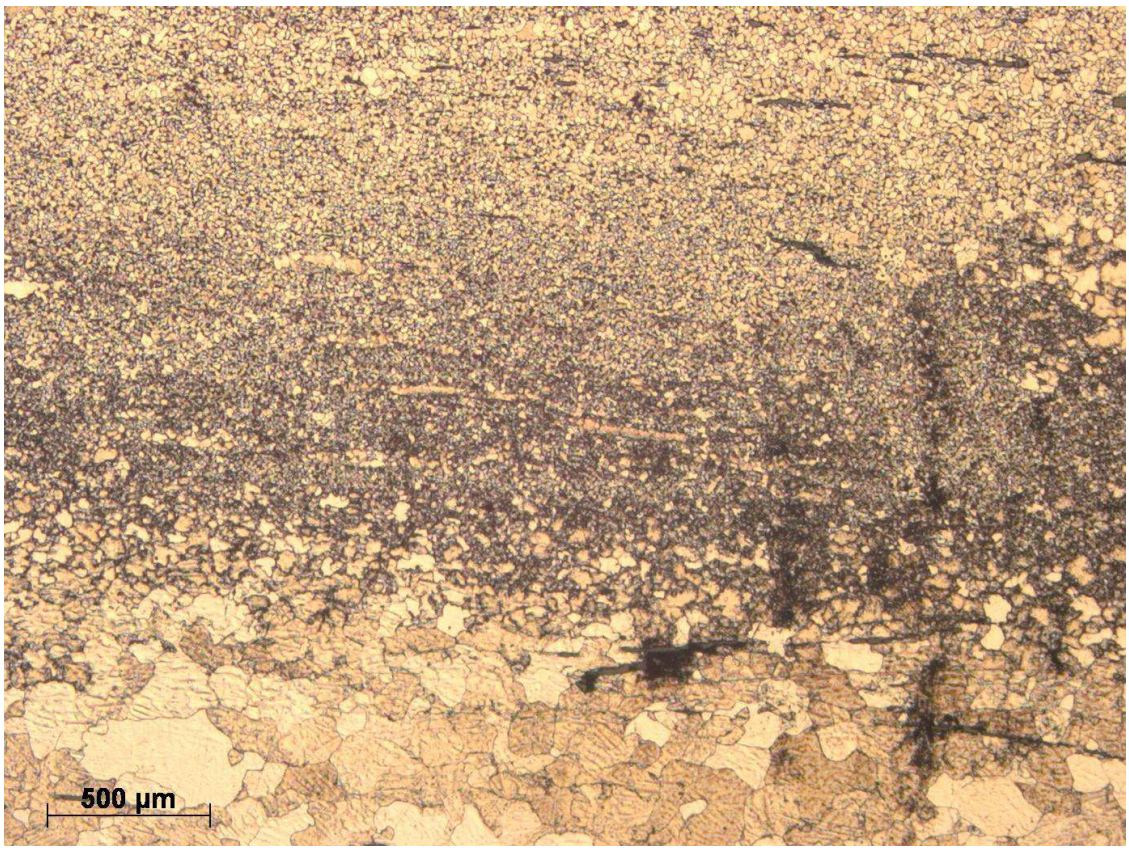

Figure 15: Sample ZW2-GG2Kb Macro x25 layers division; in the lower part of the image there is the inner part of the nail with greater grain size, in the upper one the external side with the smaller grains.

1.1.6 Nail ZW2-GG2R (sample ZWGG2Rb, ZW2-GG2Rd, ZW2-GG2Re and ZW2-GG2Rg)

Along the entire length of this nail, the presence of numerous layers is recognised. These layers have different features and grain size, as is clearly shown in the macro image below (fig. 16). These layers have a grain size that can be really dissimilar one to the other. In some areas there are big hexagonal grains (size around 4), in others areas an arrangement prevalently made by small grains is visible (size around 7). The last areas have an appearance that shows grains of ferrite surrounded by darker areas probably constituted by pearlite. In figure 12 the needle structure, that is possible to distinguish, is a Widmanstätten ferrite, the darker areas probably form pearlite (fig. 17), but in this case is not possible a precise distinction only with the use of an optical microscope.

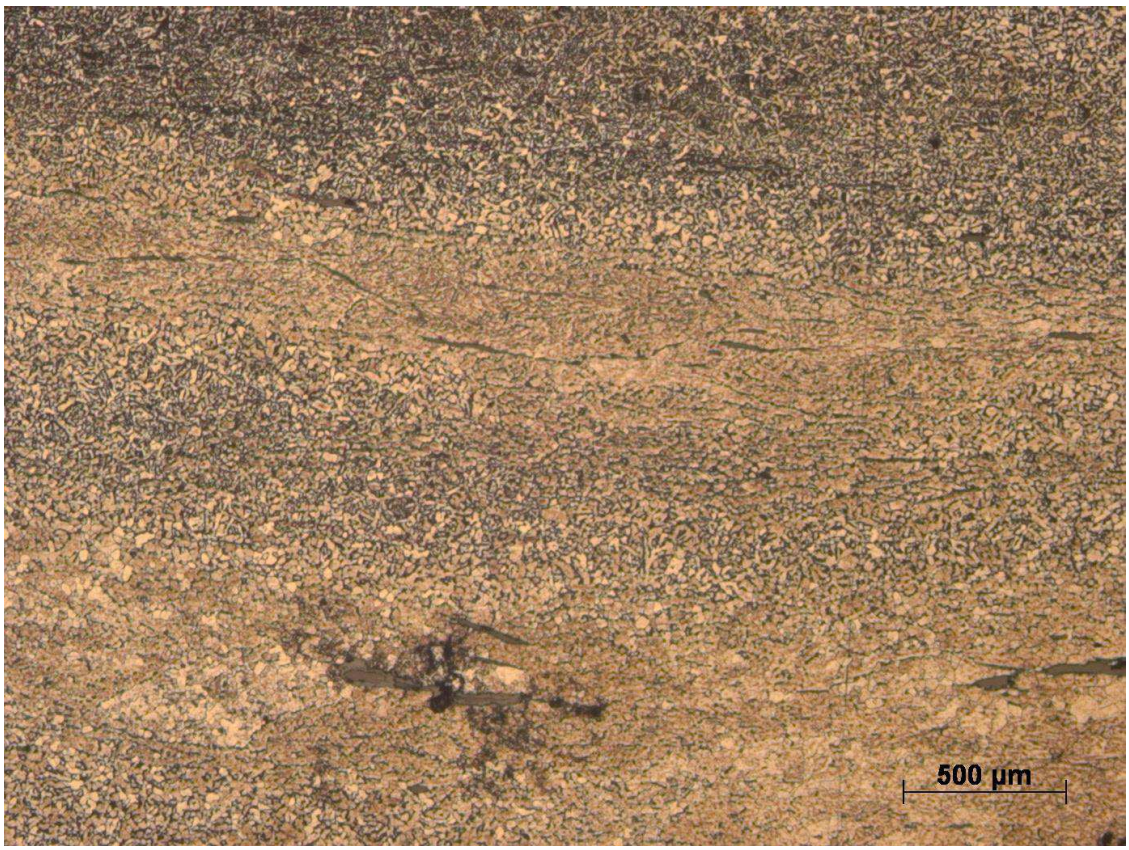

Figure 16: Sample ZW2-GG2Rb macro x25 of the layered structure.

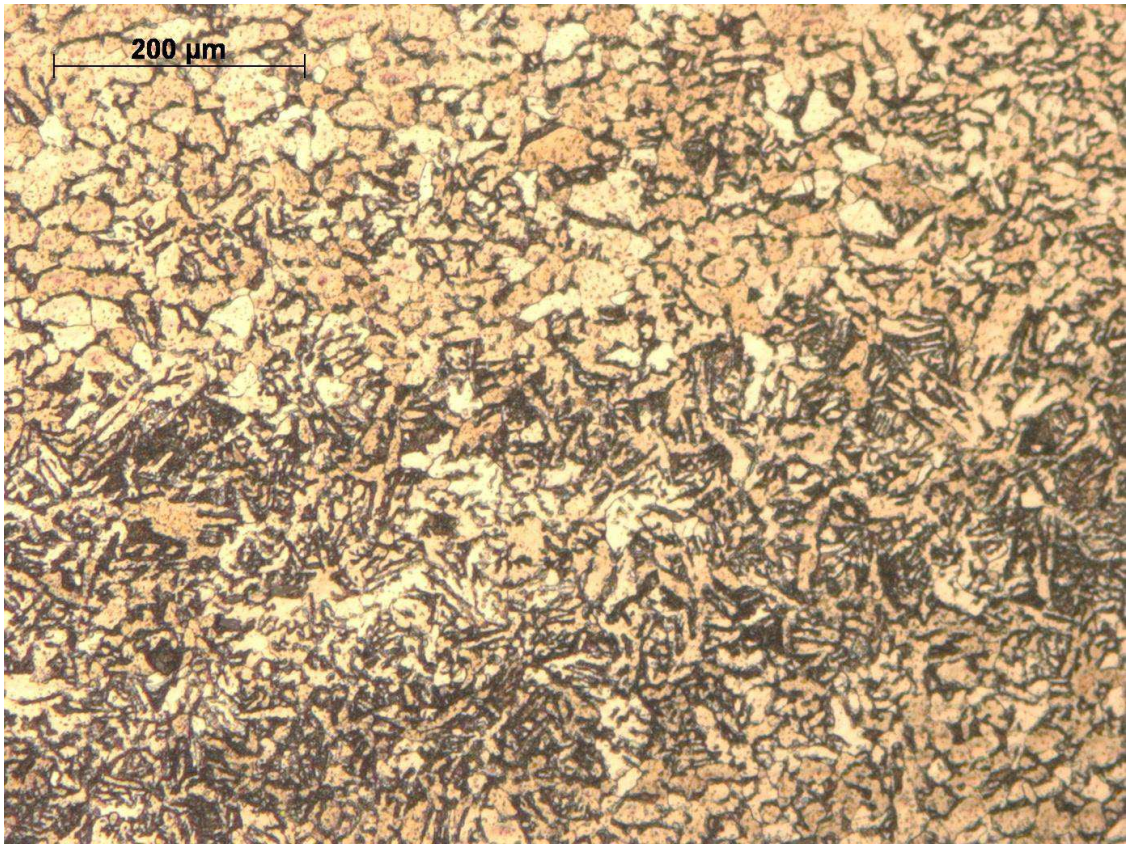

Figure 17: Sample ZW2-GG2Re x100 detail of the division between two layers, the lower one is characterized by a Widmanstätten appearance of the ferrite.

1.2 Zwammerdam 4:

1.2.1 Nail ZW4-6 (sample ZW4-6c, ZW4-6f and ZW4-6 g)

This nail shows a layered structure that starts in *sample c* and goes on till *sample f*. This arrangement is divided into approximately three areas. The first one, which belongs to one external side, has a fine grain structure (size around 7). The second one, located in the central region of the nail, has large grains (size between 2 and 3). The last one, which belongs to the other external side, has a complex structure, with secondary ferrite, with a pattern like the Widmanstätten one, surrounded by darker areas that can be formed probably by pearlite (fig 18), but with the only use of the optical microscopy is not possible to precisely divide the three structures. The tip (*sample g*) shows a different pattern, which is not characterized by different layers, but by a decrease in grain dimensions till the extreme tip, where the grain size is around 7.

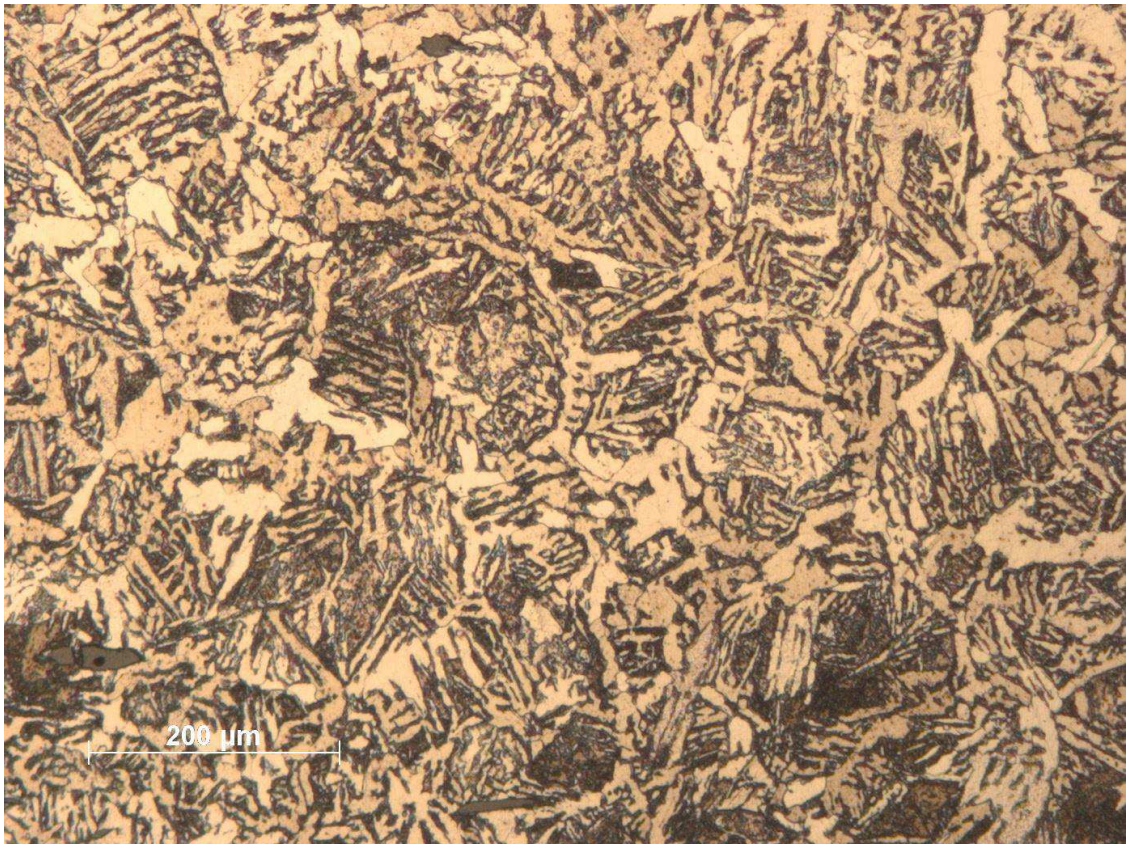

Figure 28: Sample ZW4-6c x100 secondary ferrite structures

1.2.2 Nail ZW4-7 (sample ZW4-7 b, ZW4-7c, ZW4-7f and ZW4-7h)

The *samples b* and *c*, taken from the upper part of the stem show a layered pattern. The layer's configuration is complex with a no clear division between one to the other. One of the two external sides is characterized by the presence mixed structure of secondary ferrite or acicular secondary cementite; the other one has a different arrangement with small grains (size around 6). In the central part of the samples is present a dark layer surrounded by two stratums of acicular ferrite with a structure similar the Widmanstätten pattern.

Sample f has a different arrangement. The acicular ferrite strata are not present anymore; the grains size is increased (around 5) and the presence of phosphorus watery effect can be clearly seen. These features continue in the tip (*sample h*) but here a clear division line can be noticed between the layers where is present or not the phosphorus. The grain size in the tip is between 6 and 7.

1.3 Zwammerdam 6:

1.3.1 Nail ZW6-7 (sample ZW6-7cv, ZW6-7dv, ZW6-7bh, ZW6-7eh, ZW6-7fh and ZW6-7gh)

The main characteristic of this nail is the small dimension of the grains. All over the nails from the upper part till the tip the grain size is around 7, in the curved section of the nail (*samples eh*, *fh*. and *gh*) the grain size decreases further till arrive around 9. This situation is particularly clear in the right section of the *sample fh*, where is possible to notice the formation of these small grains between the grain boundaries (fig 19). Along the entire length of the nail can be detected the presence of phosphorus layers; this situation is particularly visible in *sample dv* (fig. 20). In particular areas of the *samples cv*, *dv* and *bh* can be registered the presence of a acicular ferrite, surrounded by pearlite.

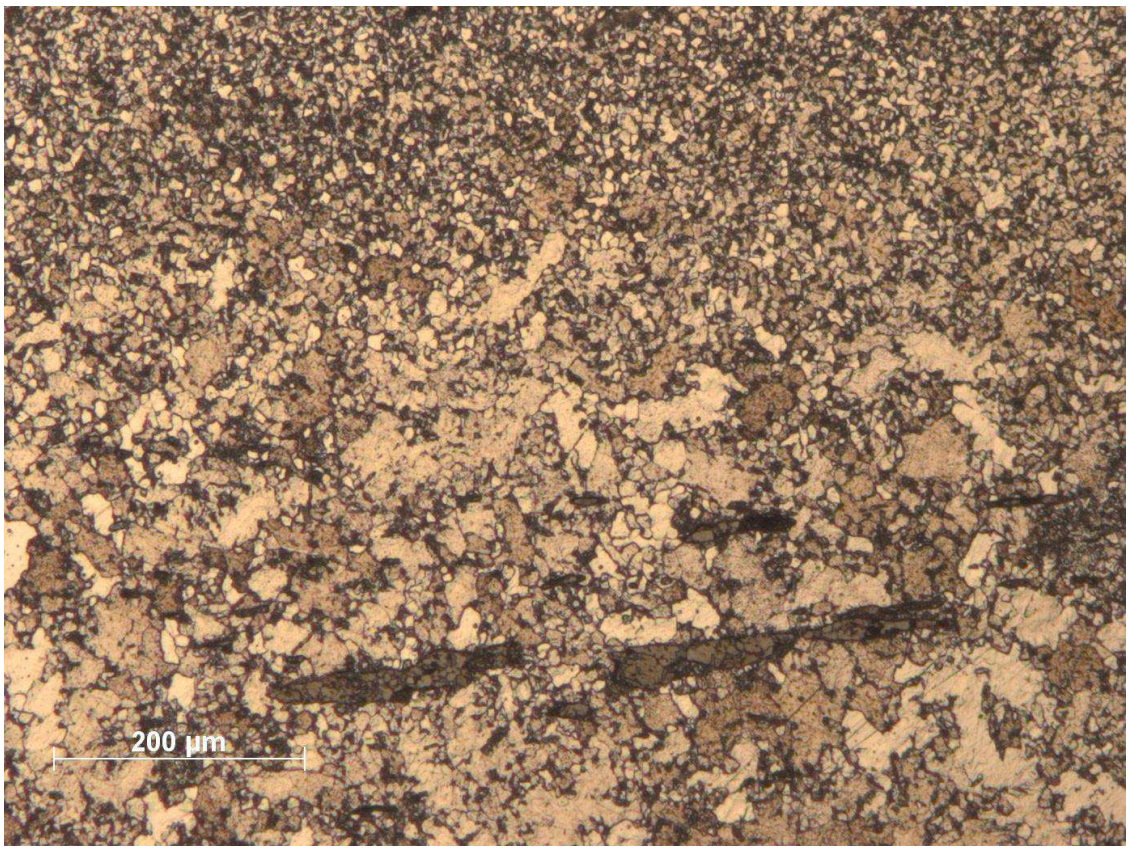

Figure 39: Sample ZW6-7eh detail of the small grains that surround the bigger ones

Figure 20: Sample ZW6-7dv phosphorus layer

1.3.2 Nail ZW6-8 (samples ZW6-8b, ZW6-8e, ZW6-8f and ZW6-8g)

The central part of the *samples b* and *e* is characterized by a stratum with a grain size around 1; furthermore these grains shown slip lines (fig 21). This central core is surrounded by a complex structure of many layers with different features; the division line is very clear and is indicated by the phosphorus effect. In combination with this situation the grain size decreases till 5. Inside *sample f* the central stratum with big grains disappears, but are still visible areas with the phosphorus effect, areas without it and areas in which the grains have an elongated shape. In the left side of this sample areas with the presence of a low grade of acicular ferrite are recognized. Except for the presence of these last areas, this situation is practically the same also in the *sample g*; the grains size in these two samples is between 7 and 8.

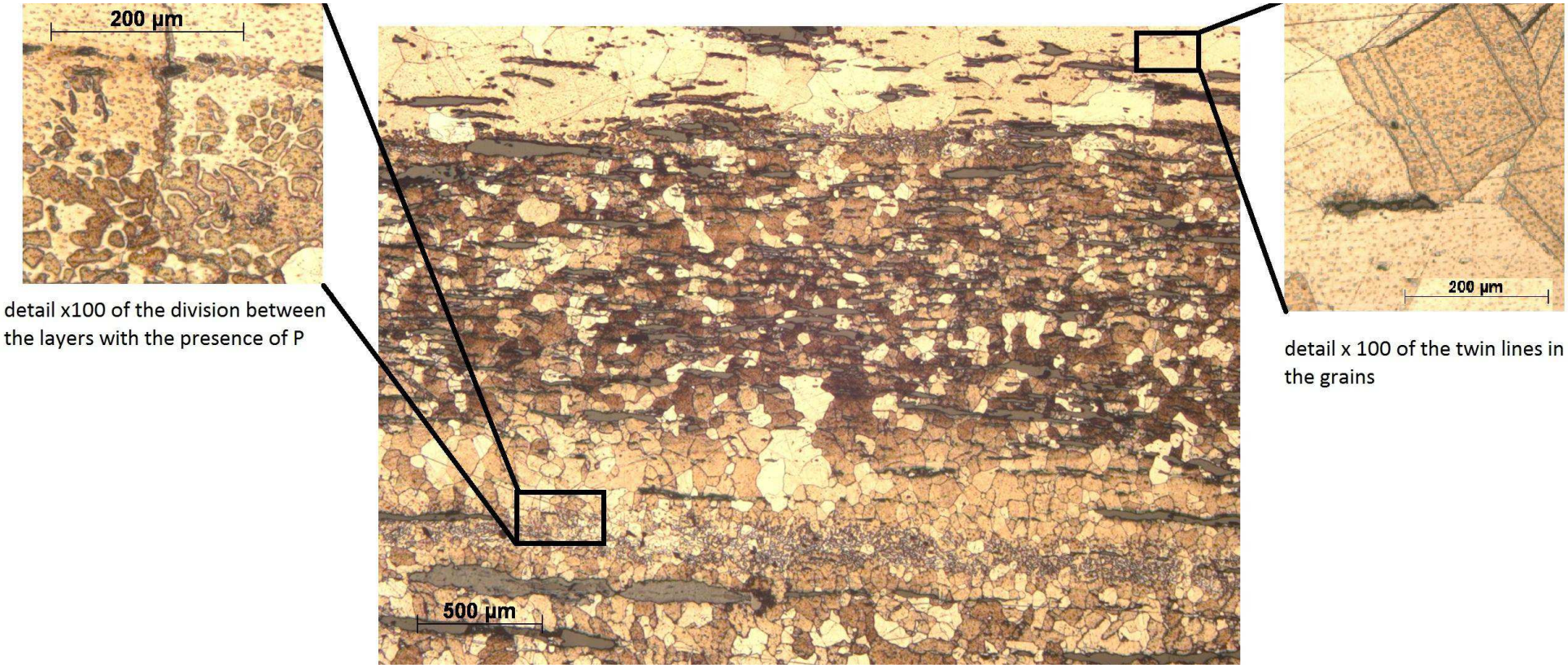

Figure 21: Sample ZW6-8b macro x25 with details of the different layers. The detail images are not directly related to the position show in the image.

1.3.3 Nail ZW6-9 (sample ZW6-9b, ZW6-9f and ZW6-9g

This nail has shows a homogeneous structure with only some layer in which can appreciate a change in the grain size. The central stratum of *samples b* and *f* is a layer with a grain size around 7. Going from this central area to the external side were recognized three other different layers, two with quite big grains with size around 5, dived by a thin layer again with small grains with a size around 7. The situation in practically the same also in the tip (*sample g*), the only difference is the thickness of the central layer, which is approximately 300 µm thicker than in the others samples (fig 22).

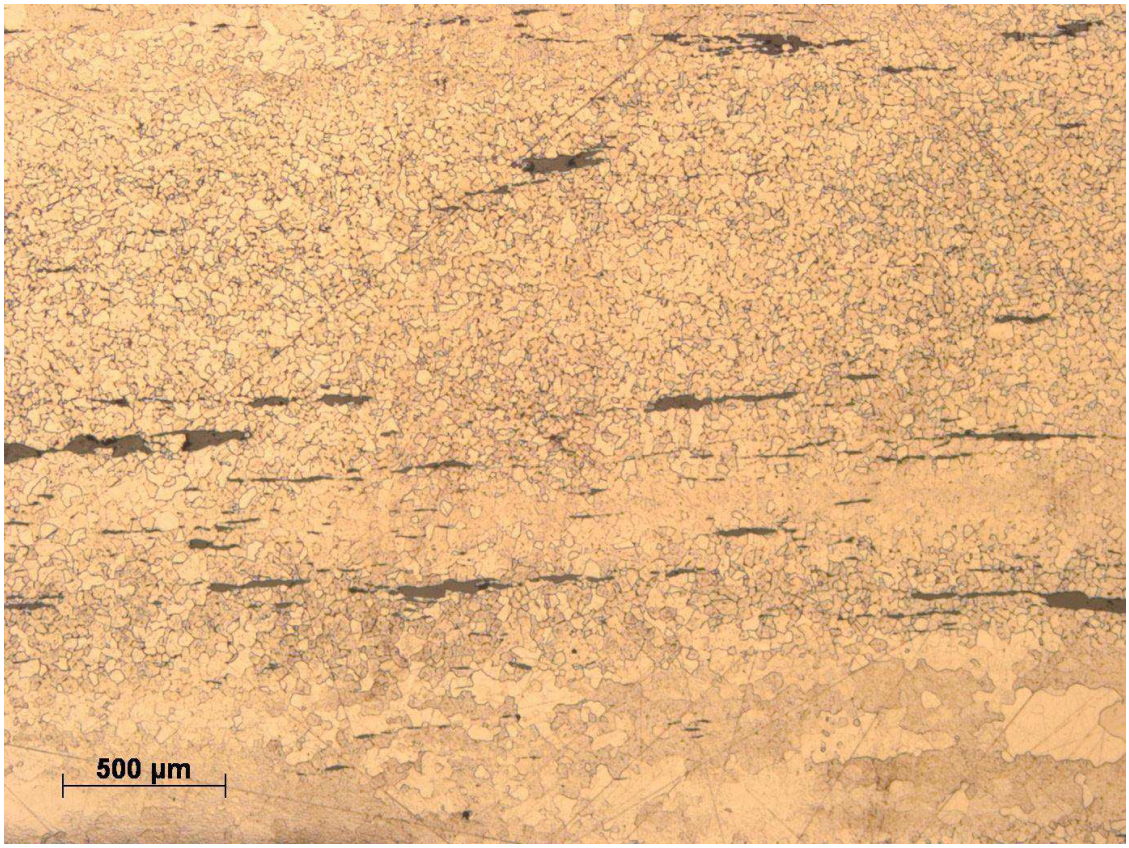

Figure 22: Sample ZW6-9g macro x25 of the layer distribution

1.3.4 Nail ZW6-10 (sample ZW6-10a, ZW6-10c, ZW6-10f and ZW6-10g)

In the selected samples is present the head of the nail itself, which shows high percentage of phosphorus and a layer with different grains size. The size of these grains starts with a value the around 6, in the external zone, value that arrive around 4 in the central area. The grains of this latter are characterized by the presence of slip lines and a wide spread

phosphorus effect. In the stem (*samples c* and *f*) is still visible the widespread presence of phosphorus effect, but differently from the head the grains size remains more homogeneous without great fluctuation or layering, and it is around 4 in the inner part and around 6-7 in the sides. A similar situation is found inside the tip.

1.3.5 Nail ZW6-13 (samples ZW6-13 b, ZW6-13d, ZW6-13f and ZW6-13g)

The grain arrangement inside the first three specimens of this nail does not show many variations, the grains maintain approximately the same size (between 3 and 4) till the tip, where, a layer with grains size around 7 is clearly visible. In many cases were observed grains characterized by split a line, the amount of the grains with this feature is in the order of tens.

1.4 Woerden 7:

1.4.1 Nail W7-8 (samples W7-8b, W7-8d and W7-8e)

In *sample b* can be easily recognized the presence of phosphorus, a situation that completely disappears inside the other two samples selected from this nail. In all the samples are visible layers with different grain size. The dimension of these grains is between 1-2 inside the central layer, and decrease till 6-7 in correspondence of the external sides of the sample. Inside the tip (*sample g*) were recognized 5 layers in the right side (fig 23), that along the length come together into a single layer which is the one that characterizes the extreme tip. In fig 24 is visible the size of the grains inside this layer[14], which is around 7.

[14] This layer is the one formed by the union of the precedent 5 different layers.

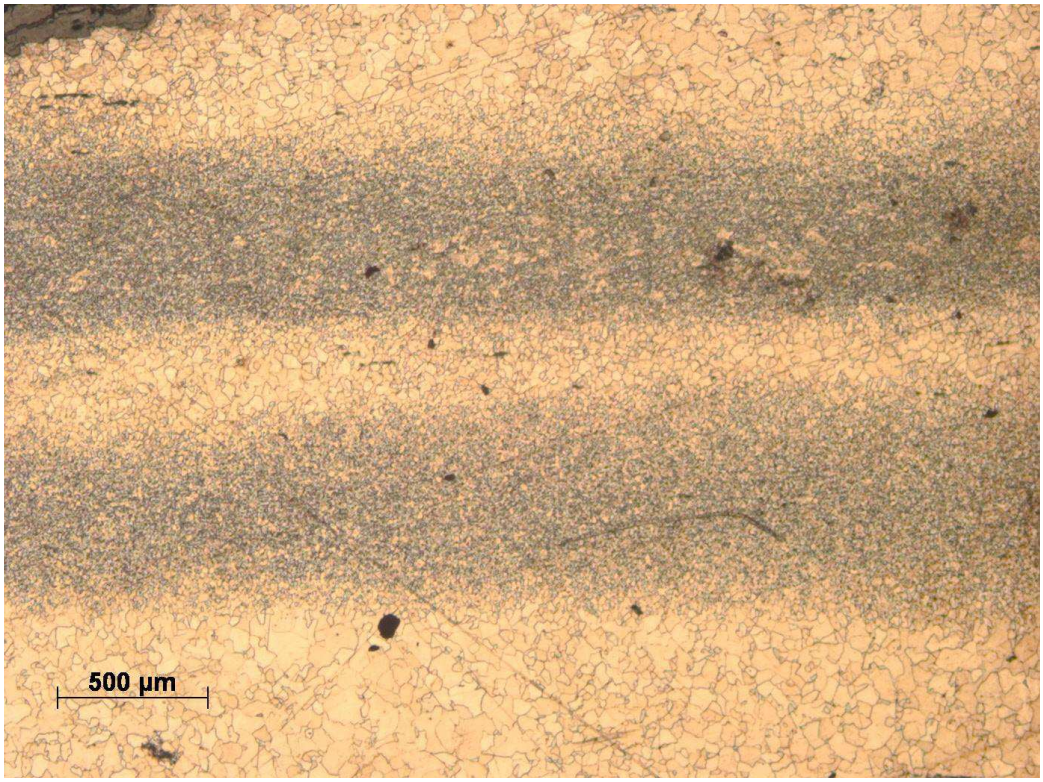

Figure 43: Sample W7-8g macro x25 different layers of the crystal structure

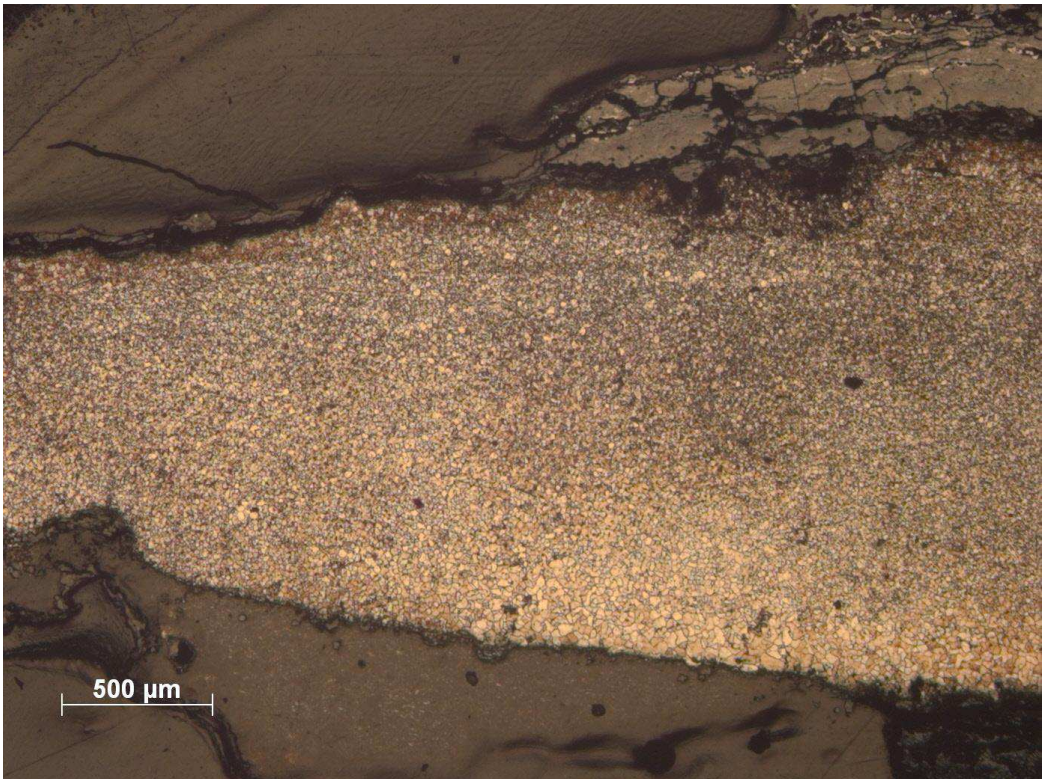

Figure 5: Sample W7-8g macro x25 extreme tip

2 SCANNING ELECTRON MICROSCOPE (SEM) WITH ENERGY DISPERSIVE X-RAY SPECTROSCOPY (EDS):

2.1 Zwammerdam 2:

2.1.1 Nail ZW2-2 (samples ZW2-2a, ZW2-2c, ZW2-2d and ZW2-2g)

The series of four samples have shown a homogeneous structure with few slag inclusions. This feature is valid for major areas of the specimens but in some areas, i.e. in the middle part of *sample c* were registered an increase in quantity and size of the slag inclusions. The major elements are silicon (Si), aluminium (Al), phosphorus (P), potassium (K) and calcium (Ca), manganese (Mn) and magnesium (Mg). These last two elements are practically presents in all the analyzed slag inclusions of this nail. Inside the head of the nail was found a slag with a high percentage of silicon (around 28 wt%), index of a glassy matrix. In that slag are also present barium (Ba) and titanium (Ti) as accessory elements.

The tip deserves a separate discussion. In this section of the nails (*sample g*) were observed a fracture and in close proximity to this were found some pollutants elements, i.e. chlorine (Cl) and sulphur (S). In the detail[15] picture taken to better understand the nature of the slag were clearly visible, in most of the cases, all the different mineral phases present, related to fayalite (Fe_2SiO_4) and wüstite (FeO) crystals, this conclusion is due not only to the chemical composition, but also to the shape of the crystal inside the slags. The fayalite inside the slag inclusion form preferentially elongated crystals, which result of a light grey under the microscope, the wüstite on the other hand create preferentially a dendritic structure.

These conclusions are derived from the observation and the chemical composition, to obtain a precise identification of the crystalline species is necessary to perform analysis like the X-rays diffraction (XRD).

[15] In this context the word detail is related to high magnification that goes from x1000 up to x4000 or more.

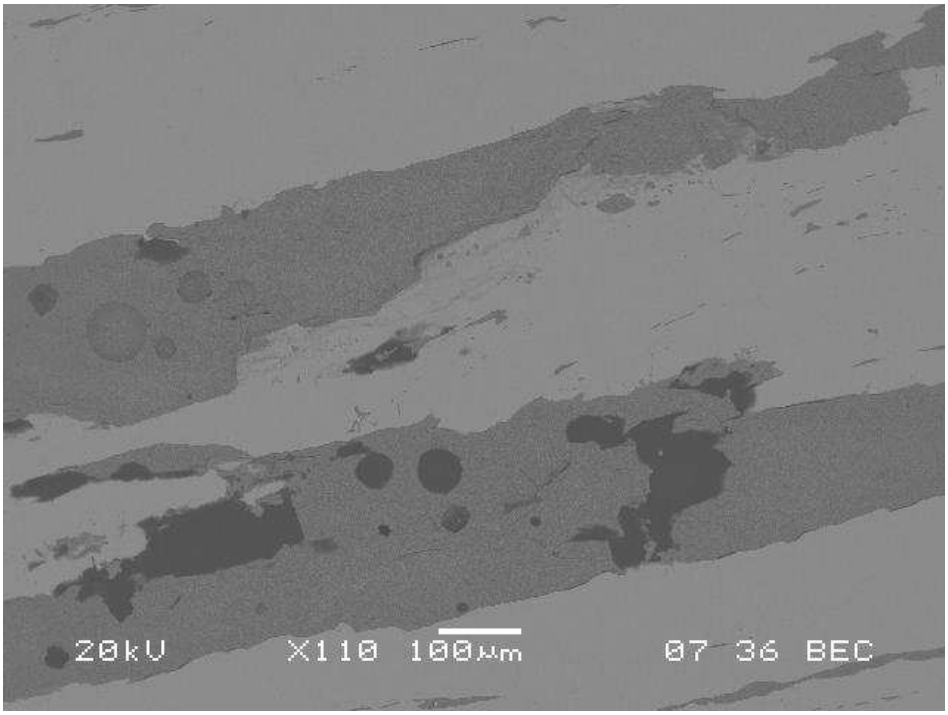

Figure 65: Backscattered electron (BES) General feature x110 of the slag inclusions from nail ZW2-2

2.1.2 Nail ZW2-3 (samples ZW2-3d and ZW2-3e)

The specimen ZW2-3d has a homogeneous surface characterized by few slag inclusions[16]. Some traces of the barium (around 0,5 wt%) can be observed in two occasions inside the slag composition. The situation in more or less the same in the lower parte of the nail (*sample e*), but here can is registered an increase of the number of inclusions.

2.1.3 Nail ZW2-GE2K (samples ZW2-GE2Kb, ZW2-GE2Ke, and ZW2-GE2Kf)

This nail is characterized by the massive presence of P inside the metal core. In fact this element is found practically everywhere over the surface of the entire series of the specimens taken from the nail. The surface of all the samples is characterized by the presence an high amount of slag inclusion, the amount of this inclusion is in the order of hundreds. These inclusions have an elongated shape. The principal elements are Si, Al, P, Ca and K, it has also been observed the totally absence of other elements like Mn, Mg and Ba. The change in composition of the slag inclusions from the head to the tip must be

[16] The amount of these inclusions is in the order of tens.

highlighted. Inside the *sample b* the composition of the inclusions is generally characterized by a low weight quantity (when present around 0,7 wt%) or a totally absence of elements like K and Ca, a feature that disappear along the length of the nail. At high enlargement (from around x1000 to around x2000) were identify more phases inside a single slag inclusions. In some particular occasion the chlorine were detect inside the slag inclusions.

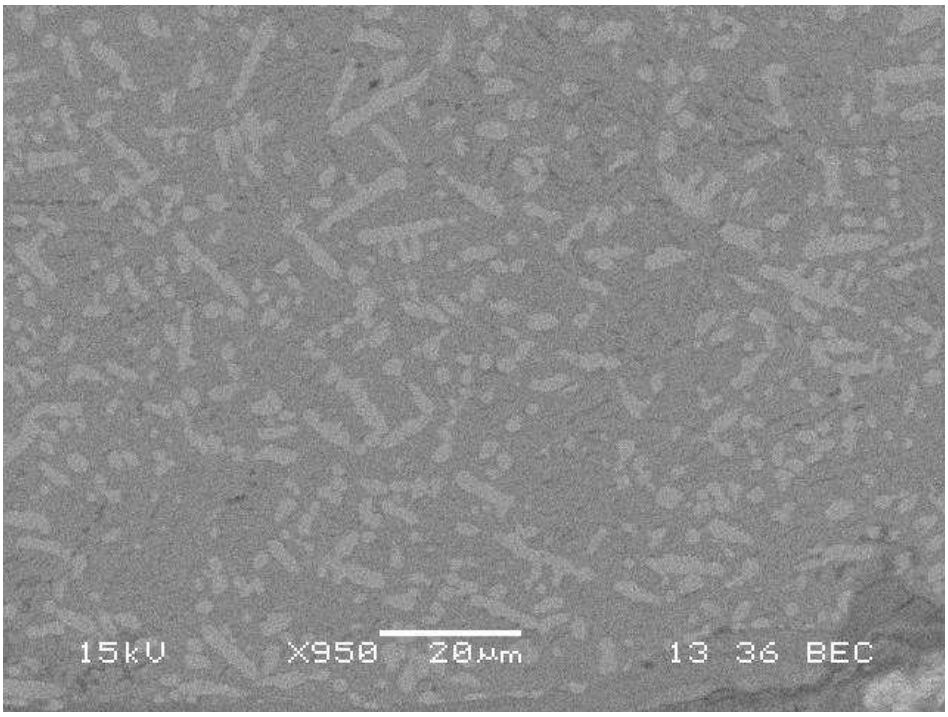

Figure 76: BES view Detail x950 of the three phases that compose a slag inclusion.

2.1.4 Nail ZW2-GE2R (samples ZW2-GE2b, ZW2-GE2Rd, ZW2-GE2Re and ZW2-GE2Rg)

The first feature that registered in the upper part of the stem of the nail (*samples b* and *d*) is related to the composition of the slag inclusions. The inclusions are characterized by a low weight percentage of potassium (around 0,6 wt% where present) and calcium (around 0,6 wt% where present), but in most of the cases these elements are totally absent, in fact the absence of P is in 19/35 and the absence of Ca is in 12/35 of the analyzed slag inclusions.

P was found inside the metal core, but the presence of this element is not widespread. In fig 22 below is possible to see the general aspect of the sample taken from this nail.

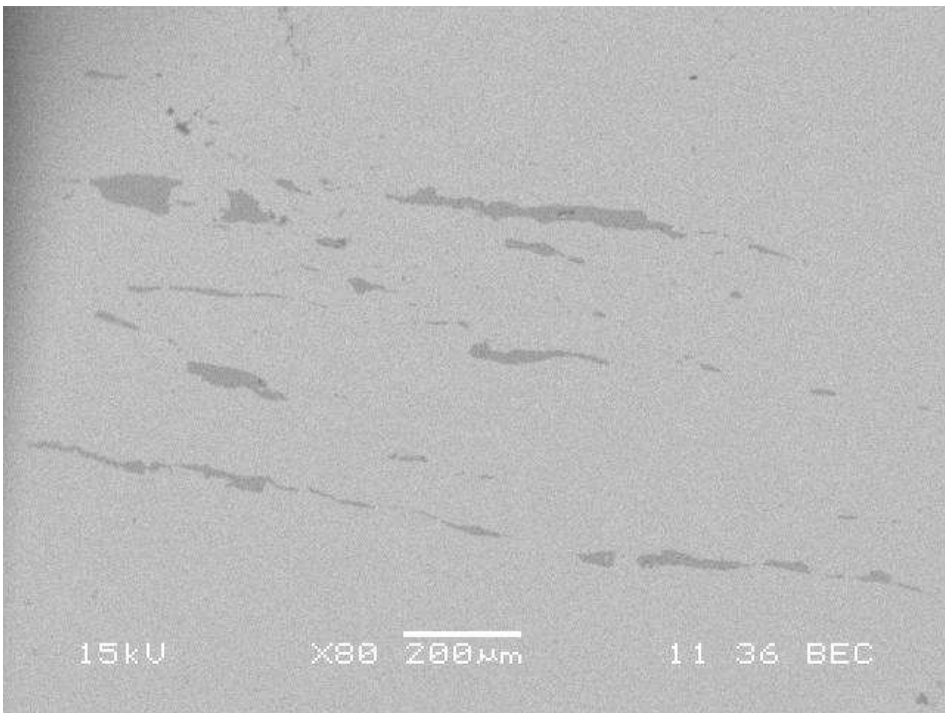

Figure 27: BEC view x80 of the layers and areas create by the slag inclusion

2.1.5 Nail ZW2-GG2K (samples ZW2-GG2Kb, ZW2-GG2Kd, ZW2-GG2Ke and ZW2-GG2Kg)

The principal feature of this nails is the high number of slag inclusions, in particular inside *samples b* and *g*. The number of the slag is in the order of hundreds. Specimen *d* has a homogeneous structure with relatively few inclusions, if compared to the previous samples. From the compositional point of view is registered the presence of P inside the metal in punctual areas of the sample, only inside the *samples d* and *e* seem that a major quantity of this element is present, in fact it was detected in 5/14 of the analyzed areas. The elements that compose the slag inclusions are Si, Al, P, K and Ca. The inclusions of the *sample b* have a low quantity of P with respect to the ones of the other specimen of this nail. The P concentration is around 0,5 wt%, when present, instead of the 1,2 wt % of the other samples. At magnification from x500 and onwards, almost all the inclusions were characterized by the presence of different phases.

2.1.6 Nail ZW2-GG2R (samples ZW2-GG2Rb, ZW2-GG2Rd, ZW2-GG2Re and ZW2-GG2Rg)

Inside this sample were registered a present of a quite high amount of slag inclusion, the number of this slags is in the order of hundreds. The EDS analyses of the inclusions inside the *sample b* have highlighted the presence Si, Al, K, Ca and P. In two cases were detected traces of titanium (around 0,50 wt%) and in one case manganese (1,23 wt%). From the point of view of the alloy composition, in 12 of 123 analyzed areas, the presence of P has detected.

2.2 Zwammerdam 4:

2.2.1 Nail ZW4-6 (samples ZW4-6c, ZW4-6f and ZW4-6 g)

The nail is characterized by a homogeneous microstructure. During the EDS analyses of the slag inclusions the presence of Si, Al, P (this element has been detected in only 14/29 of the inclusions) K, Mg and Ca were detected. The EDS have also detected titanium and manganese respectively in one and two cases. The slag inclusions of the central area of the *sample f* have shown high level of calcium, in comparison with all the others (average value above 1,00 wt% with peaks like 5,80 wt% and 7,28 wt%). The *sample c* is characterized by the presence of P inside the metal in the right side. The last feature necessary to highlight is the presence of a fracture in the tip of the nail (*sample g*) where S and Cl were detected.

2.2.2 Nail ZW4-7 (samples ZW4-7 b, ZW4-7c, ZW4-7f and ZW4-7h)

At a macroscopic vision (naked eye vision) all the samples were characterized by a high number of inclusions, in order of hundreds. The first feature to highlight is the presence of P inside only in three inclusions, in *sample*s *b* and *c*. A totally different situation was observed in *sample h*, where the presence of this element inside the inclusions is every time confirmed. In this sample the average of P is around 2% but inside 4 different slag inclusions it has arrive till 4%. The second feature to highlight is the presence of Mg practically in all the specimens of the nail, and the presence of Ba inside the *samples c* and *f*. Inside the *sample b* has identified in two different slags the presence of Ti (0,5

wt%) and Mn (around 0,9 wt%). One of the inclusions has shown a particular shape of the crystals inside it. From the chemical composition this crystal can be related to fayalite, this aspect similar to "trident" can be explained by as an effect due to the cutting and the polishing of the surface, that have cut in this so particular shape the elongated crystal typical of the fayalite (fig 28).

Inside the *sample f* is present a great fracture. Along the length of the fracture was detected a widespread presence of chlorine (in the fig 30 below is shown a crystal of halite[17]). For what concern the composition of the alloy in two cases inside the metal alloy of *sample f* the presence of phosphorus is detected.

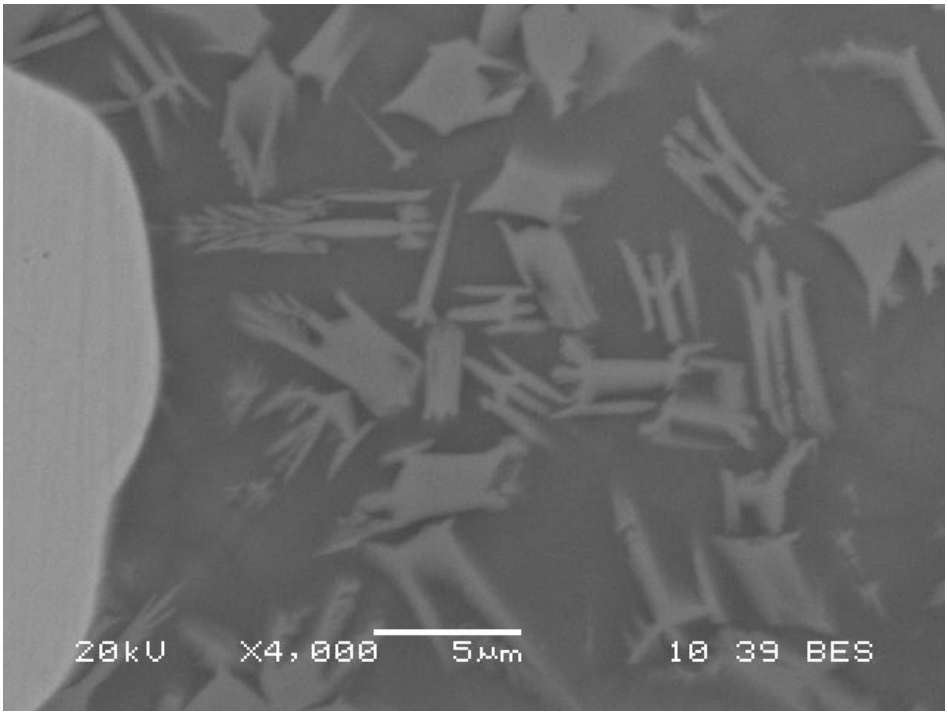

Figure 28: detail x4500, of a particular shape of the fayalite crystal inside an inclusion

[17] The Halite is a mineral formed by sodium and chlorine. The identification of the crystal show in the image with this mineral is due to the EDS analysis, in which only this two elements were detected.

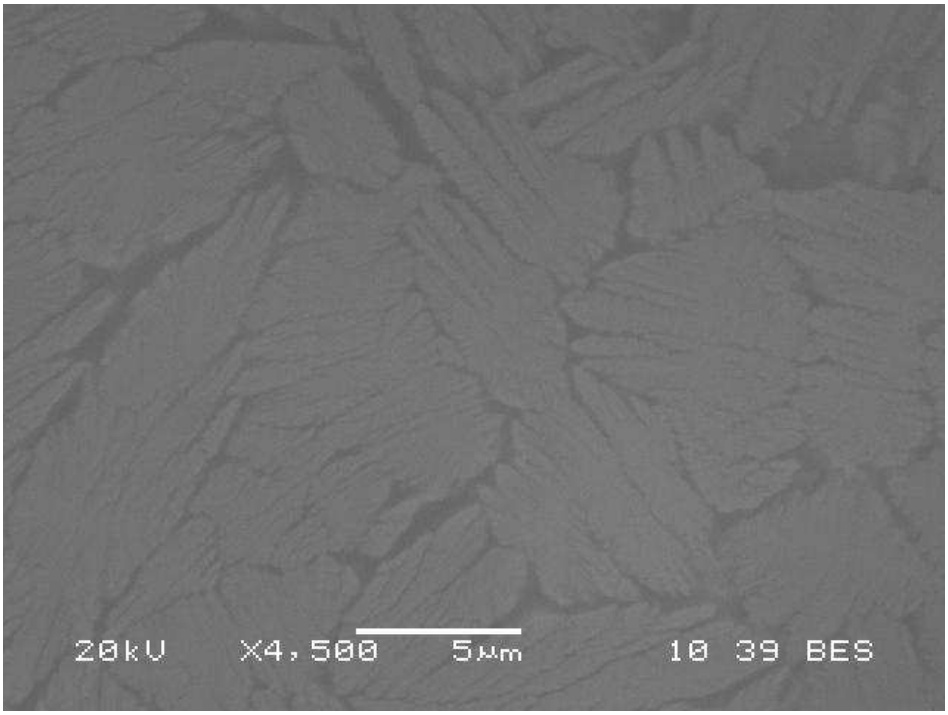

Figure 89: x4500 aspect of a slag inclusion present inside the nail ZW4-7

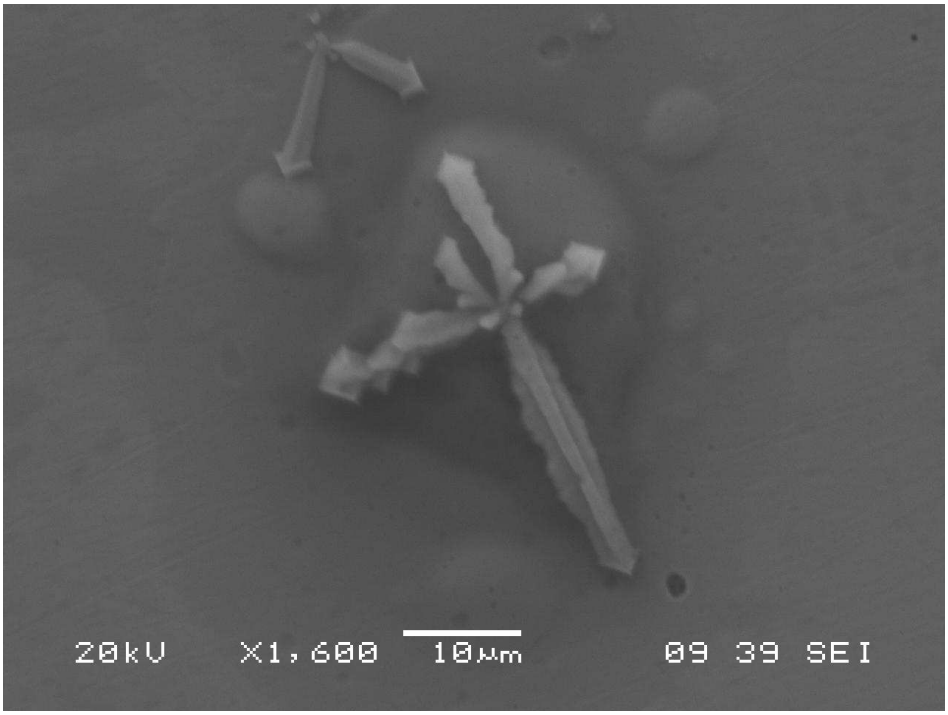

Figure 30: Secondary electron (SEI) view x1600, crystals of halite that grow from a bubble on the surface near the fracture in sample f

2.3 Zwammerdam 6:

2.3.1 Nail ZW6-7 (samples ZW6-7cv, ZW6-7dv, ZW6-7bh, ZW6-7eh, ZW6-7fh and ZW6-7gh)

The first aspect to highlight is the total absence of the P inside the iron alloy. The second important feature is the presence of Mn inside the majority of the inclusions (in 71 of 95 analysed slags) and about1 wt% of P. For the weight percentage of magnesium inside the slag must be make a division: inside the *samples bh*, *eh* and *dv*, this element is totally absent, on the other hand it is relatively abundant (in 15 of 19 analyzed slags) inside the *sample*s *fh*, *gh*. It is necessary to underline that the number inclusions seem to decrease from *samples bh* and *cv* to the *sample gh*. The presence of chlorine, inside most of the specimen of this nail, is particularly abundant inside *samples dv* and *eh*, the two specimens related to the curved section of this spike.

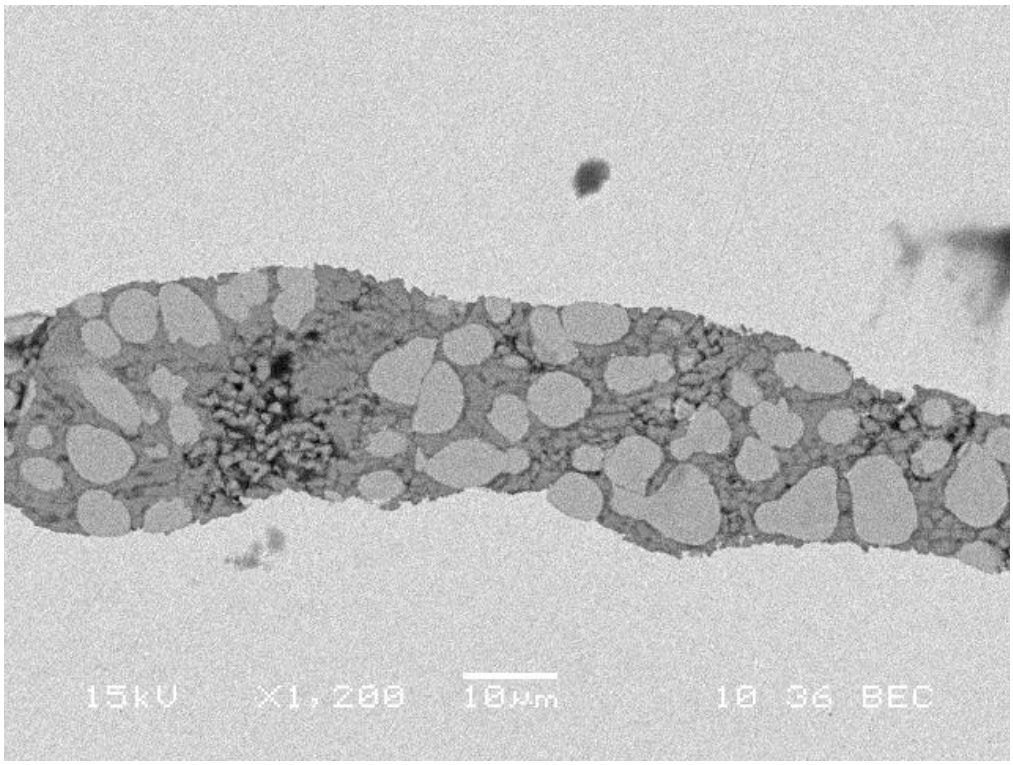

Figure 31: SEM BEC x1200 example of slag with manganese, in the darker areas, taken from sample gh

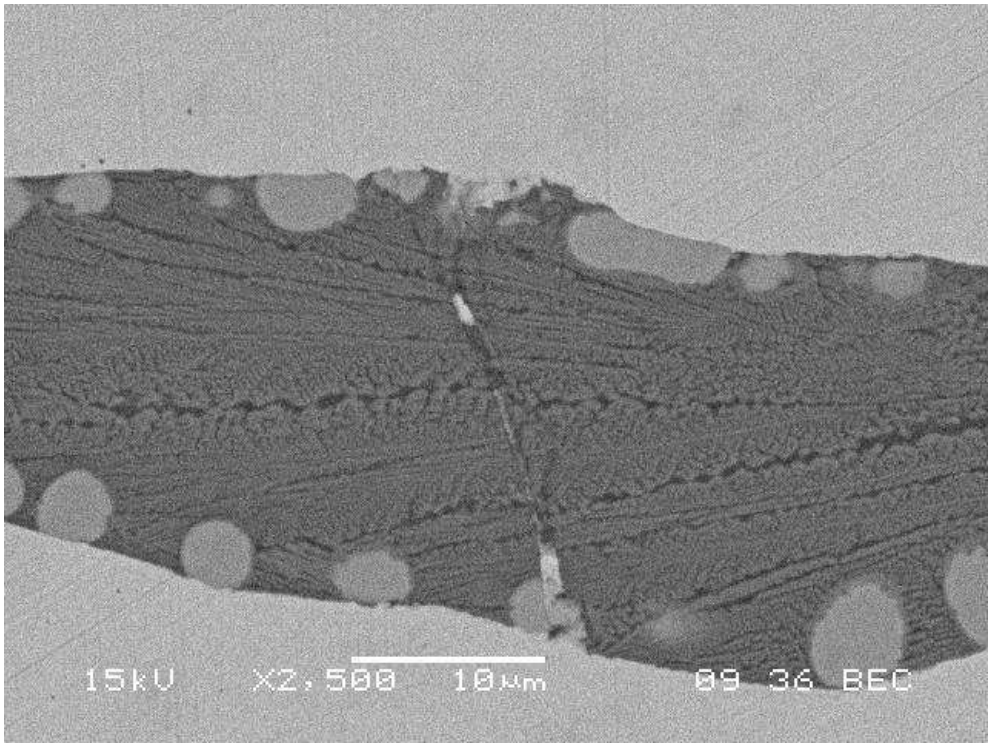

Figure 32: SEM BEC x2500 Example of the particular configuration of the crystal inside the slag inclusion inside sample eh.

2.3.2 Nail ZW6-8 (samples ZW6-8b, ZW6-8e, ZW6-8f and ZW6-8g)

The stem of this nail (*sample b*) is characterized by the presence of hundreds of inclusions, visible also with the naked eye. This sample shows two other important characteristics. The first one is related to the fracture that starts from the lower right side and goes until the lower middle of the sample. The EDS analysis of the non-metallic compounds, that surround the fracture, has shown the presence of only Ca and P, with high level of oxygen (around 30 wt%). This situation changes along the length of the crack. In a first time were detected only this three elements, then approximately in the middle of the length the composition starts to change till arrive, at the end of the fracture, to a composition comparable to a slag inclusion. The composition of the others analyzed inclusion have shown the presence of Si, AL, P, K and Ca.

Concerning the metal alloy composition has to be highlighting the presence of P. This element was particularly detected in the right areas of the *sample b*, nevertheless this

presence disappear below[18] the break. In all the other samples the presence of P is more or less located in the middle of the sample.

2.3.3 Nail ZW6-9 (samples ZW6-9b, ZW6-9f and ZW6-9g)

In first section of the nail (*sample b*) is present a long layer with slag inclusions that runs from the right side to the left one. The composition of these inclusions shows an high percentage of silicon (form 20 to 30 wt%). Inside *sample f* is visible in the right side a fracture. The contours of this break have a composition made of iron oxide [detected only Iron (fe) and Oxygen (O)], with trace of P and Ca (all around 0,5 wt%) and traces, especially in the area nearest to the external environment, of Cl and sodium (Na) (both around 0,5 wt%).

One of the most important aspects related to the tip (*sample g*) is the presence of different areas of corrosion. In particular near the extreme tip on the basis of the composition three different corrosion areas[19] can be distinguished (fig. 33):

1. The first and the greater area is composed mainly of Fe, P and O.
2. The second one, which surrounds the first one, is like an oxidized slag, where the component inside are P, Si, Al and O.
3. The third one which lies between the metal core and the other two layers is composed by Cl and O.

Concerning the metal alloy the presence of P is limited to five areas in *sample*s *f* and *g*, while it is more widespread in the *sample b* (detected in 14/21 of the analyzed areas).

[18] This area is relative the rm zone of the division of the sample (see chapter about technical, instrumentation and analyses).

[19] This zones can be recognized under the microscope by different level of grey and after from the EDS analysis by the elemental composition.

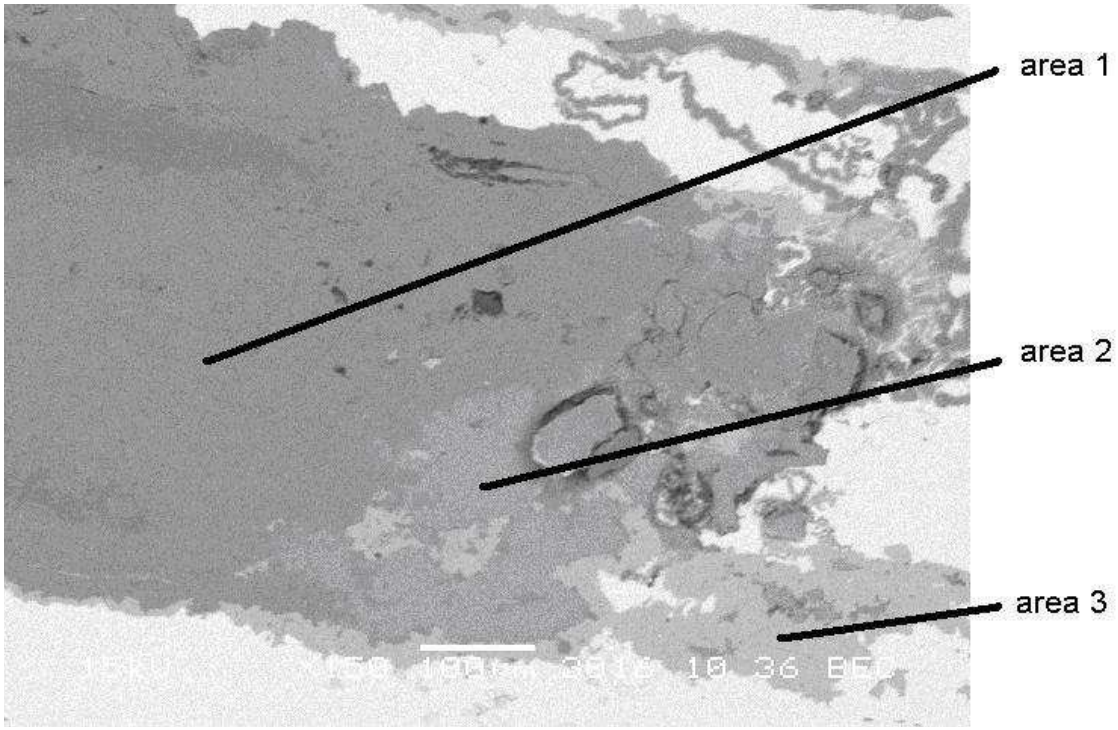

Figure 33: SEM imagine x150 that show the 3 different zones of corrosion

2.3.4 Nail ZW6-10 (samples ZW6-10a, ZW6-10c, ZW6-10f and ZW6-10g)

Sample a represents the nail's head. In this particular specimen there are inclusions with a width around 400 μm and length that arrive to 1 mm or more, which starts in the stem of the nail up to the borders of the head, placed in the left side. On the right side the EDS has identify P inside the metal alloy. This element was also identified in many places along the entire length of the nail, i.e. in *sample c* it is detected in all the external side, inside *sample f* it is detected in the central area of the left and of the right side; in *sample g* it is founded in the central area of the specimen. The elements that the slag inclusions are composed of are Si, Al, P, K, Ca and Mg.

2.3.5 Nail ZW6-13 (samples ZW6-13 b, ZW6-13d, ZW6-13f and ZW6-13g)

The first three samples selected from this nail have a homogeneous structure with few elongated slag inclusions; the amount of the inclusion is in the order of tens. This situation is different in the tip of the nail (*sample g*), where the amount of the inclusions is greater and a layer of them arrive till the edge of the tip (this layer is also visible by

naked eye) on one of the external sides. The composition of these inserts is various. In the first three samples the elements which compose the few inclusions are Si, Al, P, K and Ca. In the tip's area the composition changes; K and Ca are detected less often but in higher amount (around 0,8 wt%). No traces of P were detected inside the metal.

2.4 Woerden 7:

2.4.1 Nail W7-8 (samples W7-8b, W7-8d and W7-8e)

The *sample b* shows at a macroscopic observation slag inclusions visible by naked eye; the inclusions have a length around 1,5 mm and a width of 500 μm. This huge dimension allows, in most of the cases, the formation of two or three different phases that can be easily distinguished under the microscope. The *sample d*, on the contrary, is characterized by a homogeneous structure, with a lower amount of inclusions; the number of these inclusions is in the order of tens. Two of the slags, located in the right side (the nearest to the specimen b) have the same characteristics of the slags present in the *sample b*. The tip of the nail (*sample e*), has a homogeneous structure; with a low amount of inclusions, the number of this inclusions is in the order of tens. The slags have a similar composition, 9one to each other, from the head to the tip. The detected elements are: Si, Al, P, K, Ca, Mg and Mn. Concerning the presence of P inside the alloy, it is detected only inside *sample b* and in *sample e*.

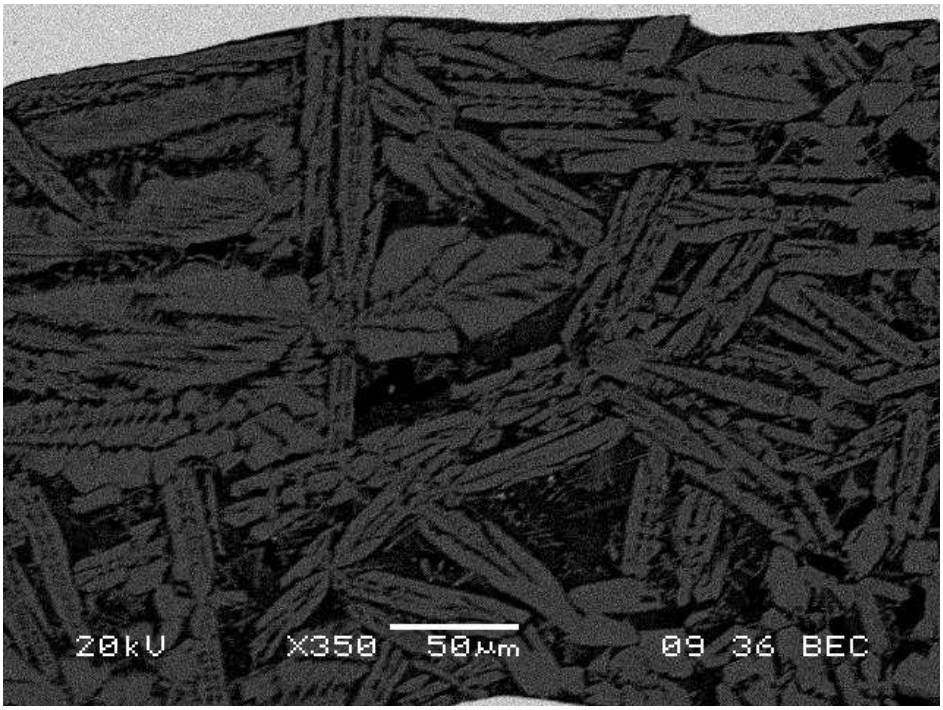

Figure 34: detail x350 of the structure visible in the slag of the sample b

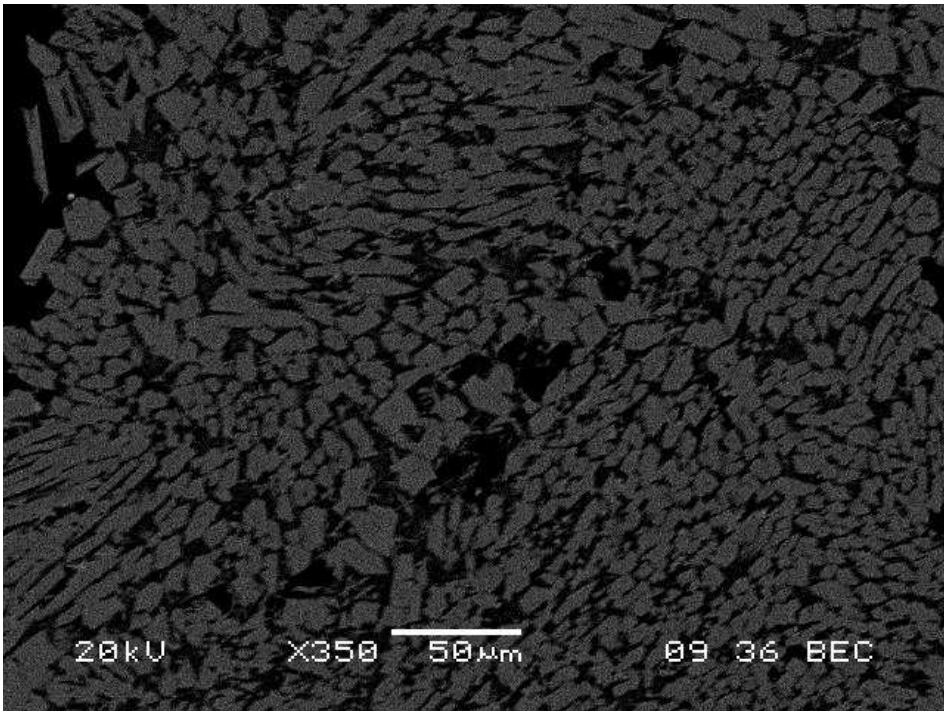

Figure 35: detail x350 of the second structure visible in the slag of sample b

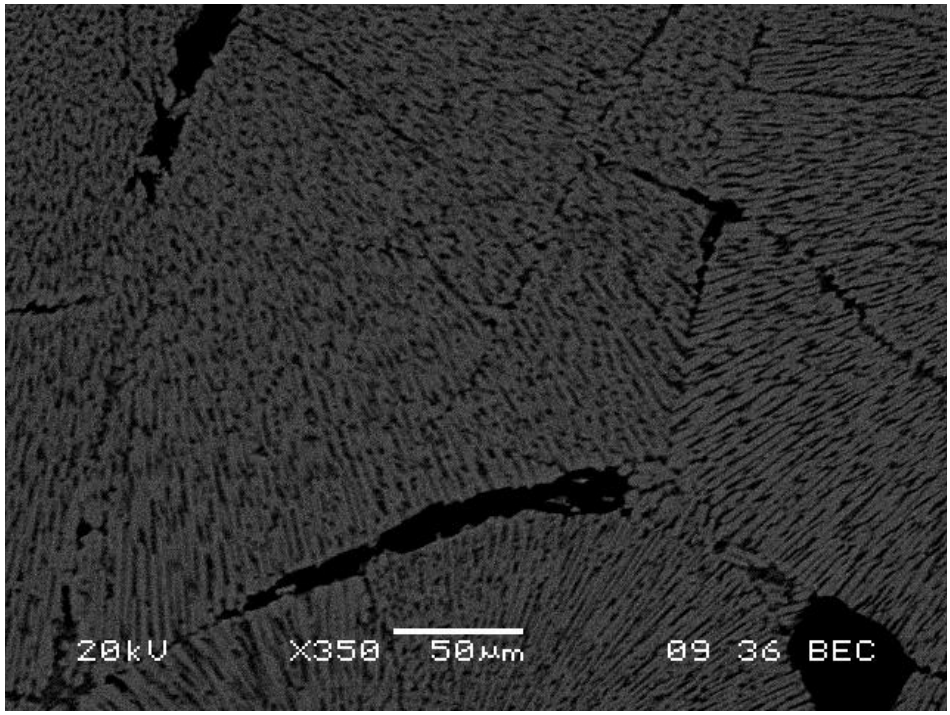

Figure 36: detail x350 of the third structure visible in the slag of sample b

3 VICKERS'S HARDNESS TEST:

This section presents the results obtained from the hardness tests. For a better presentation the data will be presented in a simplified scheme where is clearly show where the tests are performed and the values obtained. All the pictures represent the selected samples; divided by lines that represent the cutting process.

3.1 ZWAMMERDAM 2

3.1.1 Nail ZW2-2 (samples ZW2-2a, ZW2-2c, ZW2-2d and ZW2-2g)

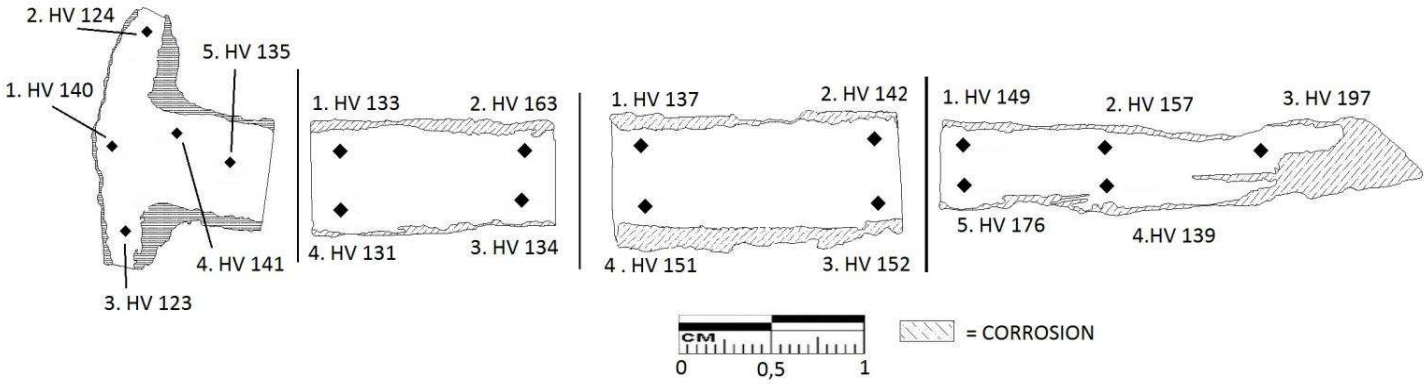

Figure 97: nail Zwamerdam2-2 with the indication of the performed hardness tests

As can be seen in the figure above (fig. 37) different zone of hardness are present in the entire length of the nail, with a general increase of the hardness from the head (*sample a*) till the tip (*sample f*), where the hardness have a value of HV 197. In the head of the nails (*sample a*), the values of the hardness are inside a range, which have a maximum of HV 140 in the central area, and minimum value of HV 123, which characterize the external part of the nail's head. The average value of the hardness in this nail is around HV 149.

3.1.2 Nail ZW2-3 (samples ZW2-3d and ZW2-3e)

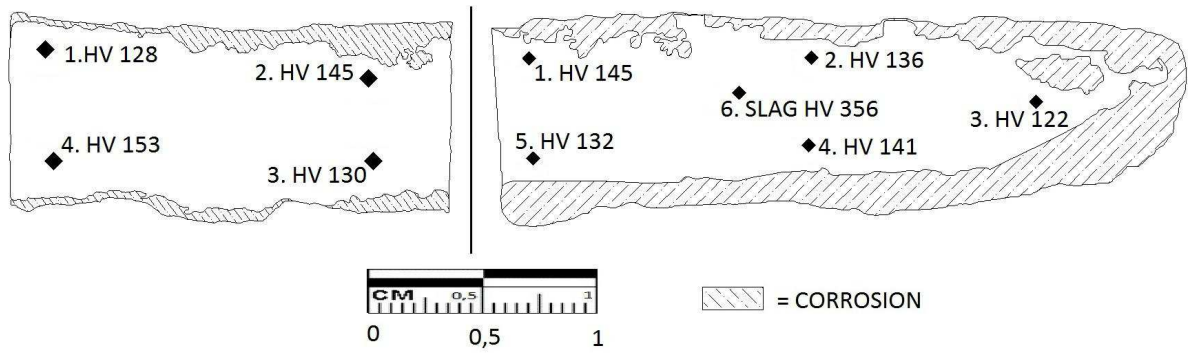

Figure 108: nail Zwammerdam2-3 with the indication of the performed hardness tests

The two selected samples show an average hardness of HV 137, with no particular increasing of hardness along the stem till the tip. In the *sample e* the test was performed also inside a slag inclusion, which resulted in a high value of hardness HV 356, about three times the hardness of the metal.

3.1.3 Nail ZW2-GE2K (samples ZW2-GE2Kb, ZW2-GE2Ke, and ZW2-GE2Kf)

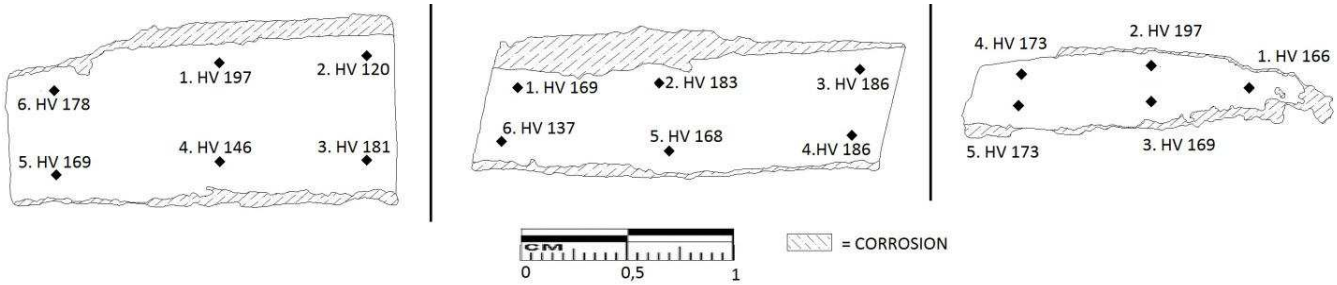

Figure 119: nail Zwammerdam 2-GE2K with the indication of the performed hardness tests

The average hardness of this nail is around HV 161. Along the length of the stem areas with different hardness were found increasing from the upper part of the stem (*sample b*) till the tip (*sample f)*. In fact inside the tip (*sample f*) the highest value of the hardness was registered, for this specific nail, HV 197.

3.1.4 Nail ZW2-GE2R (samples ZW2-GE2b, ZW2-GE2Rd, ZW2-GE2Re and ZW2-GE2Rg)

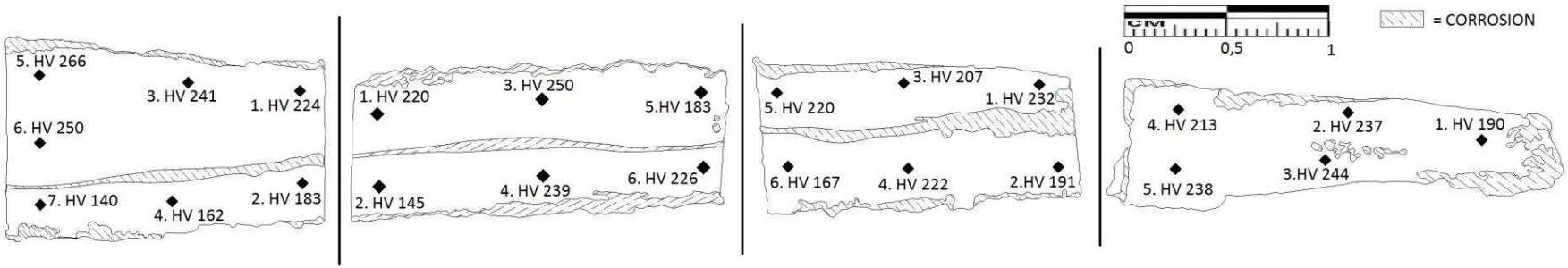

Figure 40: nail Zwammerdam2-GE2R with the indication of the performed hardness tests, the samples from the left to the right are the b, d, e and g

The nail ZW2-GE2R, as can be clearly understood by the figure above, has high hardness values along the length of the stem. The average is around HV 212, with zones where the registered value is HV 266. In the first sections of the stem (*sample*s *b* and *d*) there is a difference in hardness inside the two external sides of the samples. One area is located below the corrosion line that runs all over the length of the nails, and the other one above it. This difference in hardness slowly decreases till the right side of the *sample e* where the corrosion line and difference in hardness ends. The tip of the nail (*sample g*) does not present values that are higher compared to that of rest of the nail.

3.1.5 Nail ZW2-GG2K (sample ZWGG2Kb, ZW2-GG2Kd, ZW2-GG2Ke and ZW2-GG2Kg)

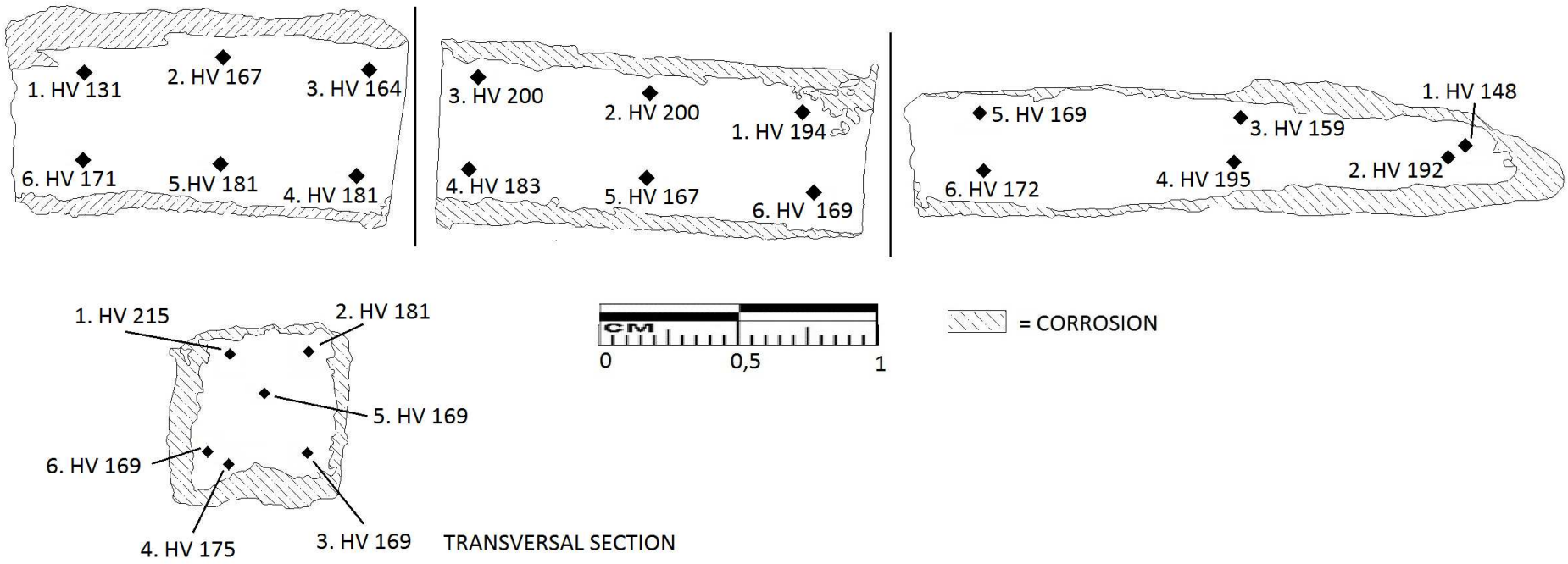

Figure 12: nail Zwammerdam2-GG2R with the indication of the performed hardness tests, the square section is the transversal one

As can be seen in figure 41, *sample e* allows the investigation of the hardness not only along the length of the stem, but also in the transversal section. This section clearly shows that the majority of the stem's areas have a similar hardness (in the transversal direction). Along the length of the stem different values of the hardness were measured, with an average value around HV 177. The hardness value of the tip (*sample g*) is not higher than the rest of the nail.

3.1.6 Nail ZW2-GG2R (sample ZWGG2Rb, ZW2-GG2Rd, ZW2-GG2Re and ZW2-GG2Rg)

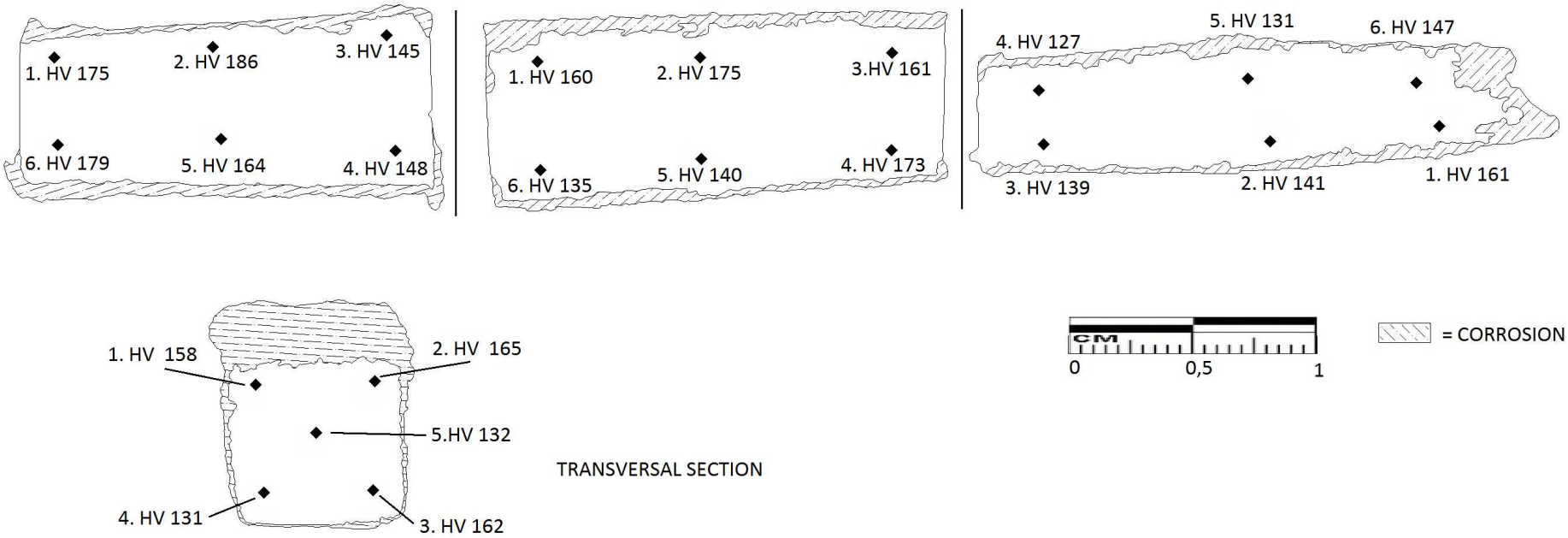

Figure 42: nail Zwammerdam2-GG2K with the indication of the performed hardness test, the square section is the transversal one.

The *sample d* is taken from the transversal section of the stem and allows the investigation the hardness also in this direction. The values of the hardness are very different. The values are inside a range, with a minimum of HV 127 and maximum of HV 186. The average is around HV 155. In the tip (*sample g*) the values are comparable to the other sections of the nail.

3.2 Zwammerdam 4:

3.2.1 Nail ZW4-6 (samples ZW4-6c, ZW4-6f and ZW4-6 g)

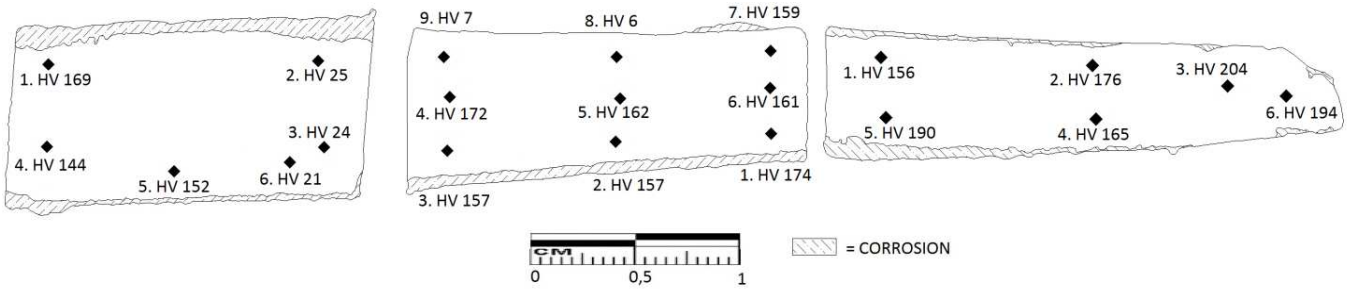

Figure 13: nail Zwammerdam4-6 with the indication of the performed hardness test

The hardness of this nail is increasing along the length of the stem, till a maximum value of HV 204 in the tip (*sample g*). The hardness increases from the upper part of the stem (*sample c*) till the tip (*sample g*). The average of the hardness in the nail is around HV 168, and the average of the tip is around HV 180.

3.2.2 Nail ZW4-7 (sample ZW4-7 b, ZW4-7c, ZW4-7f and ZW4-7h)

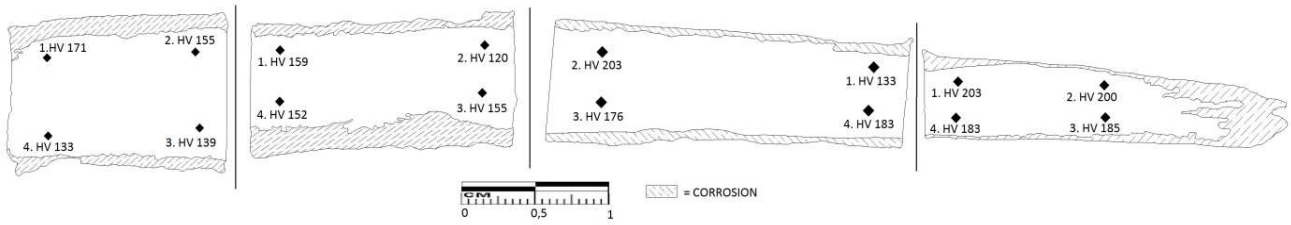

Figure 44: nail Zwammerdam4-7 with the indication of the performed hardness test

Inside this nail zones with various values of the hardness are present. This disparity in the values makes it difficult to evaluate the average hardness, which results around HV 165. However an increasing hardness from the upper part of the stem (*sample b*) to the tip (*sample h*) was measured. The tip of the nail (*sample g)* has high values of hardness, with an average value around HV 192, and a maximum of HV 203.

3.3 Zwammerdam 6:

3.3.1 Nail ZW6-7 (sample ZW6-7cv, ZW6-7dv, ZW6-7bh, ZW6-7eh, ZW6-7fh and ZW6-7gh)

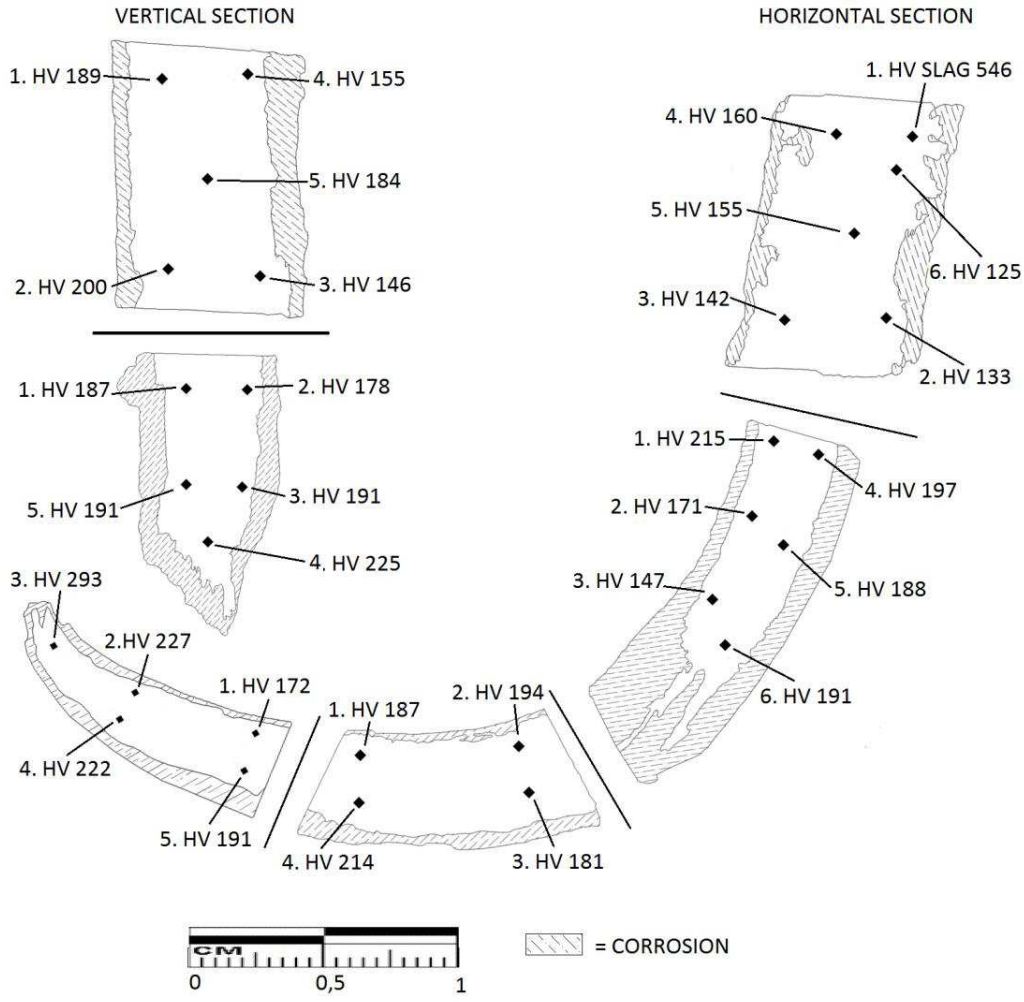

Figure 14: nail Zwammerdam6-7 with the indication of the performed hardness test

This nail is divided in two sections. The vertical section is related only to the stem until the curve, which characterizes the lower part of the nail. The horizontal section takes into account the entire length of the nail including the bending. As it is clearly shown in figure 45 a lot of different areas with different hardness are present, nevertheless a general increase of the hardness from the upper part of the stem (*samples cv* and *bh*) to the tip

(*sample gh*) was measured and the maximum value for this nail is HV 293. The average hardness for the entire nail is around HV 185. In this nail also a slag inclusion was analyzed, which proofed to be extremely hard compared to the metal alloy, with a value of HV 546.

3.3.2 Nail ZW6-8 (samples ZW6-8b, ZW6-8e, ZW6-8f and ZW6-8g)

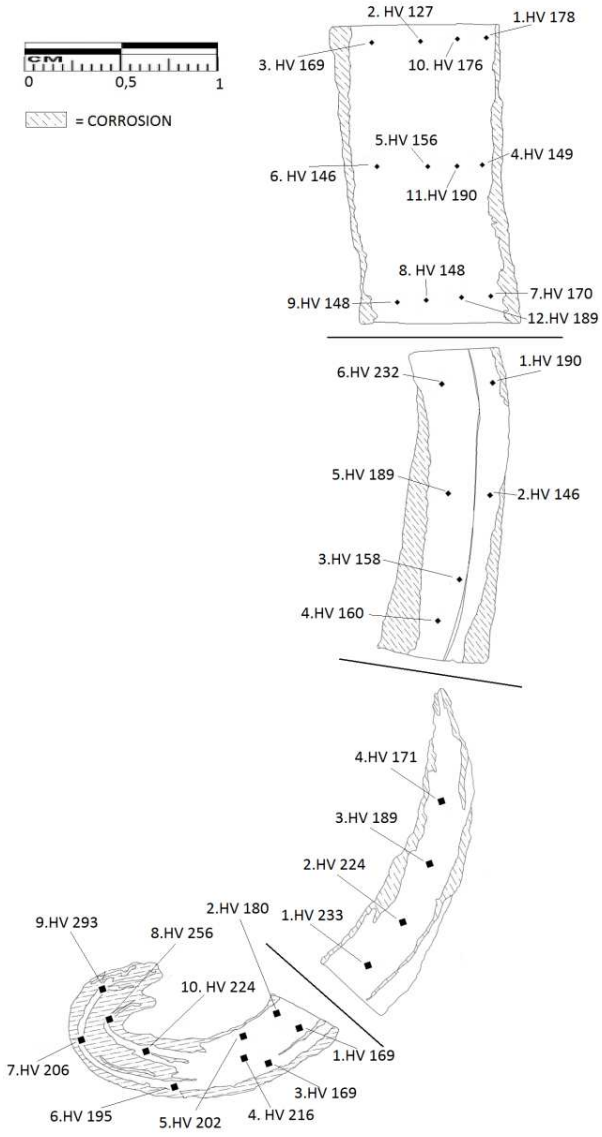

Figure 15: nail Zwammerdam6-8 with the indication of the performed hardness test

Various zones with different hardness in the upper part of the stem (*sample b*) were measured. Near the curve (*sample e*) the hardness decrease to HV 146. This decreasing effect finishes after the bending (*sample f*) where the hardness increases till the tip of the nail (*sample g*) where a maximum value of HV 293 was measured, with an average value, for this section, around HV 210. The average value for the entire nail, including the bend part, is around HV 185.

2.3.3 Nail ZW6-9 (sample ZW6-9b, ZW6-9f and ZW6-9g)

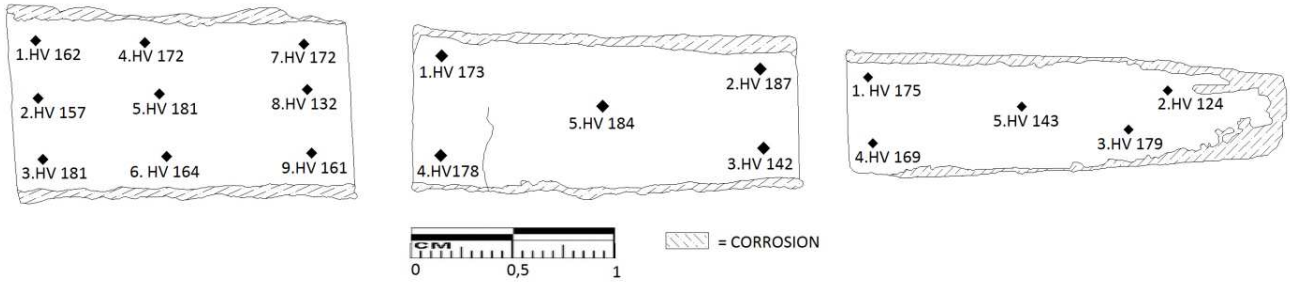

Figure 166: nail Zwammerdam6-9 with the indication of the performed hardness test

Due to the disparity in the measured values in this nail, was difficult to determine the trend along the entire length of the stem. The values registered in the tip (*sample g*) have a maximum of HV 179. On the other hand inside the stem (*sample f*) a maximum value of HV 187 was registered. The average value for the entire nail is around HV 165.

3.3.4 Nail ZW6-10 (sample ZW6-10a, ZW6-10c, ZW6-10f and ZW6-10g)

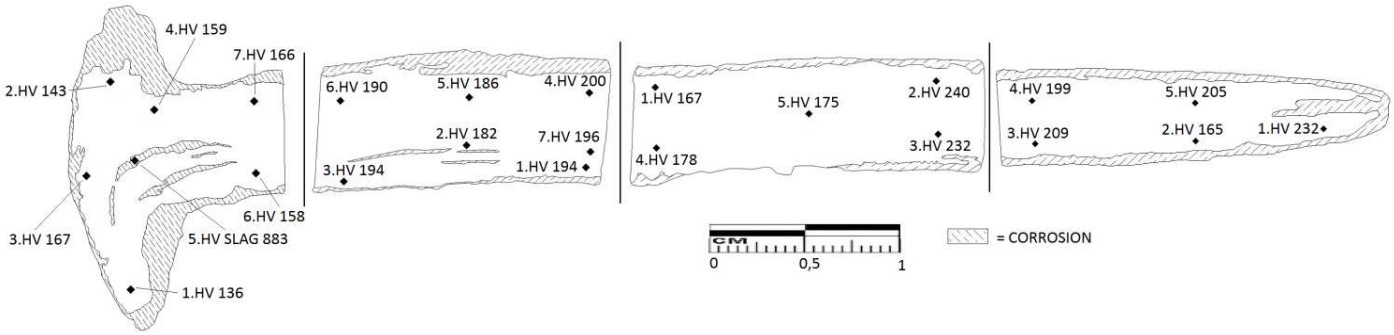

Figure 47: nail Zwammerdam6-10 with the indication of the performed hardness test

In the head of the nail (*sample a*) different values of hardness was registered, with a maximum of HV 167. The specimens selected to represent the stem (*samples c* and *f*) shows values of hardness between HV 167 up till HV 240, inside the tip (*sample g*) the values registered are lower, with a maximum of HV 205. The average hardness for the entire nail is around HV 212.

3.3.5 Nail ZW6-13 (samples ZW6-13 b, ZW6-13d, ZW6-13f and ZW6-13g)

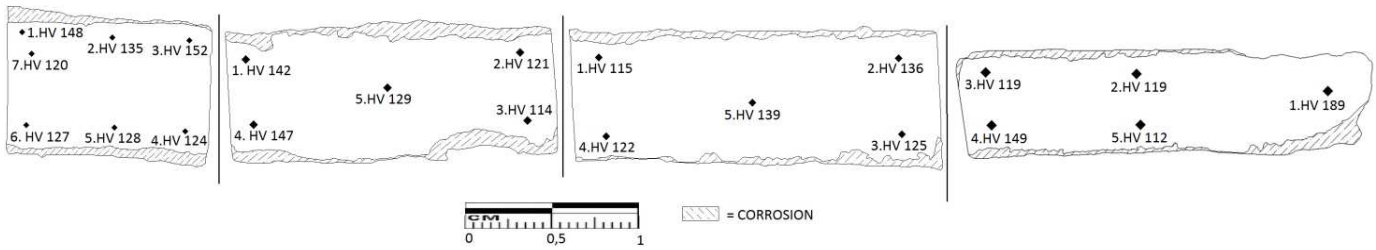

Figure 48: nail Zwammerdam6-13 with the indication of the performed hardness test

In first section of the stem (*sample b*) there is a difference between the two external sides. In the upper part the values around HV 150 in the lower one the values are around HV 126. A similar situation is present inside the second section of the stem (*sample d*) where in the left side values greater than the ones on the right side were registered. Despite these differences, the general value of the hardness along the entire stem is not so high; in fact the majority of the collected values are around HV 125. This also accounts for that of the tip (*sample g*), but the value collected from the very last area of the tip is HV 189. The average hardness is around HV 129.

3.4 Woerden 7:

3.4.1 Nail W7-8 (samples W7-8b, W7-8d and W7-8e)

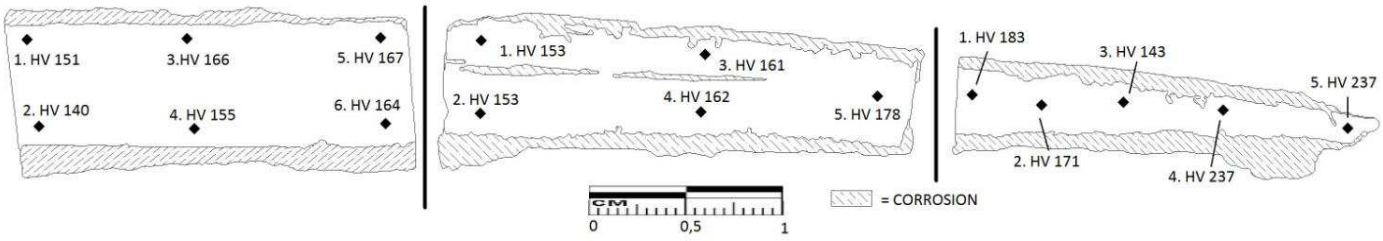

Figure 17: nail Woerden7-8 with the indication of the performed hardness test

Along the entire nail from the stem to the tip there is an increase of the hardness. The analyses have given a value of HV 237 inside the tip of the nail, and the average value of

the other section of the nail is HV 160. Along the nail there are areas with a different hardness, with values inside a range with a minimum value of HV 140 up to a maximum of HV 178.

4 LASER ABLATION – INDUCTIVELY COUPLED PLASMA – MASS SPECTROMETRY RESULTS:

The results obtained from the Laser Ablation-Inductively Coupled Plasma-Mass Spectrometry (LA-ICP-MS) are plotted in a table with the average values of all the analyzed elements. In this case, for a complete understanding of the value and of their meaning, some annotations are required.

The first note is about the multiple averaging of the data. To obtain these values a calibration with the standard glass N610 was done. This calibration affects also the measurements of the samples because it is on the base of this standard that the instrument evaluates the weight percentage in part per million (ppm) of the selected elements.

The standards glass N610 contains a standardized weight percentage quantity of all the elements that can be detected by the mass spectrometer. The second note is about the preliminary processing to obtain the raw data. The software requires the weight percentage value, transformed in ppm, of a known element to make a second calibration of the data. Therfore, it was decided to insert the weight percentage of silicon as a reference. The average value of the silicon inside the slag inclusion taken from the energy dispersive X-ray spectroscopy (EDS) system was given to the software was,. To have a precise and better evaluation of these data it is necessary to perform other tests, with the same instrument on more samples and on more reference ones to have a bigger amount of data useful for the comparison. For a better evaluation of the obtained data a comparison with other elemental analyses, like the electron probe micro analyzer (EPMA) or the ion beam technique could be useful.. It is better to perform the tests without using so many averaging, i.e. using the precise weight percentage value instead of the average one. One important reference for this research is the study made by dr. Thomas Birch of the St. Andrews University. In his work is analyzed, with this technique, the iron production in the northern Europe and in particular in Denmark. It is also on the basis of him work that the elements to analyze were outlined.

The complete series of analyzed elements is:

Mg26, Si29, P31, Ca43, Ca44, Sc45, Ti47, V51, Cr52, Mn55, Co59, Zn67, As75, Rb85, Sr88, Y89, Zr90, Nb93, Mo95, Sb121, Cs133, Ba137, La139, Ce140, Pr141, Nd146, Sm147, Sm149, Sm152, Eu151, Eu153, Gd157, Tb159, Dy161, Dy163, Ho165, Er167, Tm169, Yb172, Lu175, Hf178, Ta181, W182, W183, Pb208, Th232, U238. In table 1 not all the analyzed elements are listed, some of them, i.e. cobalt and arsenic, due to their siderophile nature have not been used for the matching of the trace elements inside the slag inclusion.

The number of analyzed slag inclusions used to evaluate the average quantity of trace elementsvaries from ship to ship. This fact is due to number of the inclusions suitable for the test, because inside the metal numerous slags[20] are presents but, in majority of the cases, the shape of these inclusions made the performing of the test, with the chosen settings impossible. The selected spot size, 60 μm,was larger than the height of most of the inclusions but when the spot size would be decreased further, it would probably has affected the results since theT data that could be obtained were related to a volume comparable to a single crystal of the inclusion. In that case, the data obtained in that way could not represent the entire composition of the slag inclusion

Inside the nails of the ships Zwammerdam 2, 4 and 6 respectively 7, 8 and 12 slag inclusions were analyzed, in Woerden 7 16 slag inclusions and in the reference sample of Heeten only 5 inclusions were analyzed. This amount of inclusions is the result of the exclusion of the unsuitable ones. The factors used to discriminate the suitable inclusions to the unsuitable ones are directly linked to the chromatogram given by the instrument after the test. From this chromatogram the different sections analyzed during the ablation with the laser were distinguished Therefore is it possible to understand if the instrument was analyzing the slag inclusion or the metal alloy. Subsequently, it was decided which measurements were suited to provenance the iron alloy.

[20] The amount of inclusion present inside the analyzed sample is in the order of hundreds, as seen in the results chapter.

ppm	Sc 45	V 51	Cr 52	Rb 85	Sr 88	Y 89	Zr 90	Nb 93	Cs 133	La 139	Ce 140	Pr 141	Nd 146
ZW2	47,8 ±3,3	247,3 ±17,5	236,7 ±18,5	106,4 ±7,0	136,0 ±8,3	418,8 ±31,0	253,2 ±18,7	12,9 ±0,9	17,9 ±1,7	189,6 ±16,6	372,0 ±32,3	54,0 ±4,4	245,1 ±21,2
ZW4	6,1 ±0,5	30,9 ±1,7	37,8 ±2,6	45,9 ±2,3	195,8 ±12,2	15,4 ±1,2	225,7 ±17,9	7,1 ±0,5	1,0 ±0,1	15,7 ±1,2	32,6 ±2,5	3,7 ±0,4	14,8 ±1,2
ZW6	10,9 ±1,4	103,4 ±11,4	61,2 ±6,9	52,0 ±3,6	113,2 ±8,6	194,1 ±18,7	100,9 ±10,8	6,5 ±0,6	3,6 ±0,4	78,7 ±8,6	96,4 ±11,7	17,0 ±1,7	74,2 ±7,7
W7	10,3 ±0,7	127,0 ±8,9	152,0 ±11,3	65,0 ±4,6	89,0 ±6,3	39,0 ±3,1	126,0 ±10,3	6,9 ±0,6	8,6 ±0,6	26,7 ±2,4	47,1 ±4,5	6,7 ±0,6	28,1 ±2,6
Heeten	2,2 ±0,4	23,4 ±3,7	13,6 ±1,6	17,4 ±2,1	40,6 ±2,9	6,4 ±0,9	28,7 ±5,2	1,3 ±0,2	0,8 ±0,1	5,1 ±1,1	10,6 ±2,2	1,3 ±0,3	5,1 ±1,2

ppm	Sm 147	Eu 151	Gd 157	Tb 159	Dy 161	Ho 165	Er 167	Tm 169	Yb 172	Lu 175	Hf 178	Ta 181	W 182
ZW2	59,0 ±4,6	13,5 ±1,1	65,3 ±4,9	9,2 ±0,6	60,4 ±4,3	11,7 ±0,9	33,8 ±2,5	4,3 ±0,3	26,4 ±1,9	3,7 ±0,3	6,6 ±0,5	0,8 ±0,1	0,6 ±0,1
ZW4	2,7 ±0,3	0,5 ±0,1	2,5 ±0,3	0,3 ±0,06	2,5 ±0,2	0,5 ±0,05	1,6 ±0,2	0,2 ±0,03	1,6 ±0,1	0,2 ±0,04	6,6 ±0,4	0,5 ±0,04	0,3 ±0,1
ZW6	15,0 ±1,7	3,4 ±0,5	17,7 ±1,9	2,5 ±0,3	17,7 ±1,8	4,1 ±0,4	13,0 ±1,6	1,7 ±0,1	11,5 ±1,2	1,7 ±0,2	2,4 ±0,4	0,3 ±0,05	1,2 ±0,1
W7	6,3 ±0,6	1,4 ±0,1	6,2 ±0,6	0,9 ±0,1	5,8 ±0,5	1,1 ±0,1	3,3 ±0,3	0,4 ±0,1	3,0 ±0,2	0,4 ±0,04	3,3 ±0,3	0,4 ±0,05	2,9 ±0,2
Heeten	1,0 ±0,3	0,4 ±0,1	1,3 ±0,3	0,2 ±0,04	1,2 ±0,2	0,2 ±0,03	0,6 ±0,1	0,1 ±0,02	0,6 ±0,1	0,1 ±0,02	0,9 ±0,2	0,1 ±0,03	0,7 ±0,2

ppm	Pb 208	Th 232	U 238
ZW2	1,1 ±0,1	15,4 ±1,1	31,4 ±2,2
ZW4	0,2 ±0,04	4,6 ±0,2	1,5 ±0,1
ZW6	0,2 ±0,05	5,9 ±0,5	28,0 ±3,2
W7	16,7 ±1,2	5,1 ±0,4	11,2 ±0,8
Heeten	0,7 ±0,03	1,4 ±0,2	4,2 ±0,5

Table 1: Average values of the elements inside the analyzed slag inclusions. The averaging is made on different amount of slag inclusion. This is due to the quality of the signal and the presence of suitable inclusion inside the metal. The slags were respectively 8 for the Zwammerdam 2 and 4 ships, 12 for the ship Zwammerdam 6, 16 for the Woerden 7 ship and 5 for the samples of Heeten.

ANALYTICAL RESULTS:

In this section will be described the analytical results obtained from the instruments. The result will be dived in sections on the basis of the techniques and on the samples. The data obtained will be presented already with an order and some averaging, all the further discussion and comment about the interpretation and the management of this information will be discussed in the next chapter. As it was done in the previous chapter the presentation of the results will start with the most general feature (optical microscopy) go on till the most detailed one (LA-ICP-MS).

1 OPTICAL MICROSCOPY (OM)

In this section the will be introduced the main characteristics of the metallographic investigation. For a better selection of the images all the references to the grain size are related to the ASTM number, which is a standardized value that represents a range of grains dimension. This value has been created and normalized by American Society for Testing and Materials, which is an international association that provides standards for the industrial and technical field. In the figure 1 is shown the monograph for the grain size, estimated on the basis of the Hilliard's method. In the figure below is also possible to notice that lower is the dimension of the grain, higher is the value of the ASTM number.

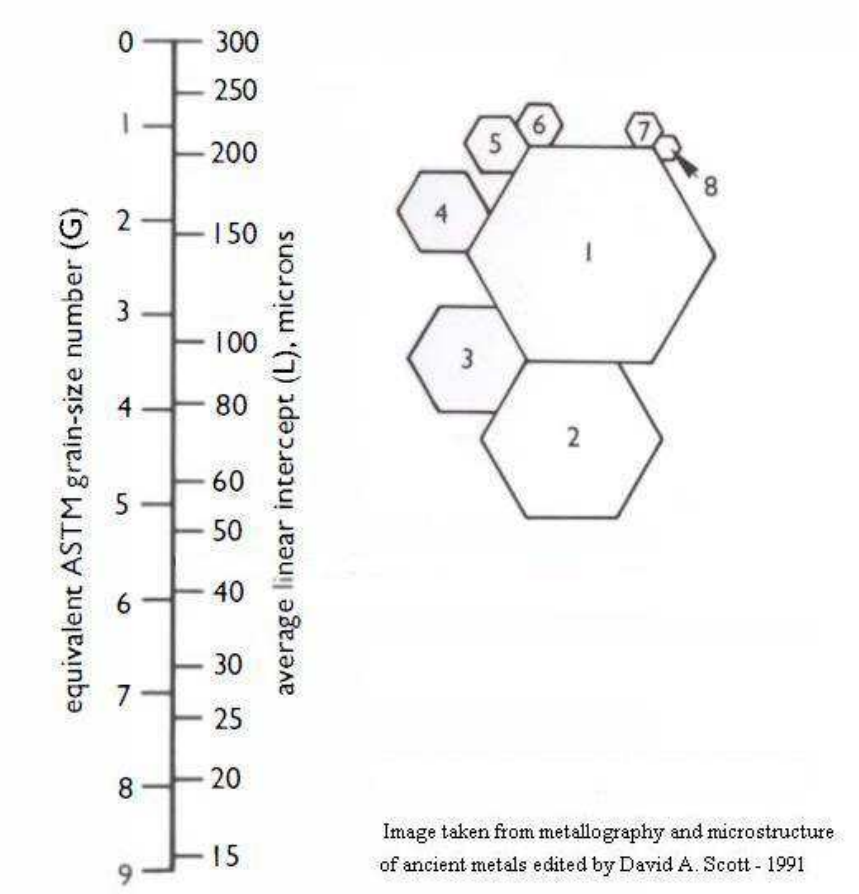

Figure 1: monograph for the grain size, estimated on the basis of the Hilliard's method- photo taken form David A. Scott -1991

1.1 ZWAMMERDAM 2:

1.1.1 Nail ZW2-2 (samples ZW2-2a, ZW2-2c, ZW2-2d and ZW2-2g)

The selected samples consists of the head of the nail (*sample a*), the stem part (*samples c* and *d*) and the tip (*sample g*). This selection allows the investigation of the changes in the texture of the metal over the entire length of the nail. What was observed is a difference in the size and in the arrangement of the metal's grains. In the head were identified areas with different grain sizes, i.e. in the inner area of the head, grains with a size between 3 and 5 (fig.2) are found. On the sides the grain size decreases until 8 (fig 3) and in some cases, i.e. inter-granular crystals, it can decrease till 9. The situation along the stem is characterised by a relatively homogeneous grain size around 4 or 5 (fig 4). In some particular areas are present small grains with a size around 7-8. The situation is quite different in the tip. In fact there are three different layers, two in the external sides where the grains size is around 8 and one in the central core, where the grains remain with size around 4 or 5, like in the stem (fig. 5).

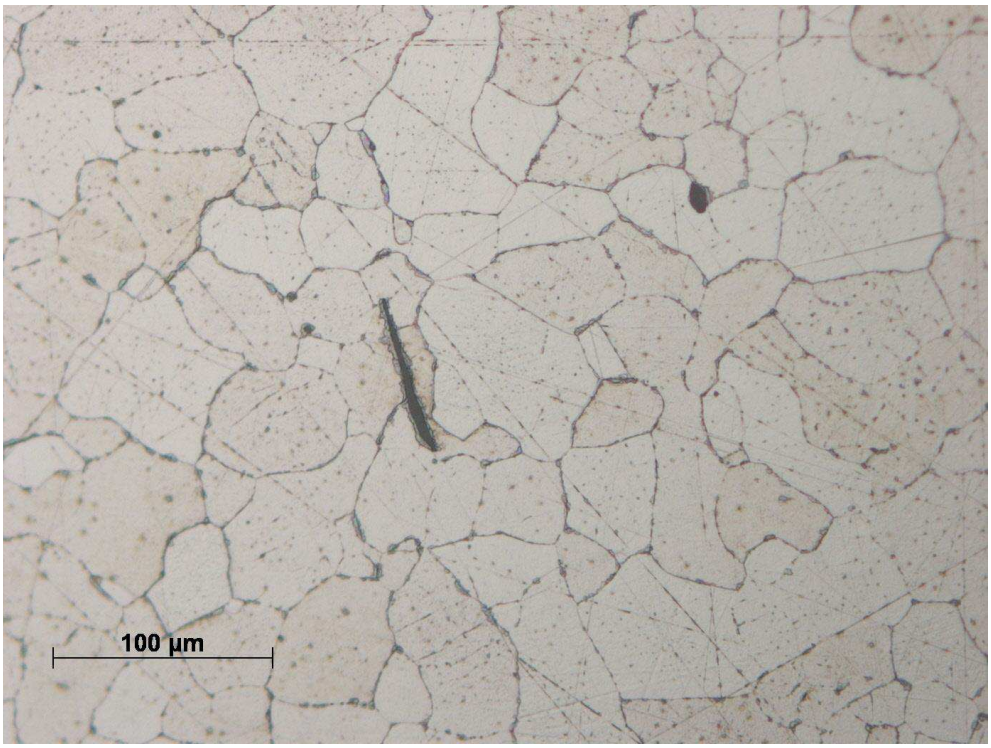

Figure 2: Sample ZW2-2a x200 difference of the grain sizes in the head of the nail.

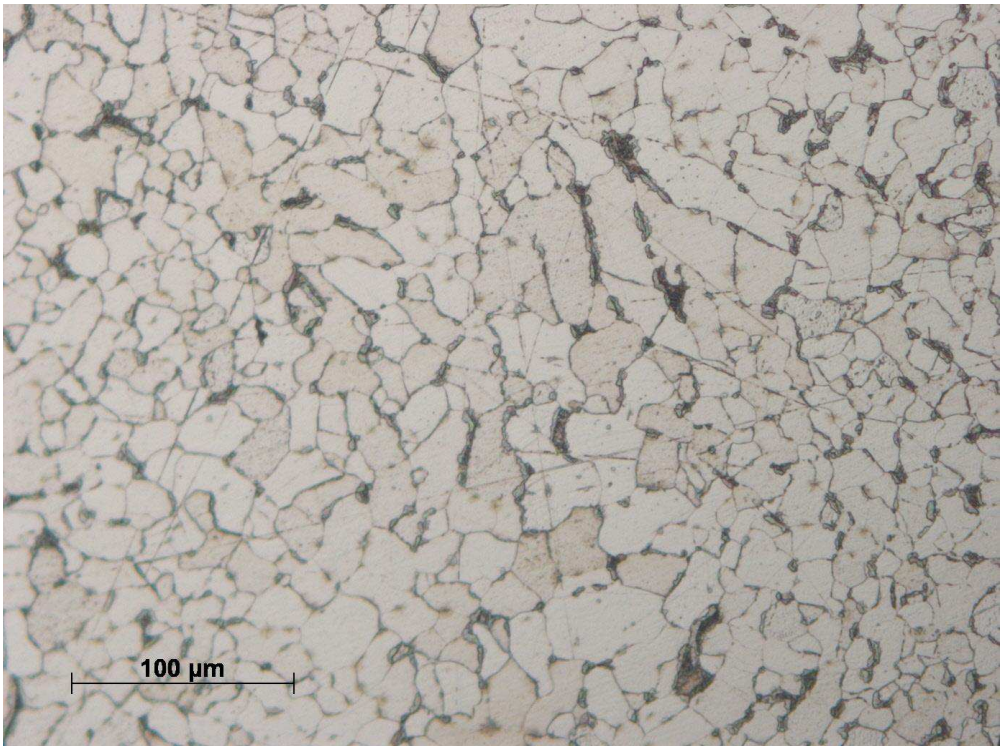

Figure 3: Sample ZW2-2a x200 right side with grain size around 8

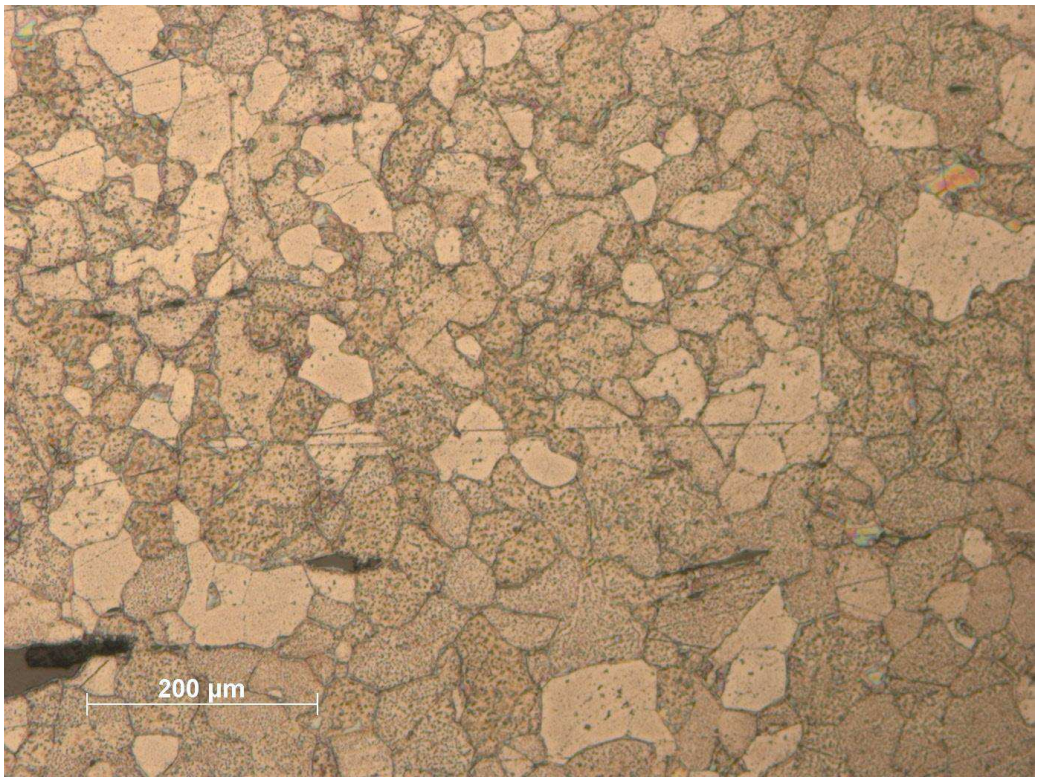

Figure 4: Sample ZW2-2d x100 grain structure of the stem

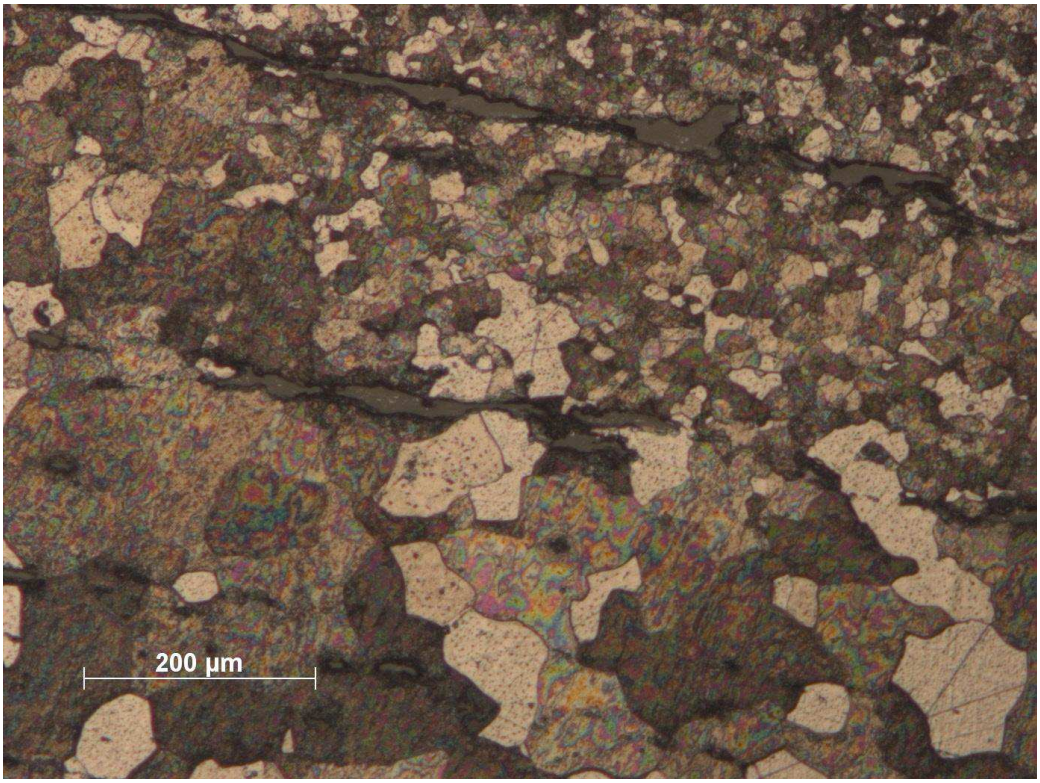

Figure 5: Sample ZW2-2g different grain size zone between the centre and the external area. The internal area is the one with big grains, the external one (in the upper part of the image) have little grains. The rainbow effect is an undesired effects created during the etching process.

1.1.2 Nail ZW2-3 (samples ZW2-3d and ZW2-3e)

The stem of this nail (*sample d*) is characterized by a homogeneous grain size. The ASTM number is around 4. A particular situation is visible in the left side of this sample. It is possible to see grains of the same size but with an elongated and flattened shape in stead of the normal crystal structure. In the tip the situation observed is different, because are present grains with a size around 3 and inside the space between these big grains were grown small grains with a size around 7. The amount of these grains is greater in the two external sides of the tip.

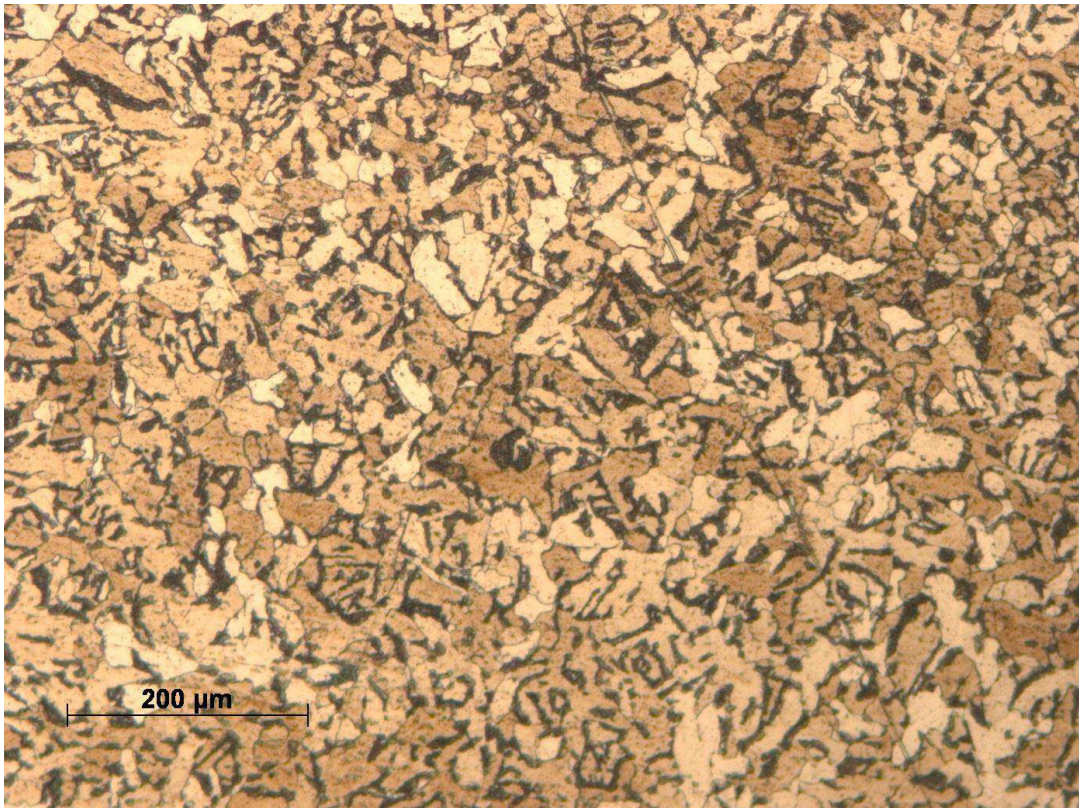

Figure 6: Sample ZW2-3d x100 elongated grains

1.1.3 Nail ZW2-GE2K (samples ZW2-GE2Kb, ZW2-GE2Ke, and ZW2-GE2Kf)

The upper part of the stem is characterized by the presence of big grains with a size around 2. At a certain point (*sample b*) can be appreciate a radical change in the grains size that goes from 2 down until 6-7 (fig 7). This situation starts in the very first section of the stem and last until the tip of the nail. From the upper part of the stem to the tip are also clearly visible areas in which it is possible to recognize the presence of the phosphorus inside the metal, the presence of this element = inside the metal is evident by a shadow or watery effect over the metal's grains. This particular effect is well describe in literature by E.G. Godfrey, 2007 (fig. 7). The figure 8 exemplifies a particular effect due to the cold working of the object: the twinning of the grains. The twinning is the structure rearrangement in a metal artefact subjected to the combined effect of cold working and re-crystallization. Twinning induces the formation of typical features evidenced by parallel-sided forms within a grain.

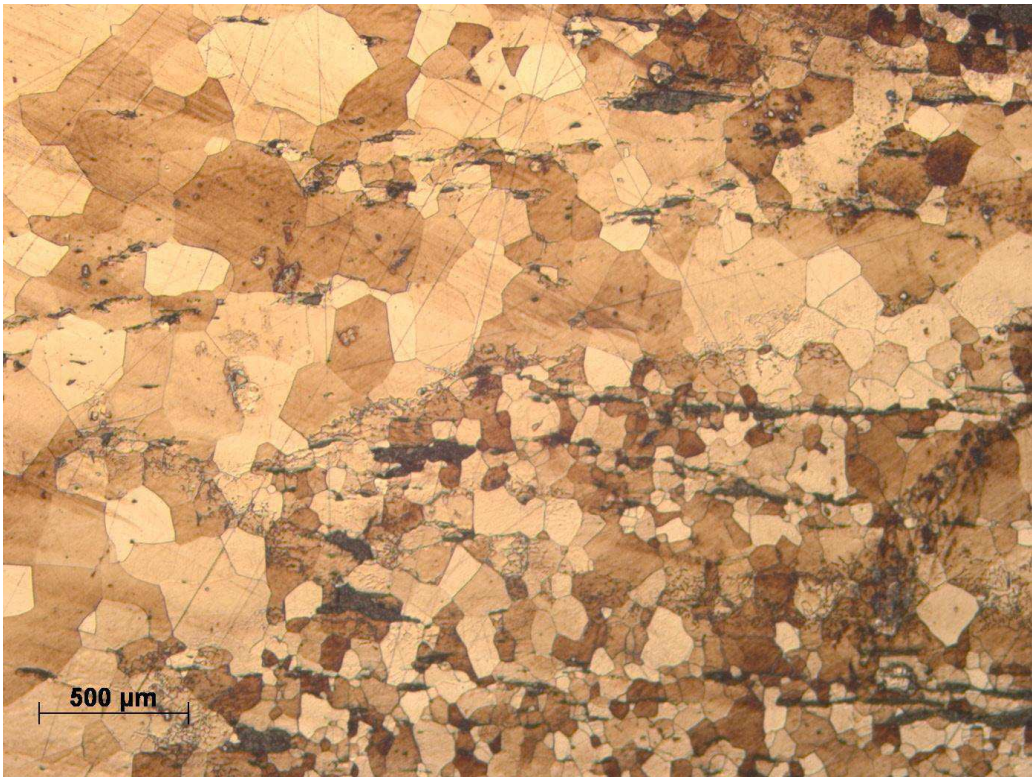

Figure 7: Sample ZW2-GE2Kbx25 division site in the grain size

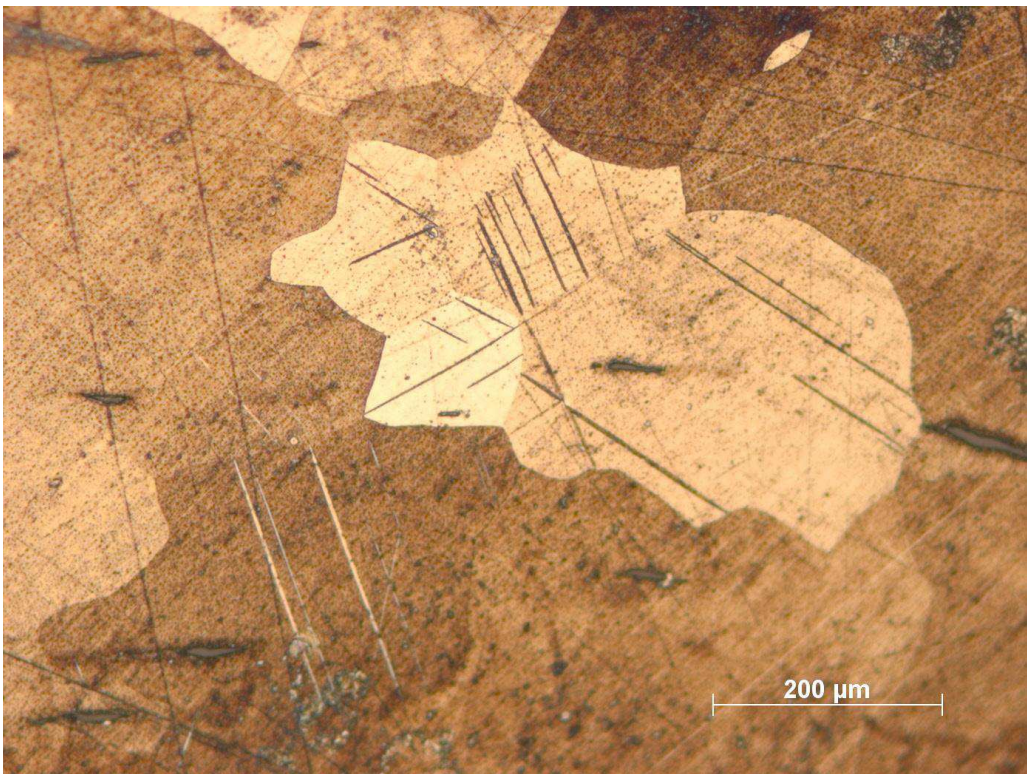

Figure 8: Sample ZW2-GE2Kb x100 twinned grains

1.1.4 Nail ZW2-GE2R (samples ZW2-GE2b, ZW2-GE2Rd, ZW2-GE2Re and ZW2-GE2Rg)

The first sample selected from this nail is characterized by the clearly presence of the phosphorus shadow effect spread all over the surface. The grain size is variable and can go from dimension of 1-2 to 6-7 in some particular areas. *Sample d* presents a variable structure with different layers and features. In the macro[1] photograph (fig. 8) are clearly visible four different layers and again the Phosphorus shadow effect. In one of the external sides was registered the presence of a combination structure of ferrite, the lighter grains, and probably pearlite, the darker areas. This layered aspect lasts also in the structure of the tip.

[1] In this context with the word macro means an enlargement of x25 in which it is possible to have an overview of the layered structures of the different specimen.

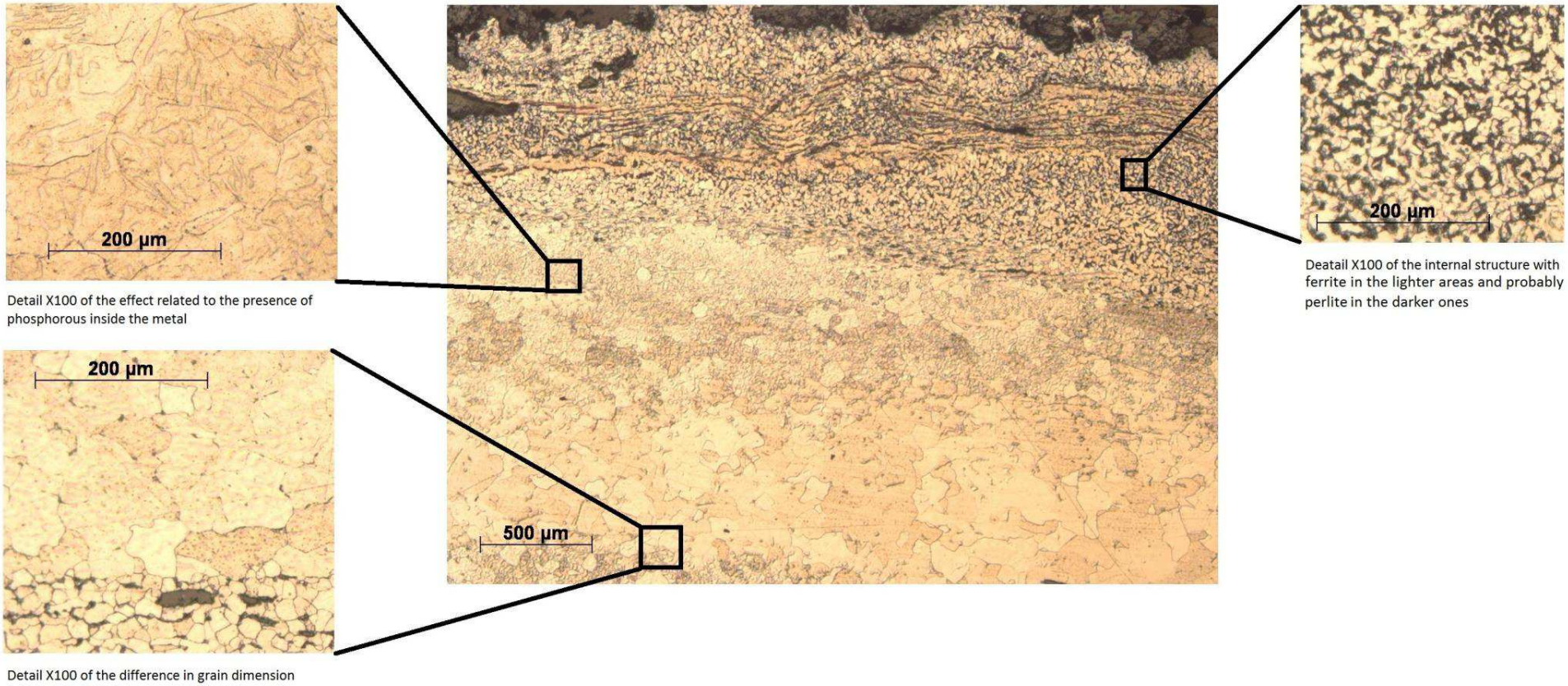

Figure 9: Sample ZW2-GE2Rd macro x25 with details of the different layers. The detail images are not directly related to the position show in the image.

1.1.5 Nail ZW2-GG2K (sample ZWGG2Kb, ZW2-GG2Kd, ZW2-GG2Ke and ZW2-GG2Kg)

The upper part of the stem (*sample b*) shows a layered structure. Inside the layers a structure with two different arrangements is visible. The first layer is situated in the one of the external sides of the specimen, is characterized by the presence of small grains with a size around 7(fig. 10). The other layer has grains with a greater size, between 3 and 4. This situation disappears along the length of the nail, in tip's direction. It is possible to notice that the grains size inside the *sample d* is quite homogeneous and is maintained around 3-4, with few variations, till the tip (*sample g*).In this last specimen is possible to appreciate a decreasing of size from around 3 to around 6, along the length of the tip itself.

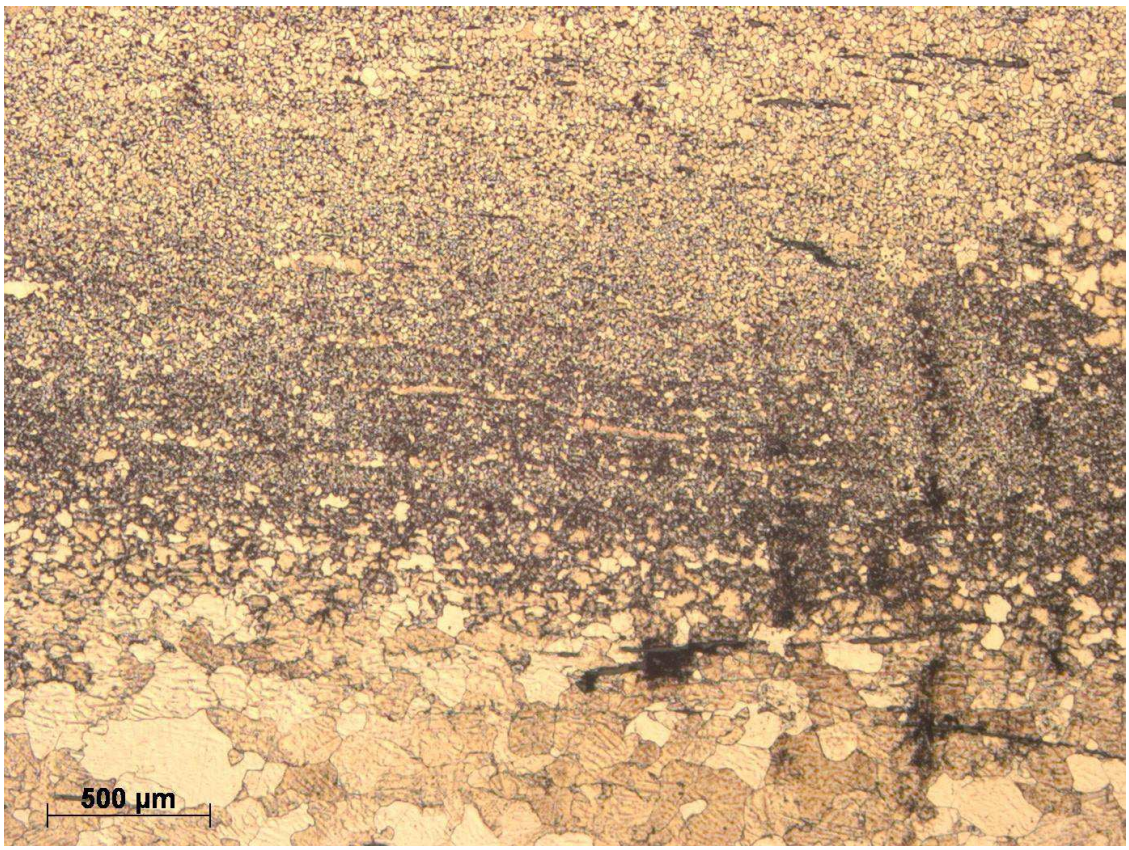

Figure 10: Sample ZW2-GG2Kb Macro x25 layers division; in the lower part of the image there is the inner part of the nail with greater grain size, in the upper one the external side with the smaller grains.

1.1.6 Nail ZW2-GG2R (sample ZWGG2Rb, ZW2-GG2Rd, ZW2-GG2Re and ZW2-GG2Rg)

Along the entire length of this nail, the presence of numerous layers is recognised. These layers have different features and grain size, as is clearly shown in the macro image below (fig. 11). These layers have a grain size that can be really dissimilar one to the other. In some areas there are big hexagonal grains (size around 4), in others areas an arrangement prevalently made by small grains is visible (size around 7). The last areas have an appearance that shows grains of ferrite surrounded by darker areas probably constituted by pearlite. In figure 12 the needle structure, that is possible to distinguish, is a Widmanstätten ferrite, the darker areas probably form pearlite (fig. 12), but in this case is not possible a precise distinction only with the use of an optical microscope.

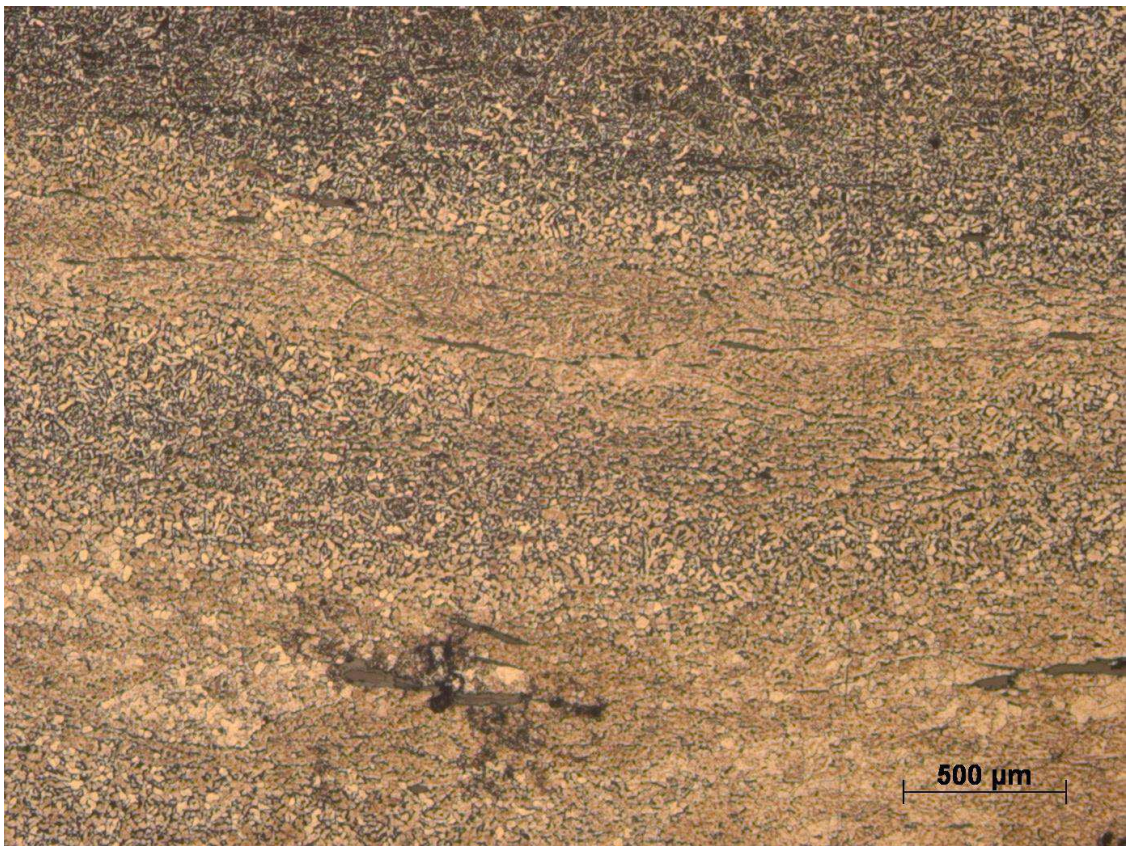

Figure 11: Sample ZW2-GG2Rb macro x25 of the layered structure.

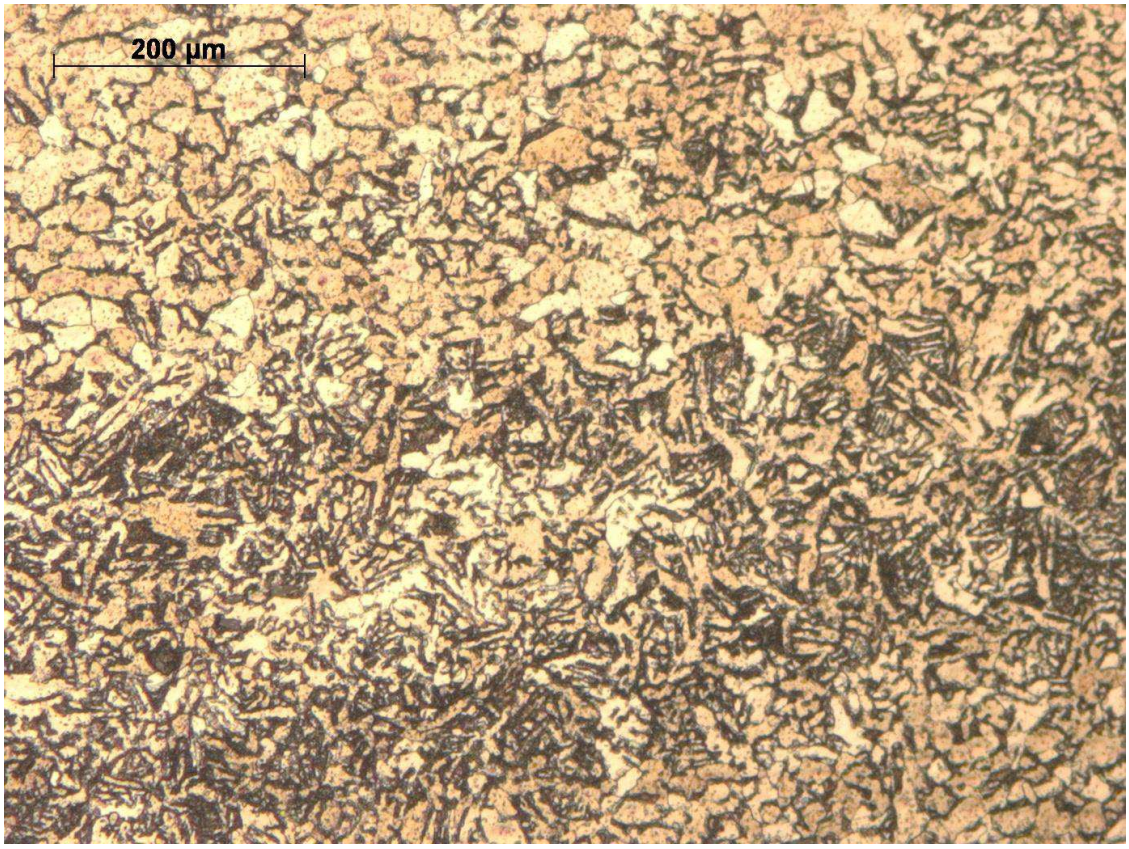

Figure 12: Sample ZW2-GG2Re x100 detail of the division between two layers, the lower one is characterized by a Widmanstätten appearance of the ferrite.

1.2 Zwammerdam 4:

1.2.1 Nail ZW4-6 (sample ZW4-6c, ZW4-6f and ZW4-6 g)

This nail shows a layered structure that starts in *sample c* and goes on till *sample f*. This arrangement is divided into approximately three areas. The first one, which belongs to one external side, has a fine grain structure (size around 7). The second one, located in the central region of the nail, has large grains (size between 2 and 3). The last one, which belongs to the other external side, has a complex structure, with secondary ferrite, with a pattern like the Widmanstätten one, surrounded by darker areas that can be formed probably by pearlite (fig 13), but with the only use of the optical microscopy is not possible to precisely divide the three structures. The tip (*sample g*) shows a different pattern, which is not characterized by different layers, but by a decrease in grain dimensions till the extreme tip, where the grain size is around 7.

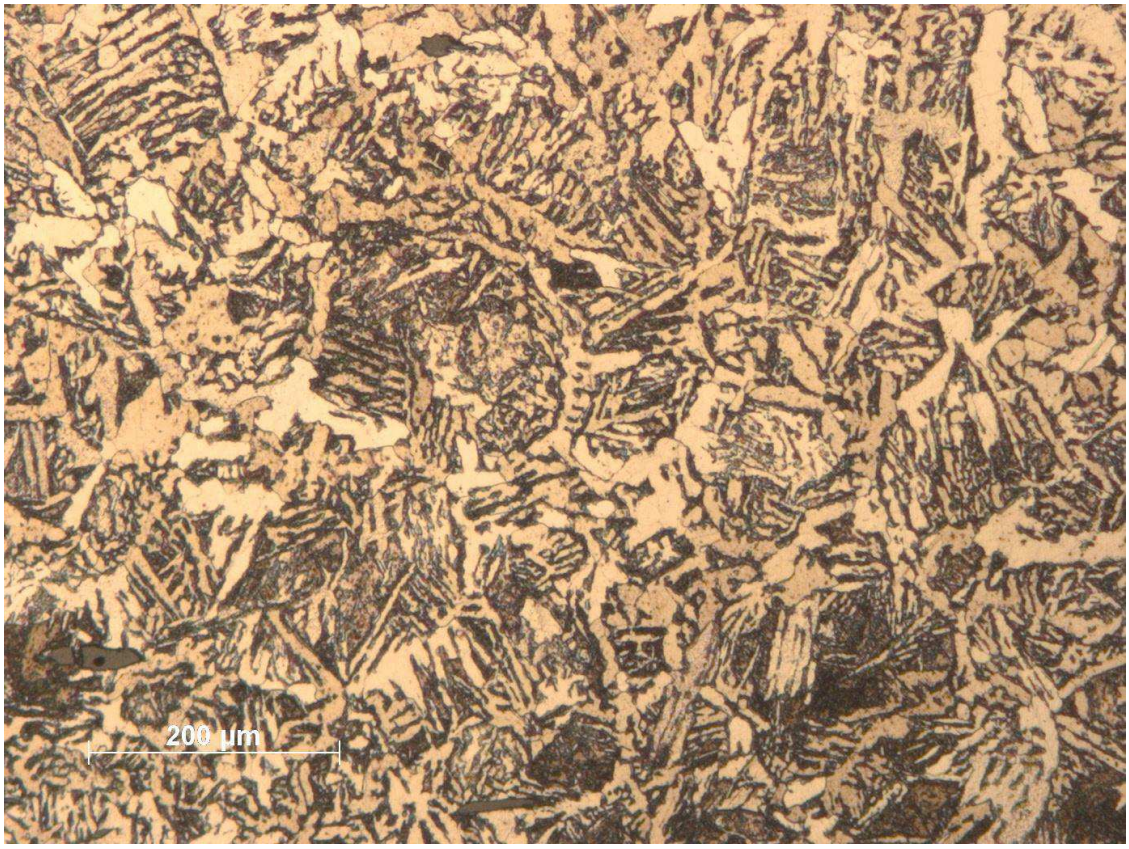

Figure 13: Sample ZW4-6c x100 secondary ferrite structures

1.2.2 Nail ZW4-7 (sample ZW4-7 b, ZW4-7c, ZW4-7f and ZW4-7h)

The *samples b* and *c*, taken from the upper part of the stem show a layered pattern. The layer's configuration is complex with a no clear division between one to the other. One of the two external sides is characterized by the presence mixed structure of secondary ferrite or acicular secondary cementite; the other one has a different arrangement with small grains (size around 6). In the central part of the samples is present a dark layer surrounded by two stratums of acicular ferrite with a structure similar the Widmanstätten pattern.

Sample f has a different arrangement. The acicular ferrite strata are not present anymore; the grains size is increased (around 5) and the presence of phosphorus watery effect can be clearly seen. These features continue in the tip (*sample h*) but here a clear division line can be noticed between the layers where is present or not the phosphorus. The grain size in the tip is between 6 and 7.

1.3 Zwammerdam 6:

1.3.1 Nail ZW6-7 (sample ZW6-7cv, ZW6-7dv, ZW6-7bh, ZW6-7eh, ZW6-7fh and ZW6-7gh)

The main characteristic of this nail is the small dimension of the grains. All over the nails from the upper part till the tip the grain size is around 7, in the curved section of the nail (*samples eh*, *fh*. and *gh*) the grain size decreases further till arrive around 9. This situation is particularly clear in the right section of the *sample fh*, where is possible to notice the formation of these small grains between the grain boundaries (fig 14). Along the entire length of the nail can be detected the presence of phosphorus layers; this situation is particularly visible in *sample dv* (fig. 15). In particular areas of the *samples cv*, *dv* and *bh* can be registered the presence of a acicular ferrite, surrounded by pearlite.

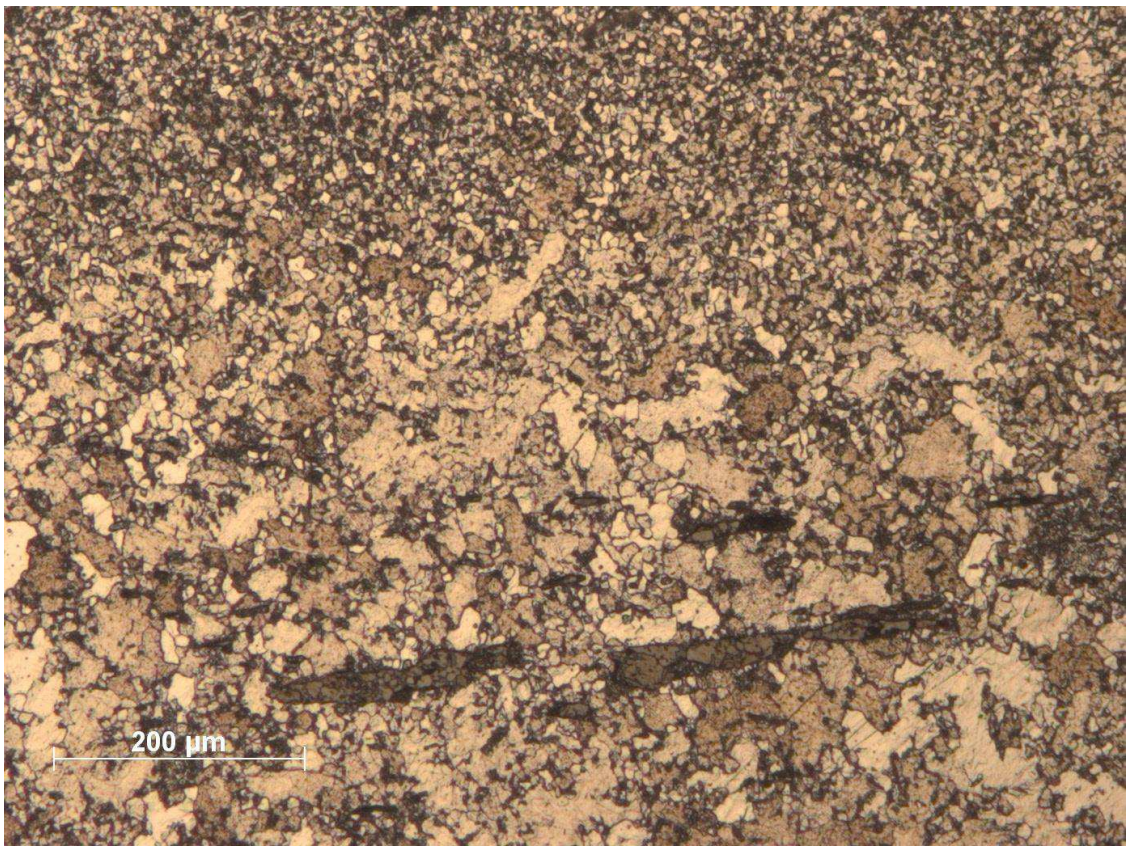

Figure 14: Sample ZW6-7eh detail of the small grains that surround the bigger ones

Figure 15: Sample ZW6-7dv phosphorus layer

1.3.2 Nail ZW6-8 (samples ZW6-8b, ZW6-8e, ZW6-8f and ZW6-8g)

The central part of the *samples b* and *e* is characterized by a stratum with a grain size around 1; furthermore these grains shown slip lines (fig 16). This central core is surrounded by a complex structure of many layers with different features; the division line is very clear and is indicated by the phosphorus effect. In combination with this situation the grain size decreases till 5. Inside *sample f* the central stratum with big grains disappears, but are still visible areas with the phosphorus effect, areas without it and areas in which the grains have an elongated shape. In the left side of this sample areas with the presence of a low grade of acicular ferrite are recognized. Except for the presence of these last areas, this situation is practically the same also in the *sample g*; the grains size in these two samples is between 7 and 8.

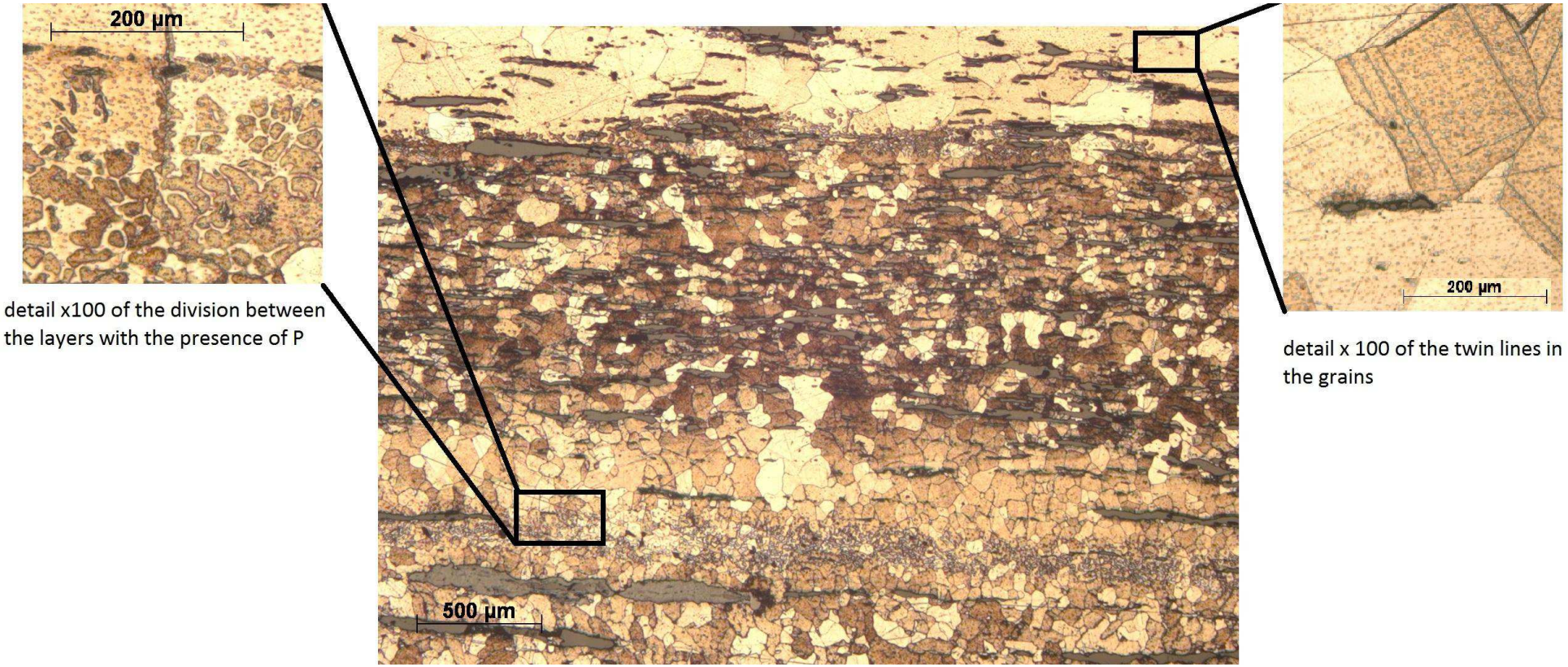

Figure 16: Sample ZW6-8b macro x25 with details of the different layers. The detail images are not directly related to the position show in the image.

1.3.3 Nail ZW6-9 (sample ZW6-9b, ZW6-9f and ZW6-9g

This nail has shows a homogeneous structure with only some layer in which can appreciate a change in the grain size. The central stratum of *samples b* and *f* is a layer with a grain size around 7. Going from this central area to the external side were recognized three other different layers, two with quite big grains with size around 5, dived by a thin layer again with small grains with a size around 7. The situation in practically the same also in the tip (*sample g*), the only difference is the thickness of the central layer, which is approximately 300 µm thicker than in the others samples (fig 17).

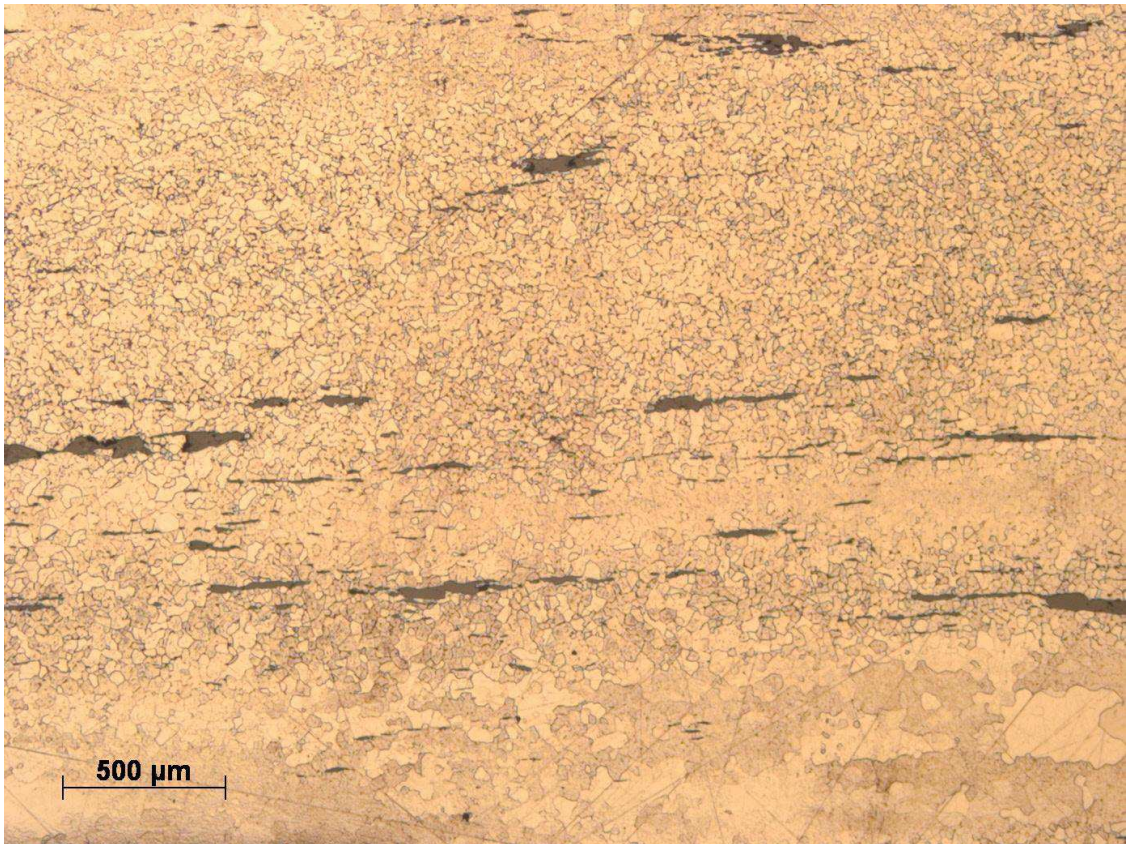

Figure 17: Sample ZW6-9g macro x25 of the layer distribution

1.3.4 Nail ZW6-10 (sample ZW6-10a, ZW6-10c, ZW6-10f and ZW6-10g)

In the selected samples is present the head of the nail itself, which shows high percentage of phosphorus and a layer with different grains size. The size of these grains starts with a value the around 6, in the external zone, value that arrive around 4 in the central area. The grains of this latter are characterized by the presence of slip lines and a wide spread phosphorus effect. In the stem (*samples c* and *f*) is still visible the widespread presence of

phosphorus effect, but differently from the head the grains size remains more homogeneous without great fluctuation or layering, and it is around 4 in the inner part and around 6-7 in the sides. A similar situation is found inside the tip.

1.3.5 Nail ZW6-13 (samples ZW6-13 b, ZW6-13d, ZW6-13f and ZW6-13g)

The grain arrangement inside the first three specimens of this nail does not show many variations, the grains maintain approximately the same size (between 3 and 4) till the tip, where, a layer with grains size around 7 is clearly visible. In many cases were observed grains characterized by split a line, the amount of the grains with this feature is in the order of tens.

1.4 Woerden 7:

1.4.1 Nail W7-8 (samples W7-8b, W7-8d and W7-8e)

In *sample b* can be easily recognized the presence of phosphorus, a situation that completely disappears inside the other two samples selected from this nail. In all the samples are visible layers with different grain size. The dimension of these grains is between1-2 inside the central layer, and decrease till 6-7 in correspondence of the external sides of the sample. Inside the tip (*sample g*) were recognized 5 layers in the right side (fig 18), that along the length come together into a single layer which is the one that characterizes the extreme tip. In fig 19 is visible the size of the grains inside this layer[2], which is around 7.

[2] This layer is the one formed by the union of the precedent 5 different layers.

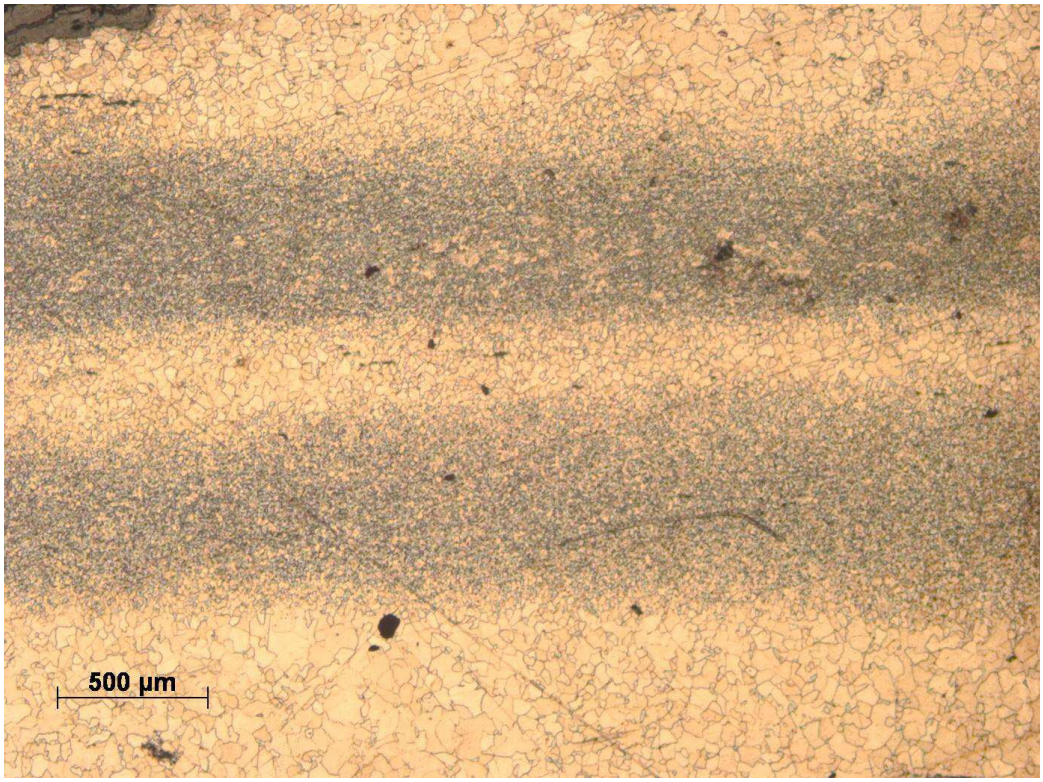

Figure 18: Sample W7-8g macro x25 different layers of the crystal structure

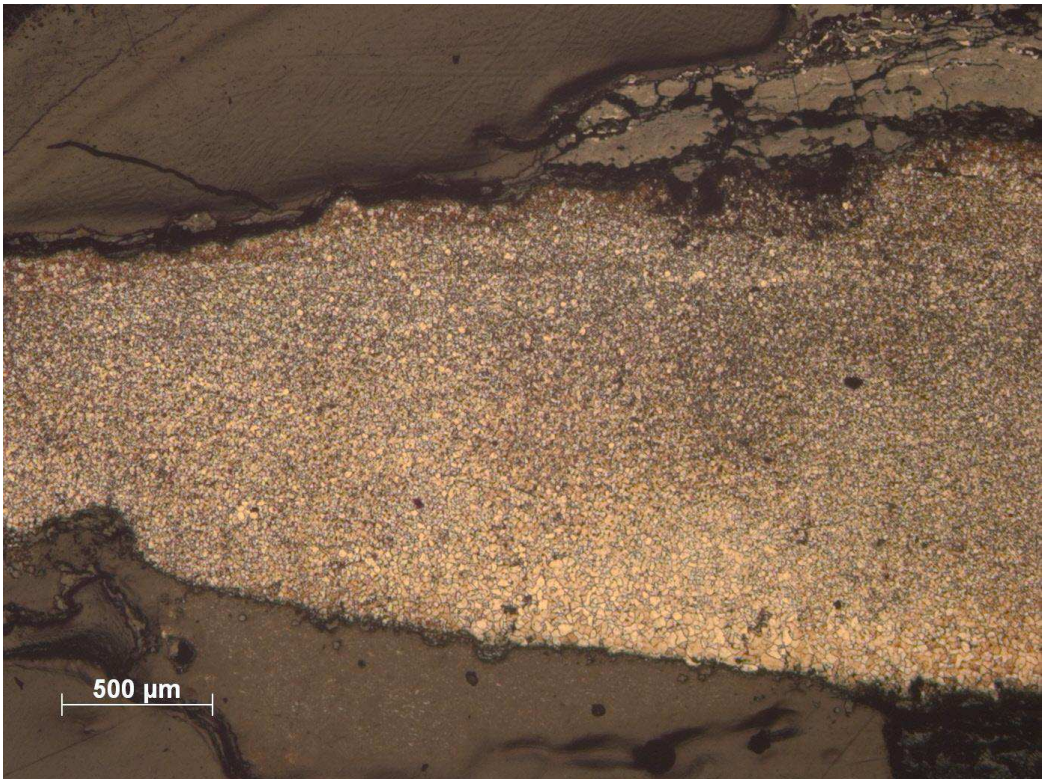

Figure 19: Sample W7-8g macro x25 extreme tip

2 SCANNING ELECTRON MICROSCOPE (SEM) WITH ENERGY DISPERSIVE X-RAY SPECTROSCOPY (EDS):

2.1 Zwammerdam 2:

2.1.1 Nail ZW2-2 (samples ZW2-2a, ZW2-2c, ZW2-2d and ZW2-2g)

The series of four samples have shown a homogeneous structure with few slag inclusions. This feature is valid for major areas of the specimens but in some areas, i.e. in the middle part of *sample c* were registered an increase in quantity and size of the slag inclusions. The major elements are silicon (Si), aluminium (Al), phosphorus (P), potassium (K) and calcium (Ca), manganese (Mn) and magnesium (Mg). These last two elements are practically presents in all the analyzed slag inclusions of this nail. Inside the head of the nail was found a slag with a high percentage of silicon (around 28 wt%), index of a glassy matrix. In that slag are also present barium (Ba) and titanium (Ti) as accessory elements.

The tip deserves a separate discussion. In this section of the nails (*sample g*) were observed a fracture and in close proximity to this were found some pollutants elements, i.e. chlorine (Cl) and sulphur (S). In the detail[3] picture taken to better understand the nature of the slag were clearly visible, in most of the cases, all the different mineral phases present, related to fayalite (Fe_2SiO_4) and wüstite (FeO) crystals, this conclusion is due not only to the chemical composition, but also to the shape of the crystal inside the slags. The fayalite inside the slag inclusion form preferentially elongated crystals, which result of a light grey under the microscope, the wüstite on the other hand create preferentially a dendritic structure.

These conclusions are derived from the observation and the chemical composition, to obtain a precise identification of the crystalline species is necessary to perform analysis like the X-rays diffraction (XRD).

[3] In this context the word detail is related to high magnification that goes from x1000 up to x4000 or more.

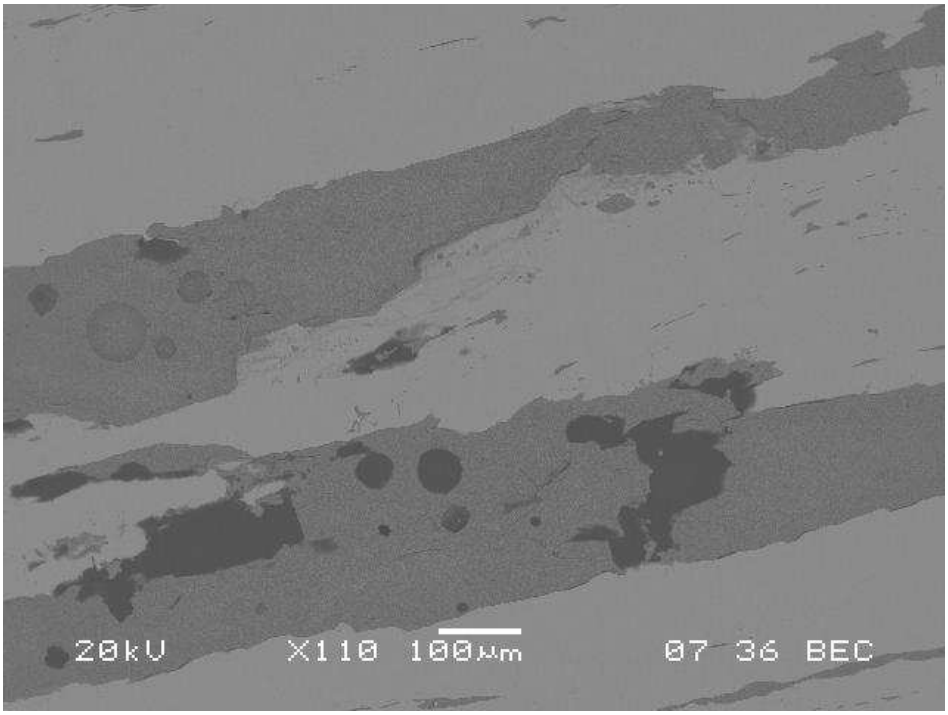

Figure 20: Backscattered electron view (BEC) General feature x110 of the slag inclusions from nail ZW2-2

2.1.2 Nail ZW2-3 (samples ZW2-3d and ZW2-3e)

The specimen ZW2-3d has a homogeneous surface characterized by few slag inclusions[4]. Some traces of the barium (around 0,5 wt%) can be observed in two occasions inside the slag composition. The situation in more or less the same in the lower parte of the nail (*sample e*), but here can is registered an increase of the number of inclusions.

2.1.3 Nail ZW2-GE2K (samples ZW2-GE2Kb, ZW2-GE2Ke, and ZW2-GE2Kf)

This nail is characterized by the massive presence of P inside the metal core. In fact this element is found practically everywhere over the surface of the entire series of the specimens taken from the nail. The surface of all the samples is characterized by the presence an high amount of slag inclusion, the amount of this inclusion is in the order of hundreds. These inclusions have an elongated shape. The principal elements are Si, Al, P, Ca and K, it has also been observed the totally absence of other elements like Mn, Mg and Ba. The change in composition of the slag inclusions from the head to the tip must be

[4] The amount of these inclusions is in the order of tens.

highlighted. Inside the *sample b* the composition of the inclusions is generally characterized by a low weight quantity (when present around 0,7 wt%) or a totally absence of elements like K and Ca, a feature that disappear along the length of the nail. At high enlargement (from around x1000 to around x2000) were identify more phases inside a single slag inclusions. In some particular occasion the chlorine were detect inside the slag inclusions.

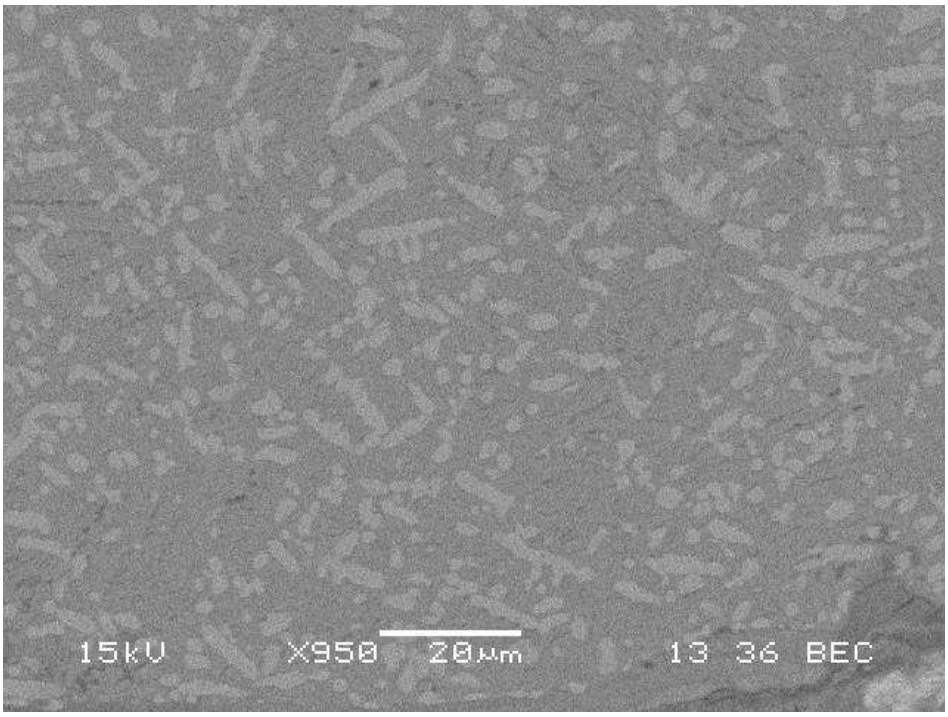

Figure 21: BEC view Detail x950 of the three phases that compose a slag inclusion.

2.1.4 Nail ZW2-GE2R (samples ZW2-GE2b, ZW2-GE2Rd, ZW2-GE2Re and ZW2-GE2Rg)

The first feature that registered in the upper part of the stem of the nail (*samples b* and *d*) is related to the composition of the slag inclusions. The inclusions are characterized by a low weight percentage of potassium (around 0,6 wt% where present) and calcium (around 0,6 wt% where present), but in most of the cases these elements are totally absent, in fact the absence of P is in 19/35 and the absence of Ca is in 12/35 of the analyzed slag inclusions.

P was found inside the metal core, but the presence of this element is not widespread. In fig 22 below is possible to see the general aspect of the sample taken from this nail.

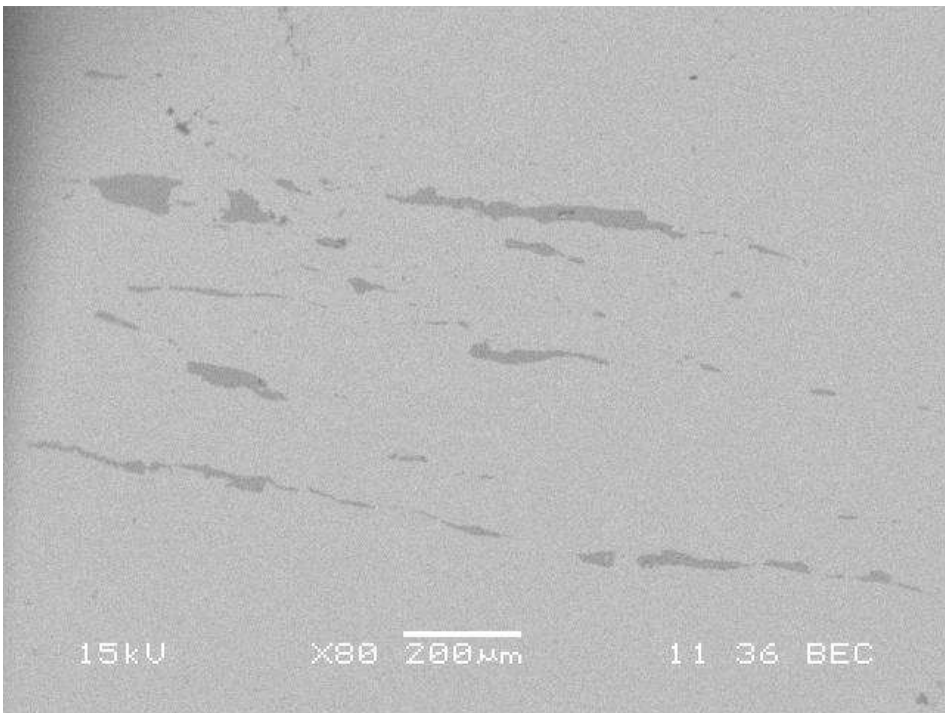

Figure 22: BEC view x80 of the layers and areas create by the slag inclusion

2.1.5 Nail ZW2-GG2K (samples ZW2-GG2Kb, ZW2-GG2Kd, ZW2-GG2Ke and ZW2-GG2Kg)

The principal feature of this nails is the high number of slag inclusions, in particular inside *samples b* and *g*. The number of the slag is in the order of hundreds. Specimen *d* has a homogeneous structure with relatively few inclusions, if compared to the previous samples. From the compositional point of view is registered the presence of P inside the metal in punctual areas of the sample, only inside the *samples d* and *e* seem that a major quantity of this element is present, in fact it was detected in 5/14 of the analyzed areas. The elements that compose the slag inclusions are Si, Al, P, K and Ca. The inclusions of the *sample b* have a low quantity of P with respect to the ones of the other specimen of this nail. The P concentration is around 0,5 wt%, when present, instead of the 1,2 wt % of the other samples. At magnification from x500 and onwards, almost all the inclusions were characterized by the presence of different phases.

2.1.6 Nail ZW2-GG2R (samples ZW2-GG2Rb, ZW2-GG2Rd, ZW2-GG2Re and ZW2-GG2Rg)

Inside this sample were registered a present of a quite high amount of slag inclusion, the number of this slags is in the order of hundreds. The EDS analyses of the inclusions inside the *sample b* have highlighted the presence Si, Al, K, Ca and P. In two cases were detected traces of titanium (around 0,50 wt%) and in one case manganese (1,23 wt%). From the point of view of the alloy composition, in 12 of 123 analyzed areas, the presence of P has detected.

2.2 Zwammerdam 4:

2.2.1 Nail ZW4-6 (samples ZW4-6c, ZW4-6f and ZW4-6 g)

The nail is characterized by a homogeneous microstructure. During the EDS analyses of the slag inclusions the presence of Si, Al, P (this element has been detected in only 14/29 of the inclusions) K, Mg and Ca were detected. The EDS have also detected titanium and manganese respectively in one and two cases. The slag inclusions of the central area of the *sample f* have shown high level of calcium, in comparison with all the others (average value above 1,00 wt% with peaks like 5,80 wt% and 7,28 wt%). The *sample c* is characterized by the presence of P inside the metal in the right side. The last feature necessary to highlight is the presence of a fracture in the tip of the nail (*sample g*) where S and Cl were detected.

2.2.2 Nail ZW4-7 (samples ZW4-7 b, ZW4-7c, ZW4-7f and ZW4-7h)

At a macroscopic vision (naked eye vision) all the samples were characterized by a high number of inclusions, in order of hundreds. The first feature to highlight is the presence of P inside only in three inclusions, in *sample*s *b* and *c*. A totally different situation was observed in *sample h*, where the presence of this element inside the inclusions is every time confirmed. In this sample the average of P is around 2% but inside 4 different slag inclusions it has arrive till 4%. The second feature to highlight is the presence of Mg practically in all the specimens of the nail, and the presence of Ba inside the *samples c* and *f*. Inside the *sample b* has identified in two different slags the presence of Ti (0,5

wt%) and Mn (around 0,9 wt%). One of the inclusions has shown a particular shape of the crystals inside it. From the chemical composition this crystal can be related to fayalite, this aspect similar to "trident" can be explained by as an effect due to the cutting and the polishing of the surface, that have cut in this so particular shape the elongated crystal typical of the fayalite (fig 23).

Inside the *sample f* is present a great fracture. Along the length of the fracture was detected a widespread presence of chlorine (in the fig 25 below is shown a crystal of halite[5]). For what concern the composition of the alloy in two cases inside the metal alloy of *sample f* the presence of phosphorus is detected.

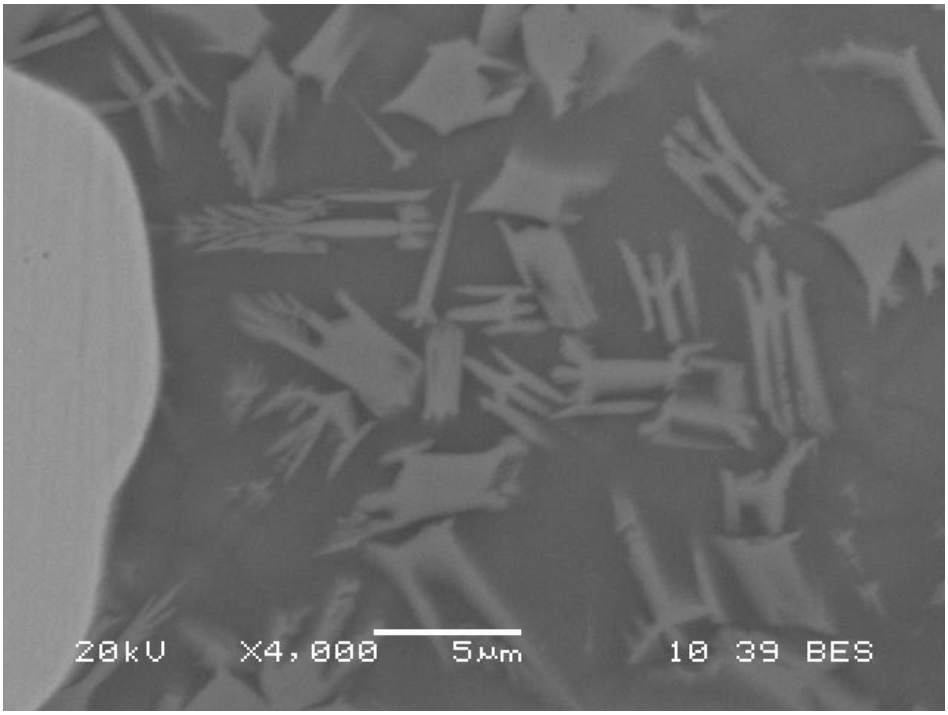

Figure 23: detail x4500, of a particular shape of the fayalite crystal inside an inclusion

[5] The Halite is a mineral formed by sodium and chlorine. The identification of the crystal show in the image with this mineral is due to the EDS analysis, in which only this two elements were detected.

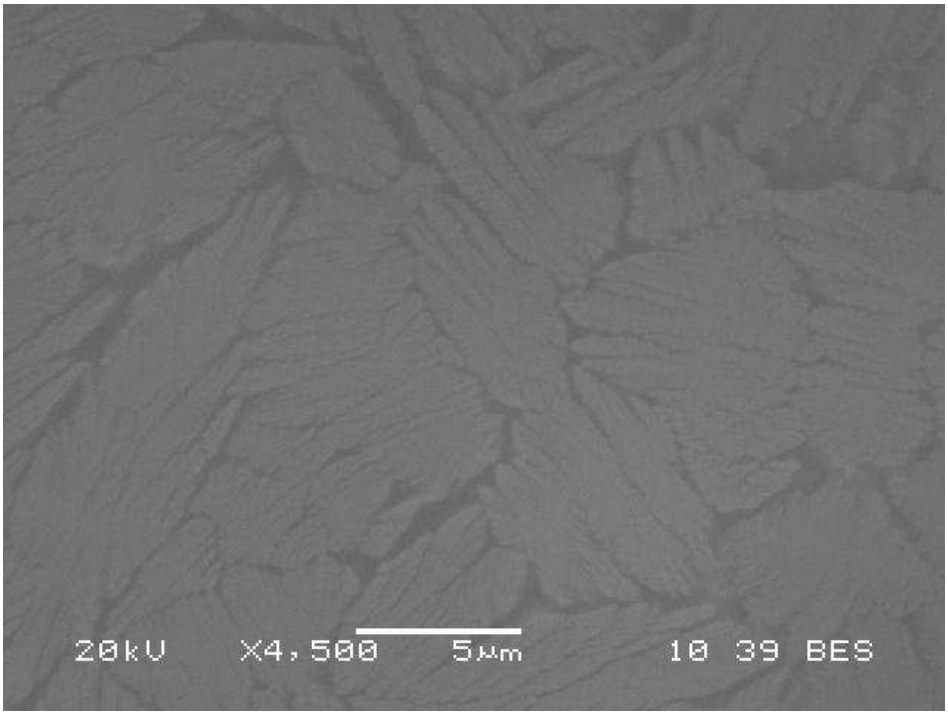

Figure 24: x4500 aspect of a slag inclusion present inside the nail ZW4-7

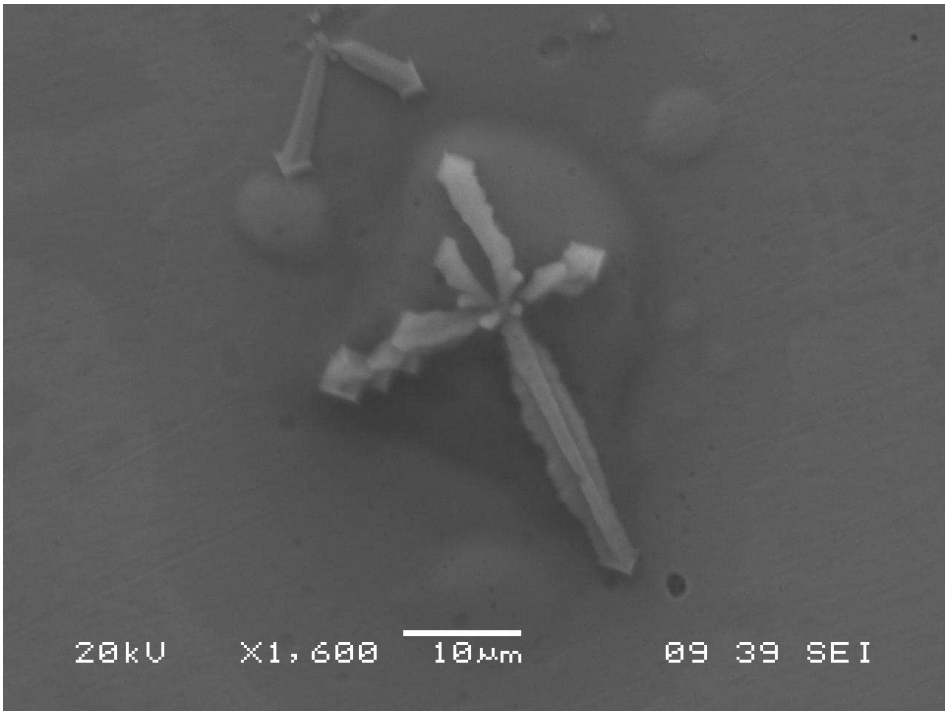

Figure 25: Secondary electron (SEI) view x1600, crystals of halite that grow from a bubble on the surface near the fracture in sample f

2.3 Zwammerdam 6:

2.3.1 Nail ZW6-7 (samples ZW6-7cv, ZW6-7dv, ZW6-7bh, ZW6-7eh, ZW6-7fh and ZW6-7gh)

The first aspect to highlight is the total absence of the P inside the iron alloy. The second important feature is the presence of Mn inside the majority of the inclusions (in 71 of 95 analysed slags) and about1 wt% of P. For the weight percentage of magnesium inside the slag must be make a division: inside the *samples bh*, *eh* and *dv*, this element is totally absent, on the other hand it is relatively abundant (in 15 of 19 analyzed slags) inside the *sample*s *fh*, *gh*. It is necessary to underline that the number inclusions seem to decrease from *samples bh* and *cv* to the *sample gh*. The presence of chlorine, inside most of the specimen of this nail, is particularly abundant inside *samples dv* and *eh*, the two specimens related to the curved section of this spike.

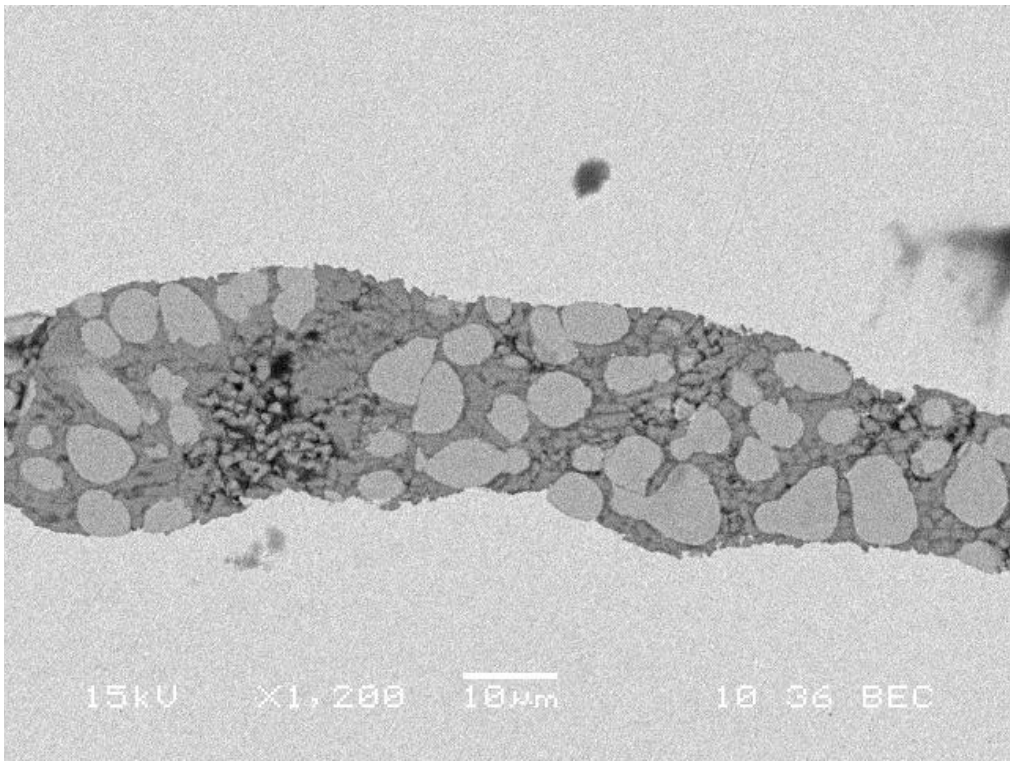

Figure 26: SEM BEC x1200 example of slag with manganese, in the darker areas, taken from sample gh

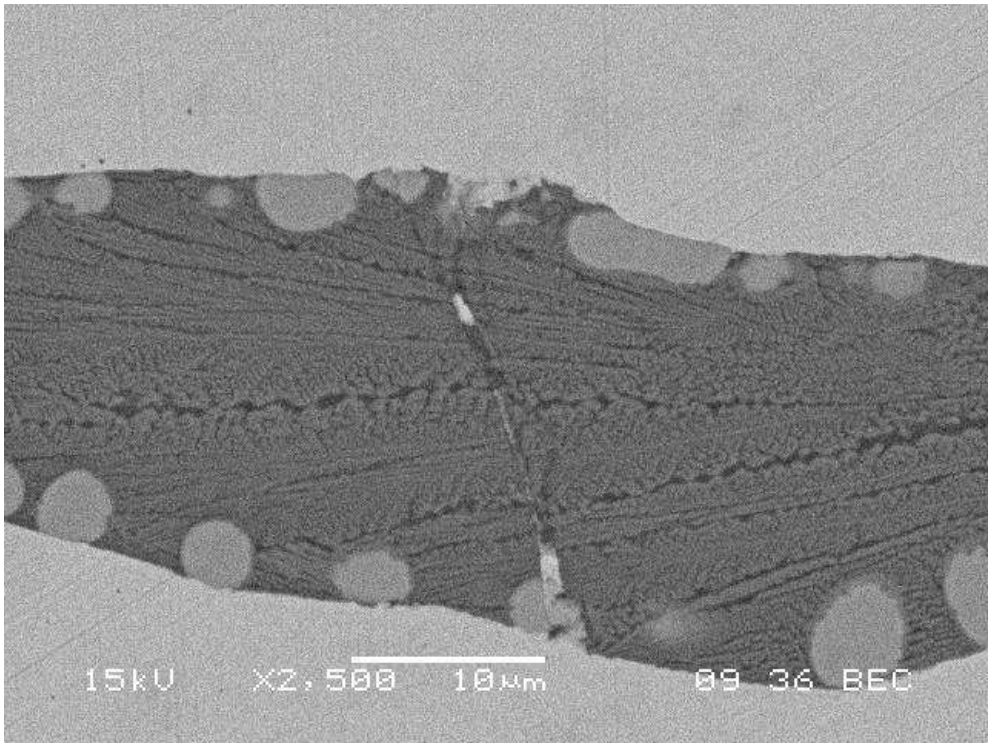

Figure 27: SEM BEC x2500 Example of the particular configuration of the crystal inside the slag inclusion inside sample eh.

2.3.2 Nail ZW6-8 (samples ZW6-8b, ZW6-8e, ZW6-8f and ZW6-8g)

The stem of this nail (*sample b*) is characterized by the presence of hundreds of inclusions, visible also with the naked eye. This sample shows two other important characteristics. The first one is related to the fracture that starts from the lower right side and goes until the lower middle of the sample. The EDS analysis of the non-metallic compounds, that surround the fracture, has shown the presence of only Ca and P, with high level of oxygen (around 30 wt%). This situation changes along the length of the crack. In a first time were detected only this three elements, then approximately in the middle of the length the composition starts to change till arrive, at the end of the fracture, to a composition comparable to a slag inclusion. The composition of the others analyzed inclusion have shown the presence of Si, AL, P, K and Ca.

Concerning the metal alloy composition has to be highlighting the presence of P. This element was particularly detected in the right areas of the *sample b*, nevertheless this

presence disappear below[6] the break. In all the other samples the presence of P is more or less located in the middle of the sample.

2.3.3 Nail ZW6-9 (samples ZW6-9b, ZW6-9f and ZW6-9g)

In first section of the nail (*sample b*) is present a long layer with slag inclusions that runs from the right side to the left one. The composition of these inclusions shows an high percentage of silicon (form 20 to 30 wt%). Inside *sample f* is visible in the right side a fracture. The contours of this break have a composition made of iron oxide [detected only Iron (fe) and Oxygen (O)], with trace of P and Ca (all around 0,5 wt%) and traces, especially in the area nearest to the external environment, of Cl and sodium (Na) (both around 0,5 wt%).

On of the most important aspects related to the tip (*sample g*) is the presence of different areas of corrosion. In particular near the extreme tip on the basis of the composition three different corrosion areas[7] can be distinguished:

1. The first and the greater area is composed mainly of Fe, P and O.
2. The second one, which surrounds the first one, is like an oxidized slag, where the component inside are P, Si, Al and O.
3. The third one which lies between the metal core and the other two layers is composed by Cl and O.

Concerning the metal alloy the presence of P is limited to five areas in *sample*s *f* and *g*, while it is more widespread in the *sample b* (detected in 14/21 of the analyzed areas).

[6] This area is relative the rm zone of the division of the sample (see chapter about technical, instrumentation and analyses).

[7] This zones can be recognized under the microscope by different level of grey and after from the EDS analysis by the elemental composition.

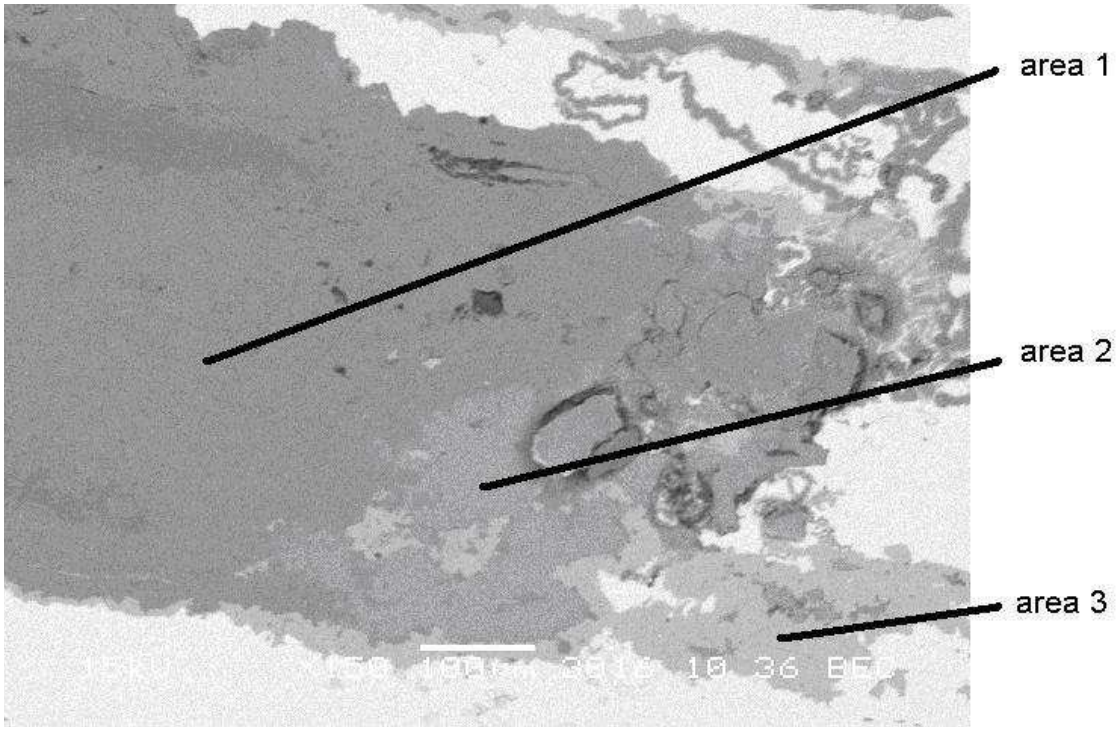

Figure 28: SEM imagine x150 that show the 3 different zones of corrosion

2.3.4 Nail ZW6-10 (samples ZW6-10a, ZW6-10c, ZW6-10f and ZW6-10g)

Sample a represents the nail's head. In this particular specimen there are inclusions with a width around 400 μm and length that arrive to 1 mm or more, which starts in the stem of the nail up to the borders of the head, placed in the left side. On the right side the EDS has identify P inside the metal alloy. This element was also identified in many places along the entire length of the nail, i.e. in *sample c* it is detected in all the external side, inside *sample f* it is detected in the central area of the left and of the right side; in *sample g* it is founded in the central area of the specimen. The elements that the slag inclusions are composed of are Si, Al, P, K, Ca and Mg.

2.3.5 Nail ZW6-13 (samples ZW6-13 b, ZW6-13d, ZW6-13f and ZW6-13g)

The first three samples selected from this nail have a homogeneous structure with few elongated slag inclusions; the amount of the inclusion is in the order of tens. This situation is different in the tip of the nail (*sample g*), where the amount of the inclusions is greater and a layer of them arrive till the edge of the tip (this layer is also visible by

naked eye) on one of the external sides. The composition of these inserts is various. In the first three samples the elements which compose the few inclusions are Si, Al, P, K and Ca. In the tip's area the composition changes; K and Ca are detected less often but in higher amount (around 0,8 wt%). No traces of P were detected inside the metal.

2.4 Woerden 7:

2.4.1 Nail W7-8 (samples W7-8b, W7-8d and W7-8e)

The *sample b* shows at a macroscopic observation slag inclusions visible by naked eye; the inclusions have a length around 1,5 mm and a width of 500 μm. This huge dimension allows, in most of the cases, the formation of two or three different phases that can be easily distinguished under the microscope. The *sample d*, on the contrary, is characterized by a homogeneous structure, with a lower amount of inclusions; the number of these inclusions is in the order of tens. Two of the slags, located in the right side (the nearest to the specimen b) have the same characteristics of the slags present in the *sample b*. The tip of the nail (*sample e*), has a homogeneous structure; with a low amount of inclusions, the number of this inclusions is in the order of tens. The slags have a similar composition, 9one to each other, from the head to the tip. The detected elements are: Si, Al, P, K, Ca, Mg and Mn. Concerning the presence of P inside the alloy, it is detected only inside *sample b* and in *sample e*.

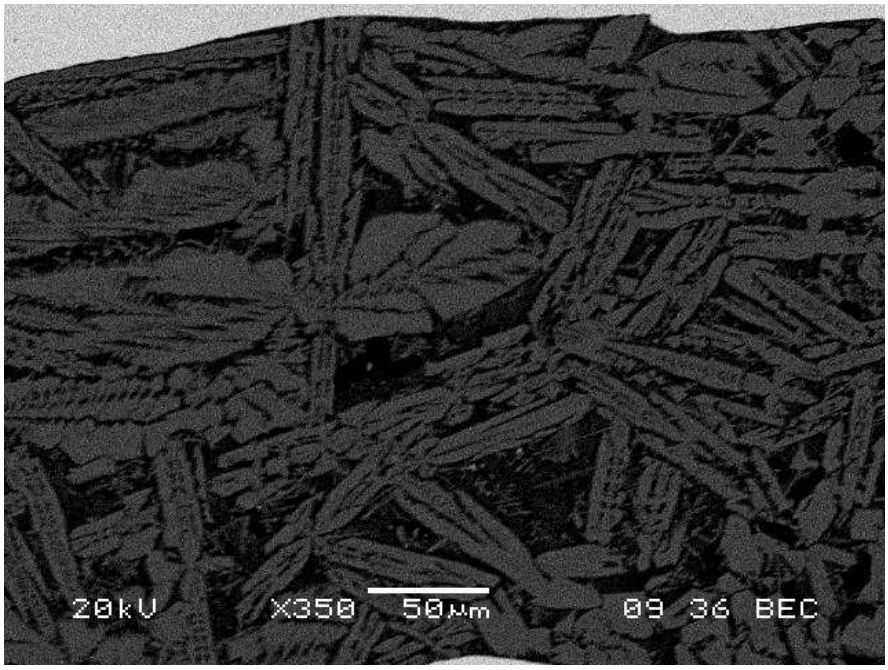

Figure 29: detail x350 of the structure visible in the slag of the sample b

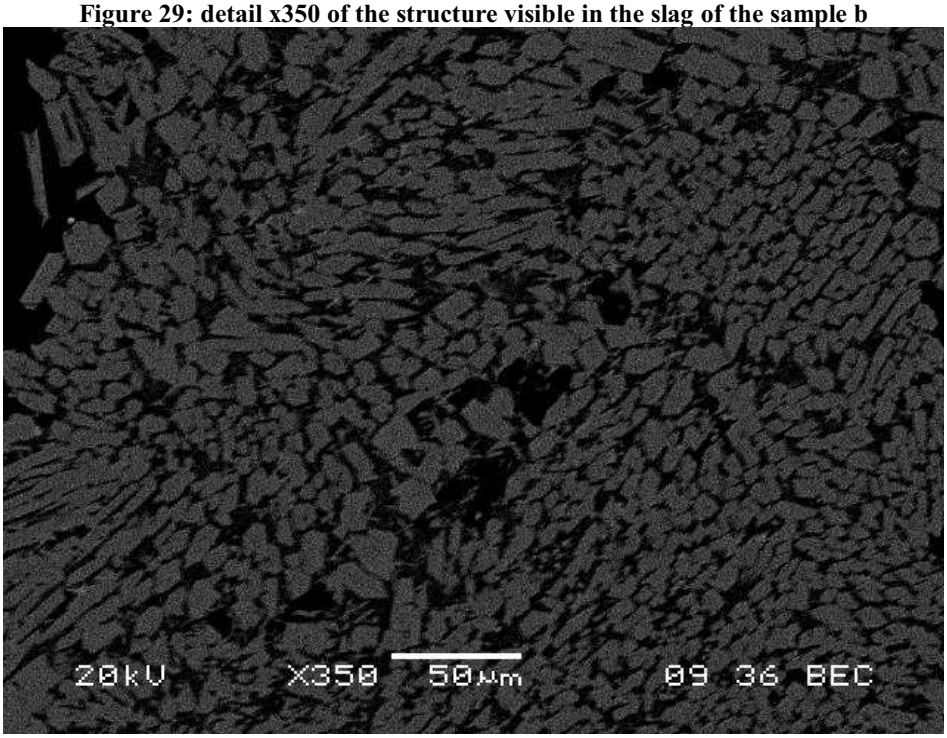

Figure 30: detail x350 of the second structure visible in the slag of sample b

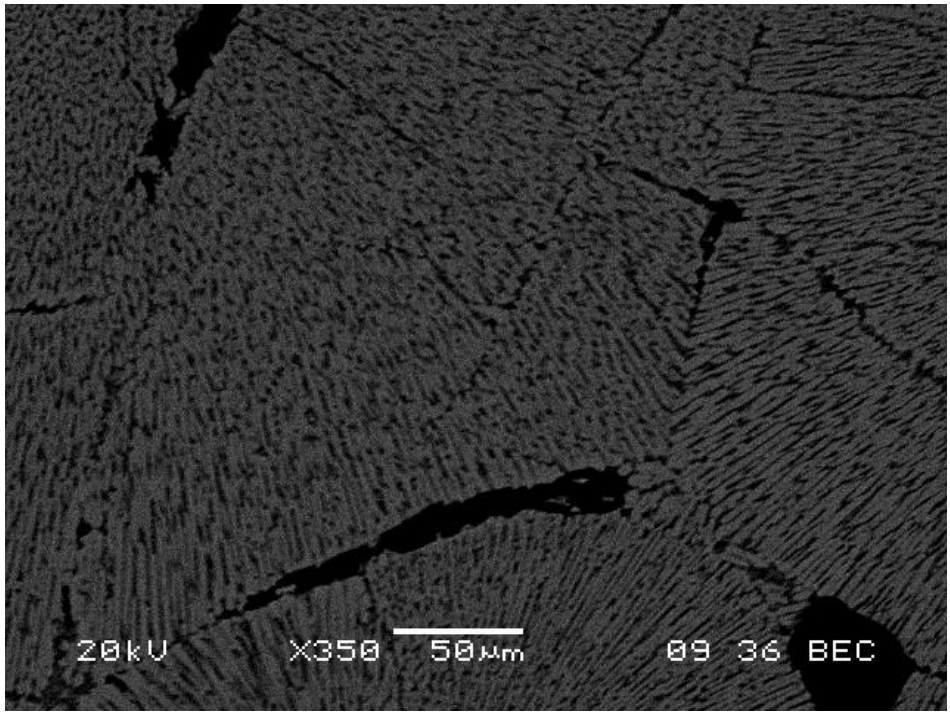

Figure 31: detail x350 of the third structure visible in the slag of sample b

3 VICKERS'S HARDNESS TEST:

This section presents the results obtained from the hardness tests. For a better presentation the data will be presented in a simplified scheme where is clearly show where the tests are performed and the values obtained. All the pictures represent the selected samples; divided by lines that represent the cutting process.

3.1 ZWAMMERDAM 2

3.1.1 Nail ZW2-2 (samples ZW2-2a, ZW2-2c, ZW2-2d and ZW2-2g)

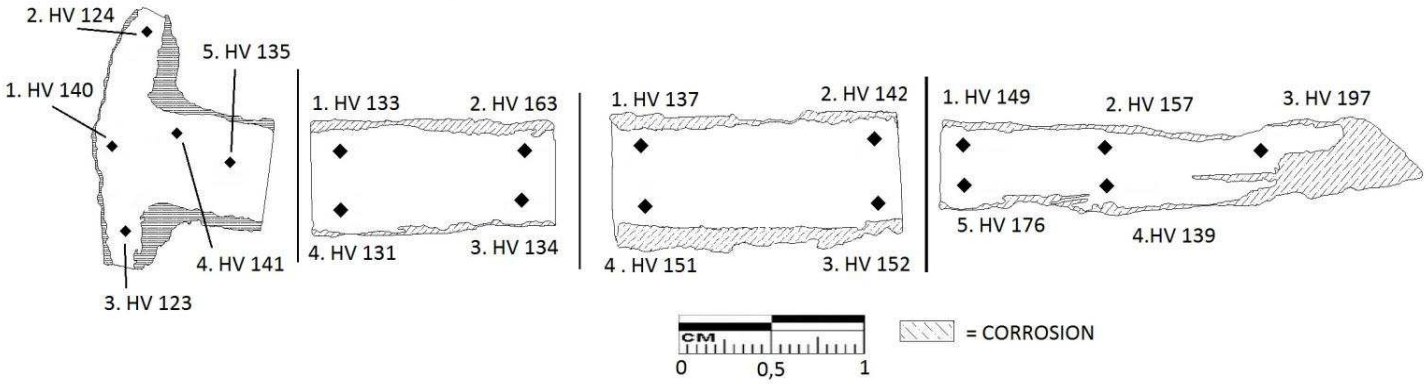

Figure 32: nail Zwamerdam2-2 with the indication of the performed hardness tests

As can be seen in the figure above (fig. 32) different zone of hardness are present in the entire length of the nail, with a general increase of the hardness from the head (*sample a*) till the tip (*sample f*), where the hardness have a value of HV 197. In the head of the nails (*sample a*), the values of the hardness are inside a range, which have a maximum of HV 140 in the central area, and minimum value of HV 123, which characterize the external part of the nail's head. The average value of the hardness in this nail is around HV 149.

3.1.2 Nail ZW2-3 (samples ZW2-3d and ZW2-3e)

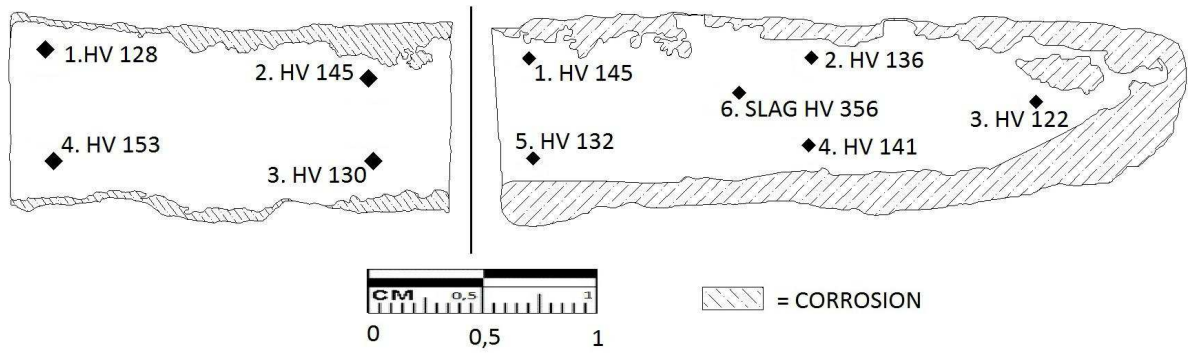

Figure 33: nail Zwammerdam2-3 with the indication of the performed hardness tests

The two selected samples show an average hardness of HV 137, with no particular increasing of hardness along the stem till the tip. In the *sample e* was performed the test also inside a slag inclusion, which have given an high value of hardness HV 356, about three times the hardness of the nail itself.

3.1.3 Nail ZW2-GE2K (samples ZW2-GE2Kb, ZW2-GE2Ke, and ZW2-GE2Kf)

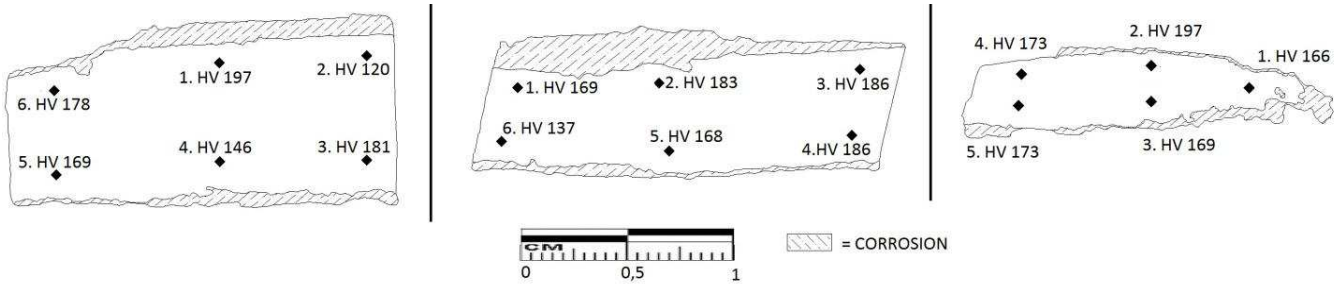

Figure 34: nail Zwammerdam 2-GE2K with the indication of the performed hardness tests

The average hardness of this nail is around HV 161. Along the length of the stem were found areas with different hardness with a general increasing of this parameter from the upper part of the stem (*sample b*) till the tip (*sample f)*. In fact inside the tip (*sample f*) was registered the highest value of the hardness, for this specific nail, HV 197.

3.1.4 Nail ZW2-GE2R (samples ZW2-GE2b, ZW2-GE2Rd, ZW2-GE2Re and ZW2-GE2Rg)

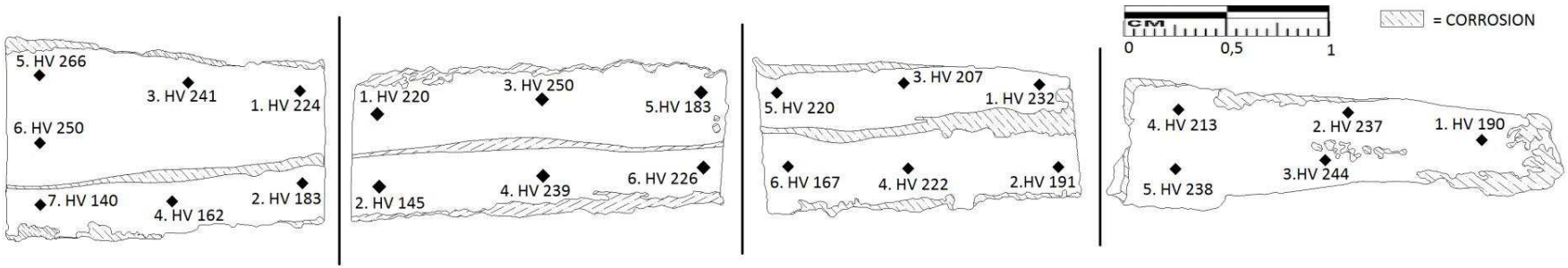

Figure 35: nail Zwammerdam2-GE2R with the indication of the performed hardness tests, the samples from the left to the right are the b, d, e and g

The nail ZW2-GE2R, as can be clearly understood by the figure above, has high hardness values along all the length of the stem. The average is around HV 212, with zones where the registered value is HV 266. In the first sections of the stem (*sample*s *b* and *d*) there is a difference of the hardness inside the two external sides of the samples. One area is located below the corrosion line that runs all over the length of the nails, and the other one above it. This difference in hardness slowly decreases till the right side of the *sample e* where there is the finishing of the corrosion line and the finishing of the difference in hardness. The tip of the nail (*sample g*) does not present values that are higher compared to the rest of the nail.

3.1.5 Nail ZW2-GG2K (sample ZWGG2Kb, ZW2-GG2Kd, ZW2-GG2Ke and ZW2-GG2Kg)

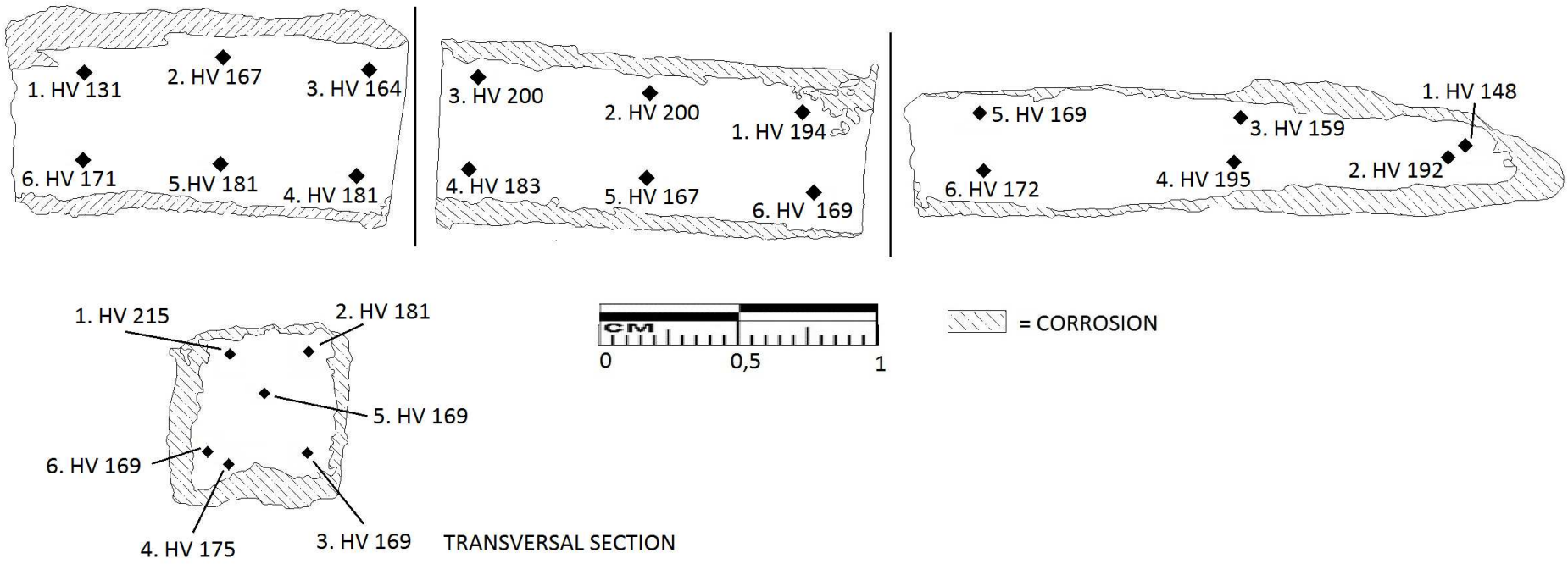

Figure 36: nail Zwammerdam2-GG2R with the indication of the performed hardness tests, the square section is the transversal one

As can be seen in the figure above (fig. 35), *sample e* allows the investigation of the hardness not only along the length of the stem, but also in the transversal section. This section clearly shows that the majority of the stem's areas have a similar hardness (in the transversal direction). Along the length of the stem were measured different values of the hardness, which has an average value around HV 177. The tip (*sample g*) does not have any hardness value higher than the rest of the nail.

3.1.6 Nail ZW2-GG2R (sample ZWGG2Rb, ZW2-GG2Rd, ZW2-GG2Re and ZW2-GG2Rg)

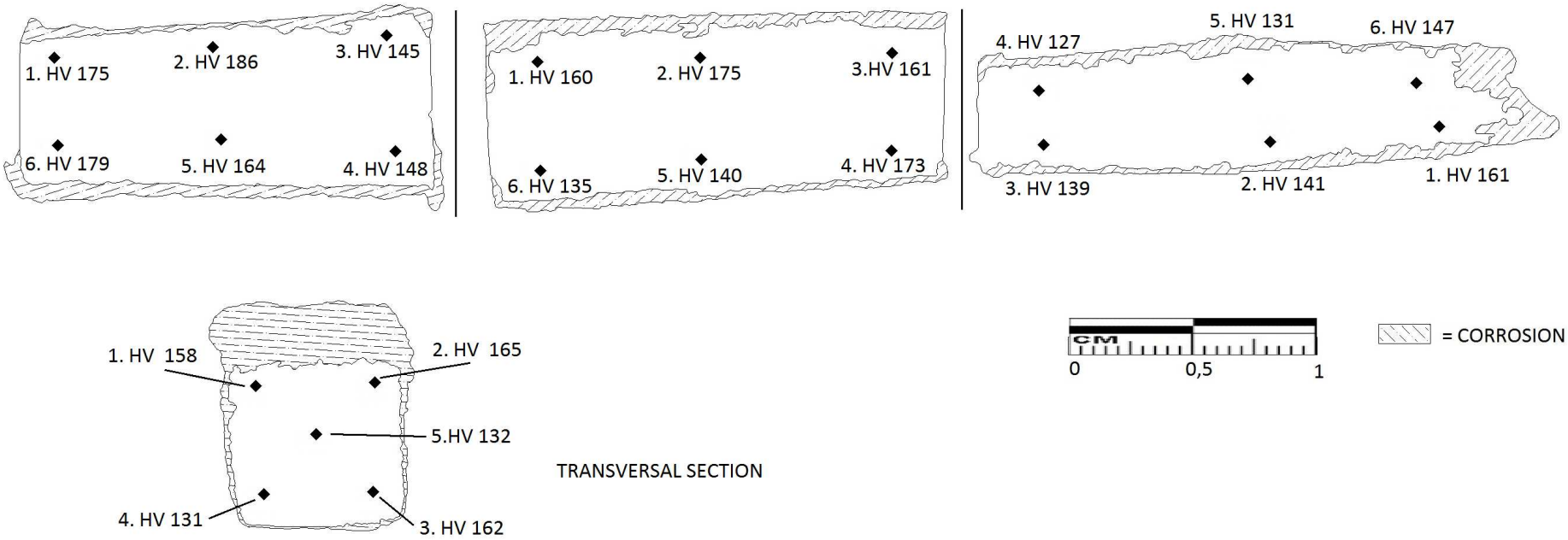

Figure 37: nail Zwammerdam2-GG2K with the indication of the performed hardness test, the square section is the transversal one.

The *sample d* is taken from the transversal section of the stem and allows the investigation the hardness also in this direction. The values of the hardness are very different. The values are inside a range, which has a minimum value of HV 127 and maximum one of HV 186. The average is around HV 155. In the tip (*sample g*) the values remain totally in line with the others sections of the nail.

3.2 Zwammerdam 4:

3.2.1 Nail ZW4-6 (samples ZW4-6c, ZW4-6f and ZW4-6 g)

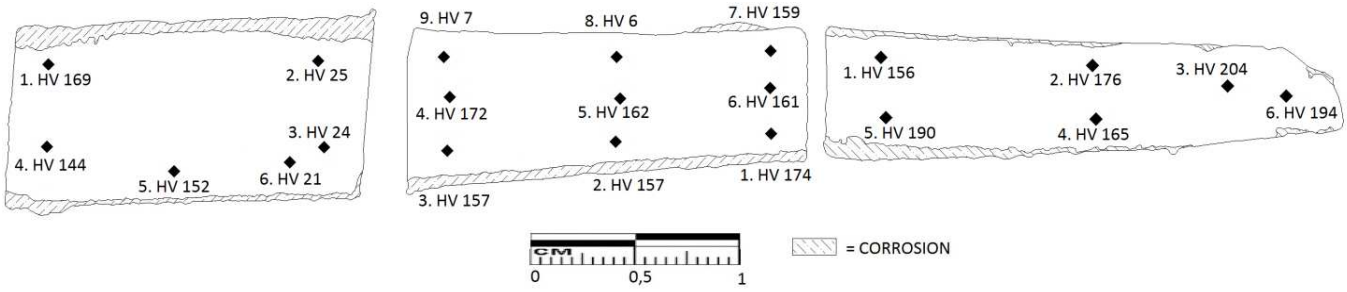

Figure 38: nail Zwammerdam4-6 with the indication of the performed hardness test

The hardness of this nail is increasing along the length of the stem, till a maximum value of HV 204 in the tip (*sample g*). It is possible to appreciate an increasing of the hardness from the upper part of the stem (*sample c*) till the tip (*sample g*). The average of the hardness in the nail is around HV 168, and the average of the tip is around HV 180. Five measurements were not taken into account for the evaluation of the hardness of this nail, because during the performing of the test the material has given a strange answer to the applied load.

3.2.2 Nail ZW4-7 (sample ZW4-7 b, ZW4-7c, ZW4-7f and ZW4-7h)

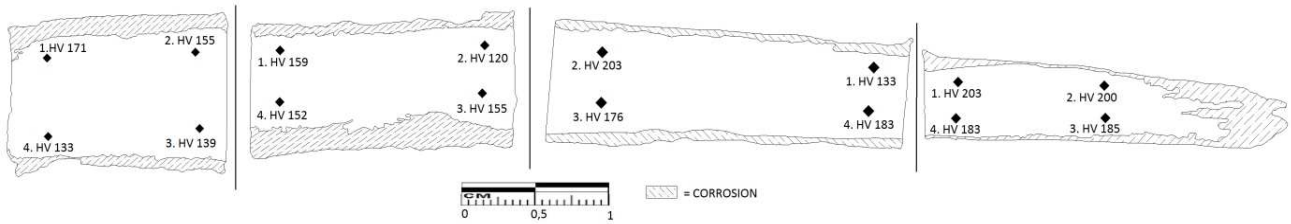

Figure 39: nail Zwammerdam4-7 with the indication of the performed hardness test

Inside this nail are present zones with various values of the hardness. This disparity in the values makes difficult an evaluation of the average hardness, which results around HV 165. In spite of this situation an increasing of the hardness from the upper part of the stem (*sample b*) to the tip (*sample h*) was measured. The tip of the nail (*sample g)* have high

values of hardness, which have an average value around HV 192, with a maximum one of HV 203.

3.3 Zwammerdam 6:

3.3.1 Nail ZW6-7 (sample ZW6-7cv, ZW6-7dv, ZW6-7bh, ZW6-7eh, ZW6-7fh and ZW6-7gh)

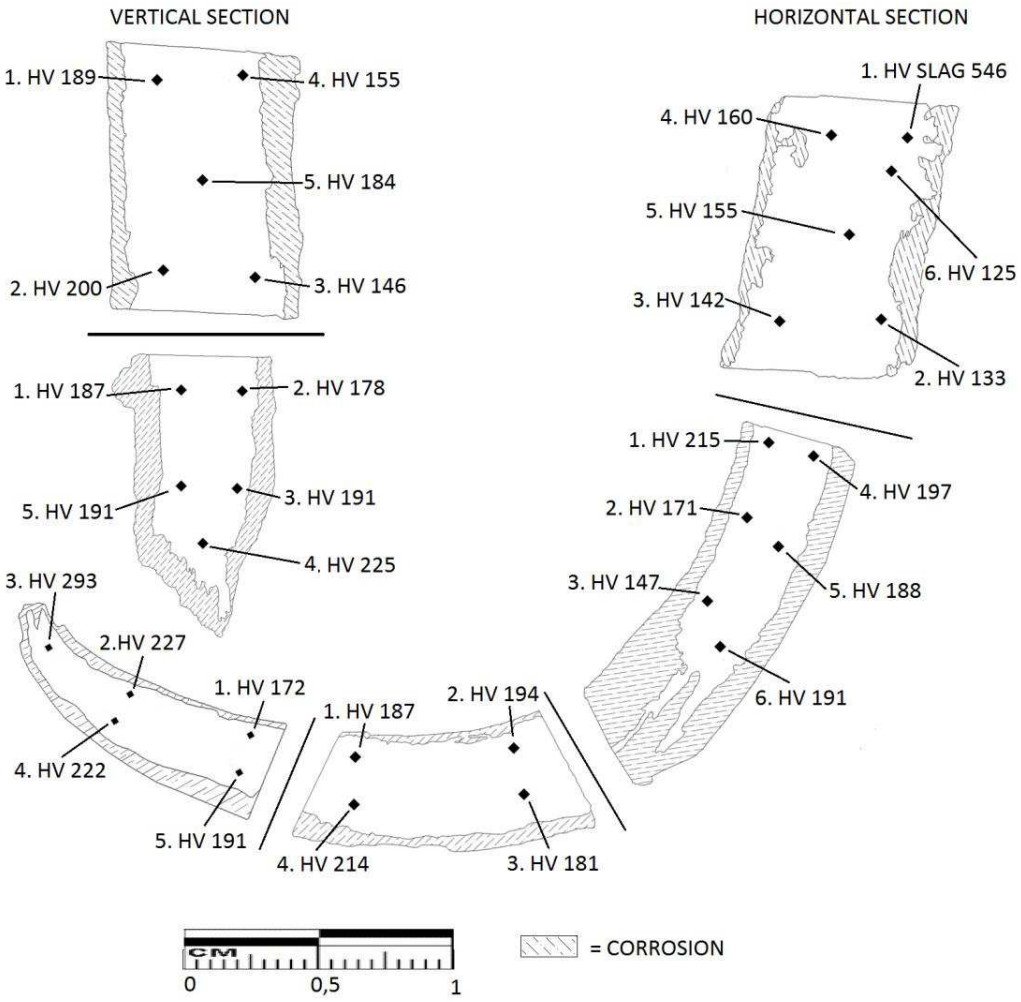

Figure 40: nail Zwammerdam6-7 with the indication of the performed hardness test

This nail is divided in two sections. The vertical section is related only to the stem until the curve, which characterize the lower part of the nail. The horizontal section takes into

account the entire length of the nail including the bending. As is clearly shown by the figure above (fig. 40) there are lots of different areas with different hardness, nevertheless there is a general increase of the hardness from the upper part of the stem (*samples cv* and *bh*) to the tip (*sample gh*), where was measured the maximum value for this nail HV 293. The average hardness for the entire nail is around HV 185. In this nail was decide to perform the test also on a slag inclusion, which resulted extremely hard compared to the metal alloy, with a value of HV 546.

3.3.2 Nail ZW6-8 (samples ZW6-8b, ZW6-8e, ZW6-8f and ZW6-8g)

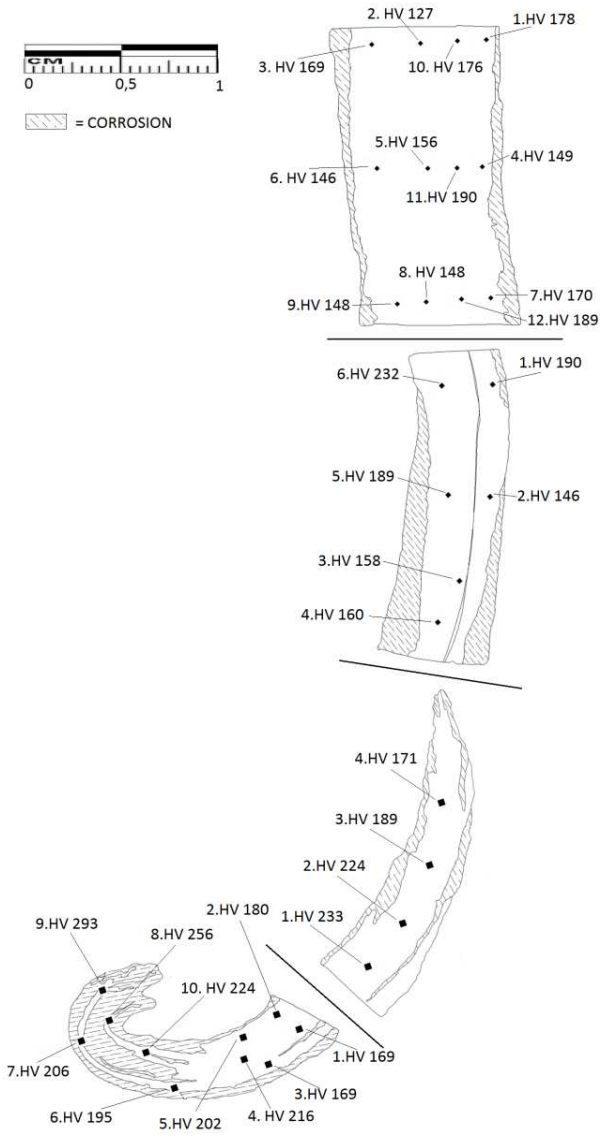

As shown in the picture (fig.41) various zones with different hardness inside upper part of the stem (*sample b*) were measured. Near the curve (*sample e*) there is a decrease of the hardness, which has a minimum value of HV 146. This decreasing effect finishes after the bending (*sample f*) where there is a reverse trend, an increase of the hardness, till to the tip of the nail (*sample g*) where a maximum value of HV 293 was measured, with an average value, for this section, around HV 210. The average value for the entire nail, including the bend part, is around HV 185.

Figure 41: nail Zwammerdam6-8 with the indication of the performed hardness test

2.3.3 Nail ZW6-9 (sample ZW6-9b, ZW6-9f and ZW6-9g)

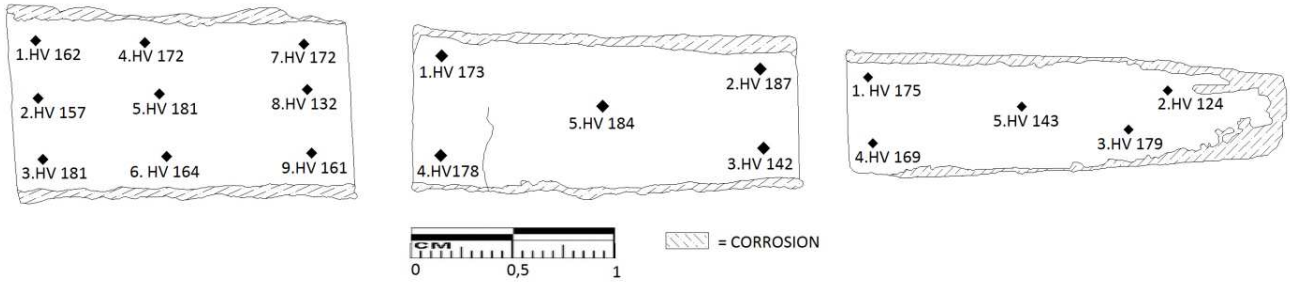

Figure 42: nail Zwammerdam6-9 with the indication of the performed hardness test

In this nail due to the disparity in the measured values, was not precisely determinate the trend along the entire length of the stem. The values registered in the tip (*sample g*) have a maximum, for this specimen, of HV 179. On the other hand inside the stem (*sample f*) was registered a maximum value of HV 187. The average value for the entire nail is around HV 165.

3.3.4 Nail ZW6-10 (sample ZW6-10a, ZW6-10c, ZW6-10f and ZW6-10g)

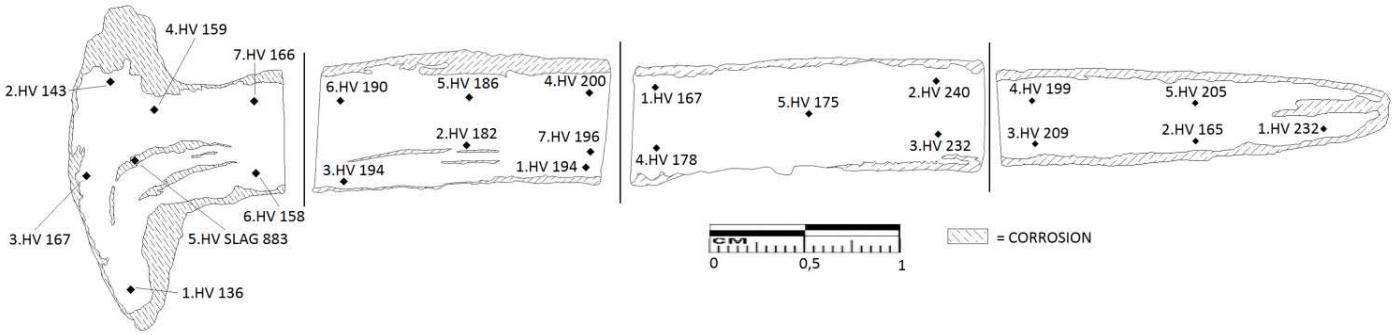

Figure 43: nail Zwammerdam6-10 with the indication of the performed hardness test

The head of the nail (*sample a*) has shown different value of the hardness on the base of the position of the measurement. The specimens selected to represent the stem (*samples c* and *f*) have shown values of hardness between HV 167 up till HV 240, the situation is quite similar inside the tip (*sample g*) but the values registered are lower, with a maximum of HV 205. The average hardness for the entire nail is around HV 212.

3.3.5 Nail ZW6-13 (samples ZW6-13 b, ZW6-13d, ZW6-13f and ZW6-13g)

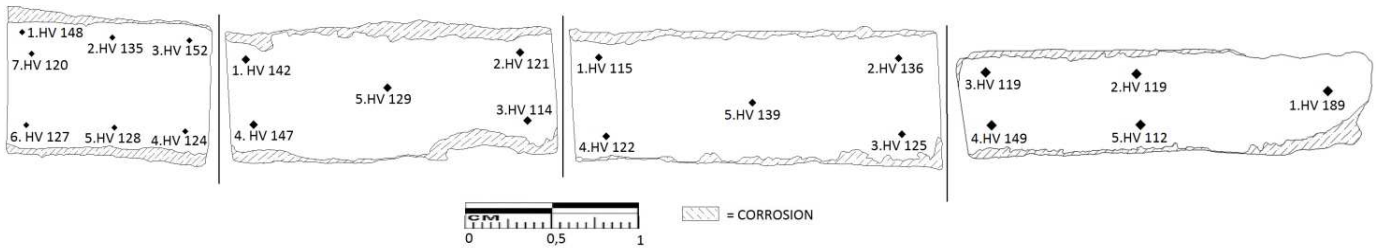

Figure 44: nail Zwammerdam6-13 with the indication of the performed hardness test

In first section of the stem (*sample b*) there is a difference between the two external sides. The areas of the upper side have hardness values higher than the lower one, in the upper part the values are around HV 150 in the lower one the values are around HV126. A similar situation is present inside the second section of the stem (*sample d*) where in the left side were registered values greater than the ones on the right side. Despite these differences, the general value of the hardness along the entire stem is not so high; in fact the majority of the collected values are around HV 125. The situation lasts also in the tip (*sample g*), but the value collected from the very last area of the tip has a value of HV 189. The average value of the hardness for the entire nail is around HV 129.

3.4 Woerden 7:

3.4.1 Nail W7-8 (samples W7-8b, W7-8d and W7-8e)

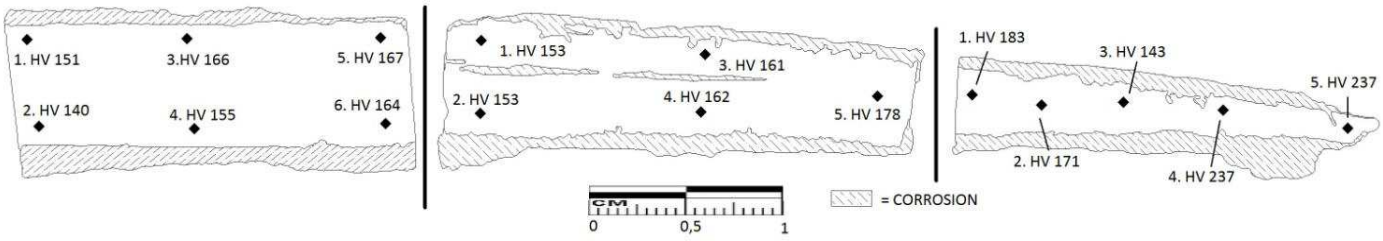

Figure 45: nail Woerden7-8 with the indication of the performed hardness test

Along the entire nail there is an increase of the hardness. The analyses have given a value of HV 237 inside the tip of the nail, instead of the average value of HV 160 of the other

section of the nail. Along the nail there are areas with a different hardness, with values that are inside a range with a minimum value of HV 140 up to a maximum one of HV 178.

4 LASER ABLATION – INDUCTIVELY COUPLED PLASMA – MASS SPECTROMETRY RESULTS:

The results obtained from the laser ablation-inductively coupled plasma-mass spectrometry (LA-ICP-MS) are plotted in a table with the average values of all the analyzed elements. In this case, for a complete understanding of the value and of their meaning, some annotations are required.

The first note is about the multiple averaging of the data. To obtain these values a calibration with the standard glass N610 were done. This calibration affects also the measurements of the samples because it is on the base of this standard that the instrument evaluates the weight percentage in part per million (ppm) of the selected elements.

The standards glass N610 is made with inside a standardized weight percentage quantity of all the elements that can be detected by the mass spectrometer. The second note is about the preliminary processing to obtain the raw data. During this passage the software requires the weight percentage value, transformed in ppm, of a known element to make a second calibration of the data. To do that was decided to insert as reference the weight percentage of silicon. The value give to the software was the average value of the silicon inside the slag inclusion, taken from the energy dispersive X-ray spectroscopy (EDS) system. To have a precise and better evaluation of these data it is necessary to perform other tests, with the same instrument on more samples and on more reference ones to have a bigger amount of data useful for the comparison. For a better evaluation of the obtained data could be useful a comparison with other elemental analyses, like the electron probe micro analyzer (EPMA) or the ion beam technique. It is better to perform the tests without using so many averaging, i.e. using the precise weight percentage value instead of the average one.

The complete series of analyzed elements is:

Mg26, Si29, P31, Ca43, Ca44, Sc45, Ti47, V51, Cr52, Mn55, Co59, Zn67, As75, Rb85, Sr88, Y89, Zr90, Nb93, Mo95, Sb121, Cs133, Ba137, La139, Ce140, Pr141, Nd146, Sm147, Sm149, Sm152, Eu151, Eu153, Gd157, Tb159, Dy161, Dy163, Ho165, Er167, Tm169, Yb172, Lu175, Hf178, Ta181, W182, W183, Pb208, Th232, U238. In the table 1

below were not plotted all the analyzed elements, some of them, i.e. cobalt and arsenic, due to their siderophile nature has not been used for the matching of the trace elements inside the slag inclusion.

The number of analyzed slag inclusions, used to evaluate the average quantity of trace elements, varies from ship to ship. This fact is due to number of the inclusions suitable for the test, because inside the metal are presents numerous slags[8] but, in majority of the cases, the shape of this inclusions made impossible the performing of the test, with the chosen settings. The selected spot size, in fact, was of 60 μm bigger than the height of most the inclusions themselves, but if the spot size was decreased further, it probably has affected the results, because the data that could be obtained were related to a volume comparable to a single crystal of the inclusion. So the data that obtained in that way could not represent the entire composition of the slag inclusion, which is one the reasons to perform this analysis.

Inside the ships Zwammerdam 2, 4 and 6 were analyzed respectively 7, 8 and 12 slag inclusion, inside the ship Woerden 7 were analyzed 16 slag inclusion, and inside the reference sample of Heeten were analyzed only 5 inclusion. This amount of inclusions is the result after the exclusion of the unsuitable ones. The factors used to discriminate the suitable inclusions to the unsuitable ones are directly linked to the chromatogram given by the instrument after the test. From this chromatogram were distinguished the different sections analyzed during the ablation with the laser, so is possible to understand if the instrument was analyzing the slag inclusion or the metal alloy, on the basis of this was decided which measurements were correct to try to understand the provenance of the iron alloy.

[8] The amount of inclusion present inside the analyzed sample is in the order of hundreds, as seen in the results chapter.

ppm	Sc 45	V 51	Cr 52	Rb 85	Sr 88	Y 89	Zr 90	Nb 93	Cs 133	La 139	Ce 140	Pr 141	Nd 146
ZW2	47,8 ±3,3	247,3 ±17,5	236,7 ±18,5	106,4 ±7,0	136,0 ±8,3	418,8 ±31,0	253,2 ±18,7	12,9 ±0,9	17,9 ±1,7	189,6 ±16,6	372,0 ±32,3	54,0 ±4,4	245,1 ±21,2
ZW4	6,1 ±0,5	30,9 ±1,7	37,8 ±2,6	45,9 ±2,3	195,8 ±12,2	15,4 ±1,2	225,7 ±17,9	7,1 ±0,5	1,0 ±0,1	15,7 ±1,2	32,6 ±2,5	3,7 ±0,4	14,8 ±1,2
ZW6	10,9 ±1,4	103,4 ±11,4	61,2 ±6,9	52,0 ±3,6	113,2 ±8,6	194,1 ±18,7	100,9 ±10,8	6,5 ±0,6	3,6 ±0,4	78,7 ±8,6	96,4 ±11,7	17,0 ±1,7	74,2 ±7,7
W7	10,3 ±0,7	127,0 ±8,9	152,0 ±11,3	65,0 ±4,6	89,0 ±6,3	39,0 ±3,1	126,0 ±10,3	6,9 ±0,6	8,6 ±0,6	26,7 ±2,4	47,1 ±4,5	6,7 ±0,6	28,1 ±2,6
Heeten	2,2 ±0,4	23,4 ±3,7	13,6 ±1,6	17,4 ±2,1	40,6 ±2,9	6,4 ±0,9	28,7 ±5,2	1,3 ±0,2	0,8 ±0,1	5,1 ±1,1	10,6 ±2,2	1,3 ±0,3	5,1 ±1,2

ppm	Sm 147	Eu 151	Gd 157	Tb 159	Dy 161	Ho 165	Er 167	Tm 169	Yb 172	Lu 175	Hf 178	Ta 181	W 182
ZW2	59,0 ±4,6	13,5 ±1,1	65,3 ±4,9	9,2 ±0,6	60,4 ±4,3	11,7 ±0,9	33,8 ±2,5	4,3 ±0,3	26,4 ±1,9	3,7 ±0,3	6,6 ±0,5	0,8 ±0,1	0,6 ±0,1
ZW4	2,7 ±0,3	0,5 ±0,1	2,5 ±0,3	0,3 ±0,06	2,5 ±0,2	0,5 ±0,05	1,6 ±0,2	0,2 ±0,03	1,6 ±0,1	0,2 ±0,04	6,6 ±0,4	0,5 ±0,04	0,3 ±0,1
ZW6	15,0 ±1,7	3,4 ±0,5	17,7 ±1,9	2,5 ±0,3	17,7 ±1,8	4,1 ±0,4	13,0 ±1,6	1,7 ±0,1	11,5 ±1,2	1,7 ±0,2	2,4 ±0,4	0,3 ±0,05	1,2 ±0,1
W7	6,3 ±0,6	1,4 ±0,1	6,2 ±0,6	0,9 ±0,1	5,8 ±0,5	1,1 ±0,1	3,3 ±0,3	0,4 ±0,1	3,0 ±0,2	0,4 ±0,04	3,3 ±0,3	0,4 ±0,05	2,9 ±0,2
Heeten	1,0 ±0,3	0,4 ±0,1	1,3 ±0,3	0,2 ±0,04	1,2 ±0,2	0,2 ±0,03	0,6 ±0,1	0,1 ±0,02	0,6 ±0,1	0,1 ±0,02	0,9 ±0,2	0,1 ±0,03	0,7 ±0,2

ppm	Pb 208	Th 232	U 238
ZW2	1,1 ±0,1	15,4 ±1,1	31,4 ±2,2
ZW4	0,2 ±0,04	4,6 ±0,2	1,5 ±0,1
ZW6	0,2 ±0,05	5,9 ±0,5	28,0 ±3,2
W7	16,7 ±1,2	5,1 ±0,4	11,2 ±0,8
Heeten	0,7 ±0,03	1,4 ±0,2	4,2 ±0,5

Table 1: schematic overview of the average values of the elements inside the analyzed slag inclusions

DISCUSSION

1 THE IDENTIFICATION AND THE CHARACTERISTICS OF THE IRON ALLOY:

Some of the features in the nails of the Zwammerdam and Woerden ships, shown under the microscope, are better explained when linked to the results obtained with the Vickers hardness test. Firstly areas with grains of ferrite are visible, signs of a very low level of carbon inside the metal (fig 50). This situation is characteristics of steel with very low content of carbon. Areas with different level of this element as well as areas with the decarburization effect were presents. In the field of ancient metallurgy the decarburisation is an effect where two areas of the iron alloy have different carbon content. This effect were observed in many nails i.e. the Zwammerdam 6-7 inwhich areas made by only ferrite are close to areas where is present ferrite plus pearlite. This is a proof of the increase of the carbon has shown in fig. 50. This type structure suggests the identification of the alloy as low carbon steel, characterizes by the presence of heterogeneous structure with high quantity of carbon. The second evaluated feature is related to the grain size all over the surface of the samples. The grain size is a characteristic linked to the working processes (Scott 1991). The general situation of the entire set of the nails shows an alloy with bigger grains of ferrite, ASTM around 2, in the middle; the external sides of the head and of the stem and in the tip on the contrary have a grain size around 7. This situation is due to successive re-heating of the iron during the working process. The iron can be work in two different way in a cold one, without the heating process, or with successive re-heating of the material to renew the malleability and the ductility, which made the material workable again. This process is called annealing (Scott 1991). The annealing process leave impressions on the crystallography; the ferrite grains undergone to a re-crystallization process, on the base of the cooling rate and on the hot working, different structures were created. In the case of these nails the results of this process are areas of small grains that interest the external sides of the

objects. This feature is observed in all the analyzed nails from all the Zwammerdam and Woerden ships. A perfect example is taken from the ZW4-7 nail where the difference in grain size between the inner and the external areas is clearly visible (fig. 51).

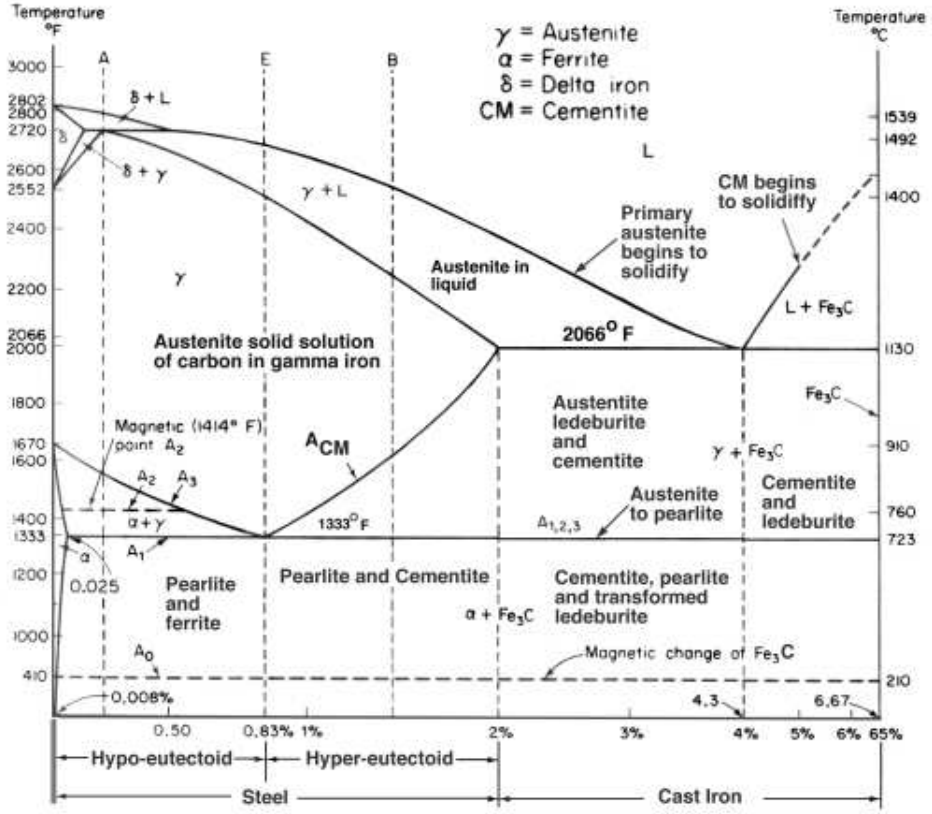

Figure 50: Diagram iron-carbon phase diagram

1.1 ZWAMMERDAM 2:

The nails taken from the Zwammerdam 2 ship show two different patterns. The first one is linked to the nails ZW2-2 and ZW2-3. These nails have a homogeneous arrangement, the structure related to a fast cooling of the artefacts are not present. It is present only a different in the grains size, from the internal area, where the bigger grains with ASTM around 3 are present, to the external and the tip one, where the ASTM number is around 7. A different situation has been observed in the ZW2-GG2K and ZW2-GE2K. The grain structure inside these nails is very heterogeneous if compare to the other nails of this ship. These nails are characterized by the presence of numerous layers; which is probably due

to different step in the production process. Pieces of iron (from different bars or residual of other work) were weld together. This process has probably created the layered structure, as last passage to obtain the finished objects, the iron has undergone to the hammering to shaping it. This hypothesis is corroborated by four different observed features:

- The highly layered structure of the iron, which could be a symptom of different working process between different layers.
- The elongated shape of the slag inclusions present inside the metal due to the hammering.
- The presence of small areas characterized by the presence of acicular ferrite with widmanstatten pattern in the inner part of the metal, symptom of a folding process. The presence of areas with this particular pattern could be another proof of the use of different iron pieces.

Figure 51: Sample ZW4-7c macro x25 in the lower part the difference in grain size is visible, possibly due to the hammering and the re-heating in the external side of the stem.

1.2 ZWAMMERDAM 4 AND 6:

One of the most interesting aspects that have to be highlighted of the Zwammerdam 4 and 6 ships is related to the cooling process. As seen in the previous chapter, inside the metal of the nails taken out from these two ships, areas with acicular ferrite were identified. This is related to a fast cooling of the material, but with only the observation under the microscope it is impossible to estimate if this cooling is previous or congruent with the smithing process of the nail. The different areas with this particular structure present inside the metal suggest that this process could be linked to the smithing of the iron bar, because is only during that process that the iron is folded and thus the layer with faster cooling can go in the inner part of the metal.

Inside the interstitial areas between the different crystals of acicular ferrite dark areas are present, which can be classified as consisting of pearlite, bainite or martensite. The evaluation of which one is the real phase involved without any other data is extremely difficult. In this case the Vickers hardness test gives useful information. A distinction between the three phases on the basis of the hardness was made. In the literature (****) it was found that the pearlite has a hardness between 200 and 300, the cementite has an hardness around 700, the bainite has an hadress between 340-700 and at least the martensite has an hardness around 800, in the Vickers test, with a load of 100 g. The range of the prearlite is precisely the one found in all the nails. This situation suggests that the darker areas are pearlite, but the presence of the other phases cannot be completely excluded since the crystals of these phases could be smaller than the dimensions of the indenter. The situation described here is particularly evident inside the nails ZW4-6 and ZW6-7 where a zone was observed with this specific characteristic (visible bright crystals of acicular ferrite and darker areas with a dimension bigger that the indenter of the Vickers test). This is clearly a heterogeneous material, with different values of carbon, different degrees of re-heating and different rates of cooling. In the right upper part of figure 52 small crystals (ASTM 7) of ferrite with few black areas between them, indicating low carbon content, is observed. In the central area acicular shaped crystals of ferrite are visible, pointing to a local faster cooling than the surrounding areas, as said before, this situation, in the inner part of the alloy, could be related to the folding process during the smithing of the bar.

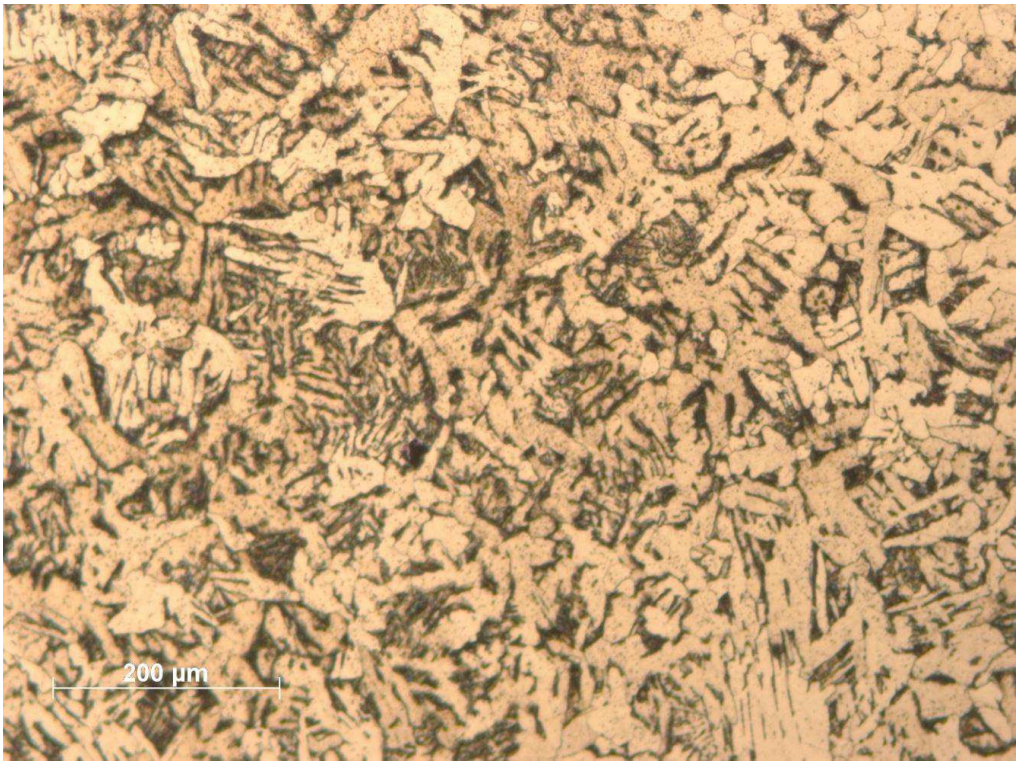

Figure 52: sample ZW4-6c x100 difference in the grain shape due to different cooling rates

Not all the nails of these ships show this feature, for example the nails taken from the Zwammerdam 6 ships have a structure that is characterized by the presence of different layers. This situation, similar to the one observed in the Zwammerdam 2 nails, but the case of Zwammerdam 6 is not the result of a massive welding of different pieces of iron. The homogeneity of the structure excludes this possibility which is probably due to a high degree of hot working of the iron. The iron was probably folded many times. The presence of different layers characterizes not only the nails of the Zwammerdam 6 ship but in general it is possible to find a layered structure in all the analyzed nails. This situation was most probably created by smithing the bloom into an iron bar. It was heated, shaped and folded by hammering when hot, to obtain the bar. The second effect of the cold working, visible under the optical microscope, is the formation of slip lines. The slip lines are the results of an intense hammering of the surface. This effect is due to the slipping of the planes of the crystalline structure. It is possible to observe this effect under the microscope because the slipping of the crystal plane create imperfections that reflect the light in a different way with respect to the surrounding crystals, thus black

straight lines are observerd inside a single crystal. A good example of this situation is visible inside the head of the nail ZW6-10 (fig 53), where most of the grains show this effect. The fact that not all the metal's crystals show this effect is due to the orientation of the grains themselves and to the polishing effect that could have cut the crystal in a way that the slip lines are invisible.

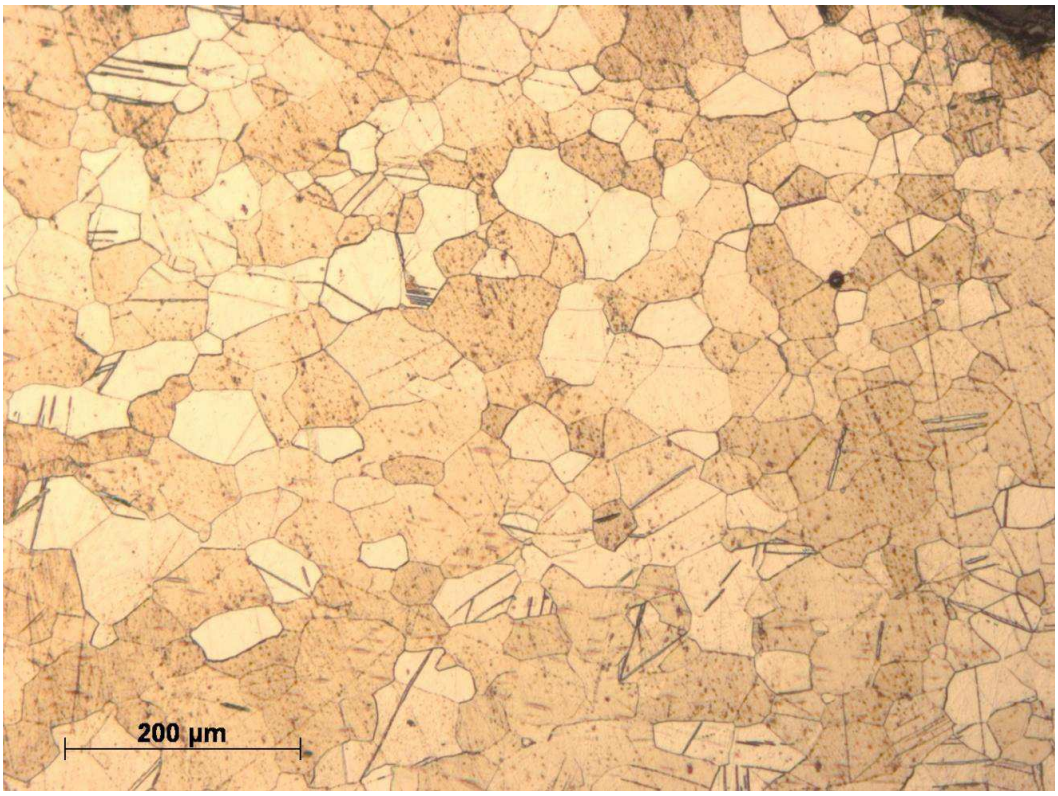

Figure 53: Sample ZW6-10a x100 slip lines inside the grains of the head of the nail

In conclusion the nails from the Zwammerdam ship are all characterized by a heterogeneous metal structure. The main features of this structure is the difference in the crystalline arrangement, due to the different carbon content, higher in the darker areas of pearlite and lower in the ferrite. In the external side the formation of grains of smaller size (ASTM 7) was observed, on the contrary in the inner part of the metal, the one generally with lower carbon content, big grains (ASTM around 3) were observed. The structure of the majority of the nails, taken from the Zwammerdam 4 and 6, is layered.

These layers are probably due to the smithing process to shape the iron into a bar or into the object.

The last aspect that has to be highlight is the difference in the structure between the straight/bended nails of Zwammerdam 2 and the other nails taken from this ship. The couple bended/straight nails are characterized by a high heterogeneous structure, with many layers and different grain size. This feature suggests the use of different iron pieces welded together, and then shaped into a nail, fact totally different if put in relation with the characteristics of the other nails of this ship.

1.3 PHOSPHORUS

The observation under the microscope has highlighted the presence of phosphorus (P) in most of the analyzed nails. According to the EDS analysis around 0,4-0,5 wt% of P was present but only in few specimens and in few areas. This discordance with the OM and the EDS is due to the detection limit of the EDS system which is around 0,1 wt%. With the used setting, with an acceleration of 15 keV, the identification is probably still difficult, to avoid this problem could be useful the use of another type of microprobe analysis, able to detect with less problem the low wt% of phosphorus inside the metal. The phosphorus effect is particularly evident in two nails of the ship Zwammerdam 2: ZW2-GE2K and ZW2-GE2R., in one of the nails taken from the ship Zwammerdam 4: ZW4-7; in two nails of the ship Zwammerdam 6: ZW6-7 and ZW6-8; and at last in one nail of the Woerden ship: W7-8. The presence of the phosphorus effect over the surface of only these nails might indicate a different origin of the raw material. The phosphorus inside the metal core originates from the phosphorus already present inside the ore used to produce the iron. The problem related to the use this data is linked with the conformation of the samples. The samples are all embedded in a resin holder which allows the investigation of only the superficial layer. This confirmation makes impossible the investigation of all the internal layers that made the nails. Thus is impossible to say if in an inner part of the other nails might be present the phosphorus.

The P distribution could be taken into account when the provenance is evaluated, without any precise data about the real weight percentage inside the metal, obtain with a specific microprobe test, is better not to take into account as provenance discrimination.

1.4 HARDNESS

The nail of the ship Woerden 7, like the nails of the ship Zwammerdam 2, is characterized by a homogeneous structure. Therefore, it is possible to study the quality of the iron alloy by the Vickers hardness test. As described in the results chapter (pag. 54-64), most of the nails have shown an increase of the hardness from the stem to the tip. If the hardness measurements are compared to the crystallographic structure of the metal it is observed that the smaller the grains, the higher the hardness of the metal. This could be an indication of the level of hammering. A clear example of that is the tip of the nail W7-8 which has a hardness of HV 237 and a grainsize of ASTM 7 (fig 54). This value is higher than the average value, which is HV 160, registered along the entire length of the nail where the grain size and is between ASTM 1 and 2. Thus the difference in hardness could be linked to the grain size, and thus to the hammering, which is more intense in the external areas than in the core. If this parameter is compared with that of the same type of objects in literature (Angus N. S., Brow G. T., Cleere H. F. 1962, E.G. Godfrey, 2007, and C. Mapelli, W. Nicodemi, R. F. Riva, M. Verdani, E. Gariboldi, 2009) and with different objects made with comparable material during a similar period (Fulford, Sim, Doig, Painter, 2005) the similarity in the obtained values is clear. Unfortunately the high diversity of the values registered makes the data not useful to a statistical evaluation, but only for a precise evaluation of the characteristics of the micro areas analyzed.

In conclusion the phosphorus was detected in less nails than what the OM have reveal. This is due to the detection limit of the instrument and to the conformation of the samples themselves. The phosphorus inside the metal core could suggest a difference in the raw material used, but without a precise evaluation of the weight percentage is better not to take into account this data for provenance discrimination. The only nails with this element inside the metal are: ZW2-GE2K and ZW2-GE2R., the ZW4-7; the: ZW6-7 and ZW6-8; and at last the W7-8.

The hardness is a parameter that allows a comparison with the literature. In this comparison the nails of the Zwammerdam and Woerden ships result comparable to the ones of the Scottish fortress of Inchtuthil. The high diversity in the registered value of the hardness makes the obtained data not suitable for a statistical evaluation.

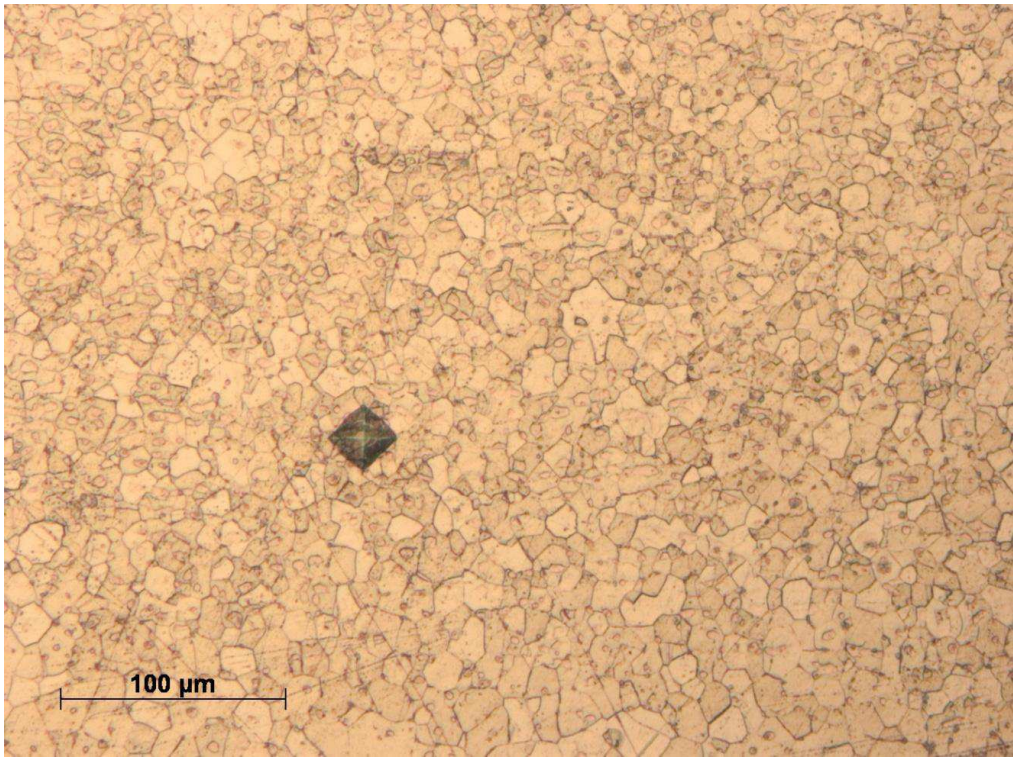

Figure 54: Sample W7-8 g x200 of the hardness test HV 237, the indentation of the diamond is clearly visible

2 THE DIVISION OF THE SHIPS ON THE BASIS OF THE ELEMENTAL COMPOSITION OF THE SLAG INCLUSIONS:

The chemical composition of the slag inclusions and the concentration of phosphorus inside the metal is analysed by EDS. To obtain the average value of the error, linked to the measurements, and the average value of the weight percentage two different formulas were applied. The first formula (1) was applied to reduce the error:

$$\sigma_y^2 = \frac{1}{\sum_{i=1}^{n}\left(\frac{1}{\sigma_i^2}\right)} \quad (1)$$

Where:

σ_y^2 = The squared value of the averaged error link to the concentration value

σ_i^2 = The squared value of every error linked to every measurement, the not squared number is given by the instrument.

With this formula a new reduced error of the measurements is obtained, which takes the quantity of the measurements to reduce the error itself into account. The more data were obtained from the instrument, the smaller and more precise the new error linked to them will be. The formula 2 is used to calculate the average value of the quantity of every chemical element found inside the slag inclusions and the metal alloy. The formula is:

$$\overline{X} = \frac{\sum_{i=1}^{n}\frac{y_i}{\sigma_i^2}}{\sum_{i=1}^{n}\frac{1}{\sigma_i^2}} \quad (2)$$

Where:

$\bar{X}$ = It is the average quantity value of the element take in consideration.

y_i = It is the value of the element given by the instrument.

σ_i^2 = It is the value of the error squared, given by the instrument and the same as in formula (1)

This formula allows obtaining an averaged quantity value of the element taken into account, in this way every value is directly linked with its specific error and the averaging process results in more precise and more accurate quantification than a standard averaging operation.

In the case of the metal alloy the problem, as said in the previous chapter, is the detection of light elements, i.e. carbon and phosphorus, because their quantity is close to the detection limit of the instrument. A specific case is the carbon content inside the metal alloy. The capacity of detection of this light element is influenced not only by the detection limit of the instrument but also by possibility of the pollution of the chamber of the SEM and the pollution of the sample, i.e. thin layer of dust/dirt. This situation creates the condition to obtain data that are affected with by many errors and thus make the use of them difficult. For all these reasons it was decided not to take into account the data relative to the carbon content given by the instruments.

The data obtained from the SEM-EDS analyses allow some observations on the different ships based on the chemical elements inside the slag inclusions. The nails of the Zwammerdam 2 are characterized by a widespread presence of manganese and magnesium. This also accounts for the Woerden 7, but in this last ship also inclusions without one of the two elements were found. In case of the other ship, i.e. Zwammerdam 4 manganese was detected in only 5 cases and in Zwammerdam 6 it was detected in 17 cases (how many inclusions were analysed which percentage of inclusions contains Mn and/or Mg). The averaged EDS values are given in Table 2

		P	Si	Al	K	Ca	Mn	Mg
ZW2-2	Wt %	0,45	24,75	8,9	2,23	2,17	3,196	0,99
	Error ±	*0,06*	*0,06*	*0,06*	*0,03*	*0,04*	*0,1*	*0,03*
Zw2-3	Wt %	1,00	3,91	0,96	0,49	0,63	0	0
	Error ±	*0,03*	*0,04*	*0,03*	*0,03*	*0,03*	0	0
ZW2-GE2K	Wt %	3,55	8,85	1,72	0,67	0,68	0	0
	Error ±	*0,04*	*0,05*	*0,05*	*0,03*	*0,03*	0	0
ZW2-GE2R	Wt %	2,09	7,12	1,63	0,28	0,41	0	0
	Error ±	*0,02*	*0,03*	*0,02*	*0,03*	*0,02*	0	0
ZW2-GG2K	Wt %	0,93	11,34	3,14	1,04	1,07	0	0
	Error ±	*0,01*	*0,03*	*0,02*	*0,01*	*0,02*	0	0
ZW2-GG2R	Wt %	0,8	10,49	4,99	1,05	0,88	0	0
	Error ±	*0,01*	*0,02*	*0,02*	*0,01*	*0,01*	0	0
ZW4-6	Wt %	8,09	2,44	0,57	1,11	0,96	0	0,61
	Error ±	*0,03*	*0,02*	*0,02*	*0,02*	*0,02*	0	*0,02*
ZW4-7	Wt %	2,00	16,56	2,48	1,99	2,96	0	0,84
	Error ±	*0,03*	*0,04*	*0,02*	*0,03*	*0,03*	0	*0,02*
ZW6-7	Wt %	1,2	10,27	3,04	2,23	2,12	3,46	0
	Error ±	*0,02*	*0,04*	*0,03*	*0,03*	*0,03*	*0,1*	0
ZW6-8	Wt %	1,34	14,3	4,02	1,34	1,48	0	0
	Error ±	*0,02*	*0,03*	*0,03*	*0,02*	*0,02*	0	0
ZW6-9	Wt %	2,2	12,42	2,4	1,53	1,62	0	0,63
	Error ±	*0,02*	*0,03*	*0,02*	*0,02*	*0,02*	0	*0,02*
ZW6-10	Wt %	1,41	11,1	3,05	1,31	1,68	0	0,67
	Error ±	*0,02*	*0,04*	*0,03*	*0,03*	*0,03*	0	*0,03*
ZW6-13	Wt %	1,2	6,63	1,86	0,74	0,67	0	0
	Error±	*0,03*	*0,04*	*0,03*	*0,04*	*0,03*	0	0
W7-8	Wt %	1,01	13,17	3,88	1,55	1,24	1,88	0,5
	Error ±	*0,02*	*0,03*	*0,02*	*0,02*	*0,02*	*0,04*	*0,02*

Table 2: averaged value of the elemental composition of the analyzed slag inclusion

The data in table 1 show that in all the ships are presents phosphorus, silicon, aluminium, potassium and calcium. Magnesium and manganese were detected only in some nails of the Zwammerdam and Woerden ships.

Based on this data it is possible to create a classification of the nails that come from different ships, but are similar in the slag composition. This aspect is particularly important in the evaluation of the production of the different ships. The fact that nails from different ships are comparable from the chemical point of view is very important

because it suggests a similarity in the used material, i.e. the nails used can come from the same iron bar or from the same place of production.

From the achieved data is possible to link the nails ZW2-2, ZW4-6, ZW4-7, ZW6-9, ZW6-10 and W7-8 on the basis of the magnesium, and the ZW2-2, ZW6-7 and W7-8 on the base of manganese. All the others nails are put in another class related to the nails without these two elements.

These observations suggest a difference in the raw material used during the production of these artefacts. Inside the slag inclusion are present elements, which during the production process were almost completely reduced, thus they influence the final composition of the inclusion themselvess. (Dillmann and L`Heritier, 2007). An example of this process is the final composition of the slag inclusion that can be constituted by three different types (Dillmann and L`Heritier, 2007):

- A complete glassy structure with a composition in prevalence of aluminosilicate compounds and very low iron content.
- An intermediary phase formed by iron oxide and aluminosilicate compounds such as fayalite (Fe_2SiO_4), which is the main situation founded inside the analyzed slag inclusions.
- A total iron oxide composition.

On the other hand there are elements, detectable by the EDS system, that are not reduced during the production process, or that are totally or in part re-oxidised REF. These elements can be interpreted to be part of compounds like MgO and MnO (when present), Al_2O_3, SiO_2, K_2O and CaO, These compounds are already inside the system during the production process, i.e. in the ore, the charcoal and the furnace lining. A clear example of this situation is the SiO_2/Al_2O_3 ratio that describes the quantity of added sand inside the metal sand during furnace lining. The graphic 1 below shows that the slag inclusions from the sample ZW6-8 are not suitable for further investigation, because in this case the ratio is a flat line. This situation means that there is an excess of Al_2O_3 that was not involved in the formation of any crystal. Thus it this excess derived for an external adding. Similar results are yielded for the samples taken from the ship ZW6-9.

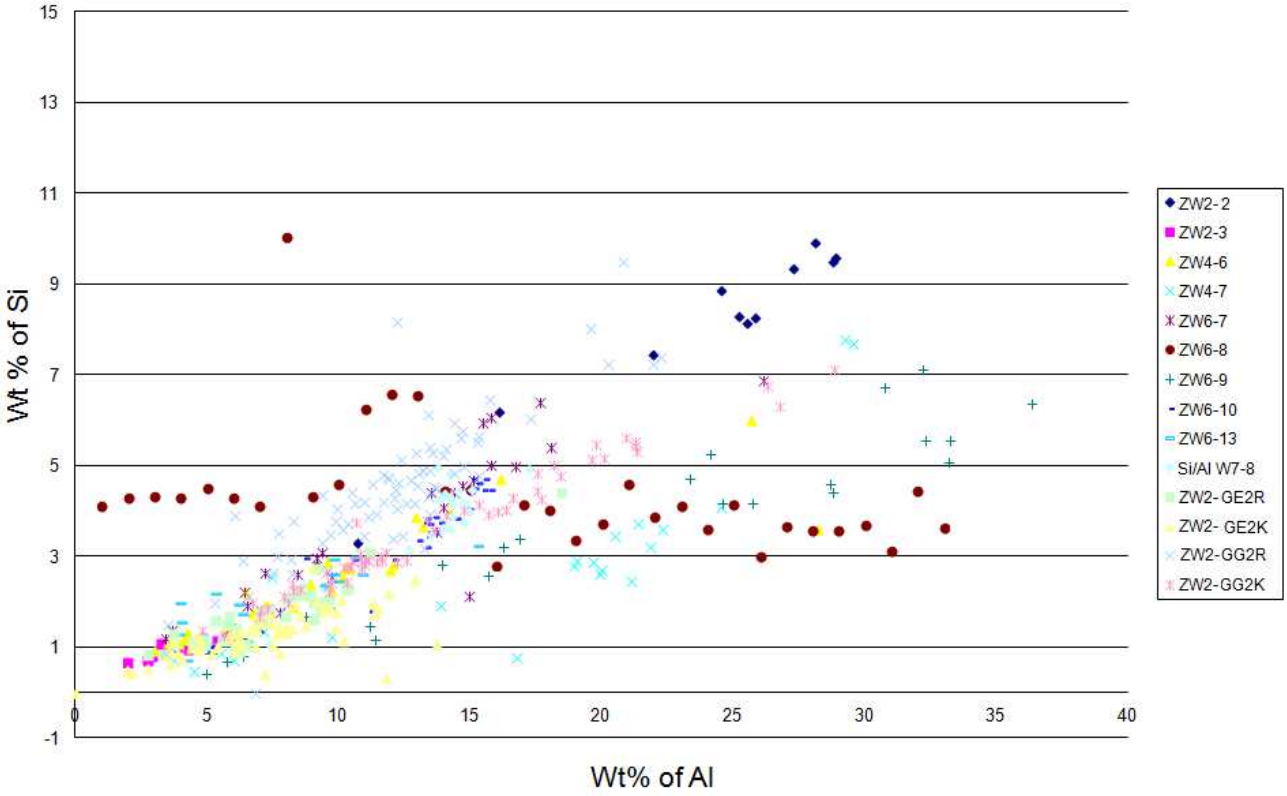

Figure 55: Elemental ratio of wt%Si and wt%Al

3 LASER ABLATION – INDUCTIVELY COUPLED PLASMA – MASS SPECTROMETRY RESULTS

The results of the EDS analyses have shown that the slag inclusions cannot be characterized by the significant presence of any particular elements, except for the silicon, but this element cannot be used for a discrimination of the provenance, because it is one of the most common elements all over the Earth's crust. For this reason the identification of a possible production site by EDS analyses is not possible. Thus it was decided to use the trace elements, based on the works of Leroy et all (2011), in order to characterize the slag inclusions and to determine if the nails could come from the place of the production site of Heeten.

The data obtained from the laser ablation- inductively couple plasma- mass spectrometry (LA-ICP-MS) have shown that there are similarities between some ships based on the concentration of elements found in the slag inclusions. The concentration of Sc, Nb, Th, in the ships Zwammerdam 6 is comparable to the one inside the ship Woerden 7; similar situation is related to the concentration of Hf and Ta in the ship Zwammerdam 2 comparable to the ship Zwammerdam 4. These similarities are related the absolute concentration of an element inside a slag inclusion, but more important is the ratio between this elements, that describe the crystallographic organization of the elements inside the inclusions.

Based on the work of Desaulty et al (2009) and Leroy et al (2011) the elements were chosen and how to manage and understand the results given by the instrument.

Only the elements that pass directly without being contaminated inside the slag during the production process, on the base of the data obtain from experimental bloomery smelting made by Leroy et all (2011) were chosen; also some other elements that pass into the slag with pollution, made by the lining or by the charcoal, are selected. Couples of elements using geochemical consideration (what do you mean) were created to manage the obtained data. Only couples of elements which can substitute each other in the crystal structure are selected. Therefore it is necessary that the elements have similar ionic radii

and similar valence. Thus was decided to follow the methodology taken from Desaulty et al (2009):

- Hf/Nb
- Y/Yb
- Th/U
- Eu/Sm
- Sm/Th
- Th/sc
- La/Yb
- Cs/Rb
- Y/La
- Ce/La

The following couples seem to be the most promising in studying the origin of the iron:

- The ratio between Eu and Sm was selected on the Eu oxidation degree, this degree can change and consequently also changes the value of the ratio from one production place to another, and thus it is useful parameter to distinguish different places of production.
- The ratio between Sm and Th was selected because these two elements have a similar behaviour during the all the phases of the sedimentary process (desegregation, transport and diagenesis), thus it is probable they have a constant ratio in the same area of production.
- The ratios between Th/Sc and La/Yb ratio are chosen because these elements are often used in the study on the modification process of the upper Earth's crust (Desalty et all 2009)

The trend of these ratios is mathematically described by the inclination of the linear relationship that links all the points together. If two classes of points, which are plotted in different areas of the graph, lie along the same line; it means that there is a connection between those classes of points. This connection describes a situation in which the quantity of the analyzed elements is different, but the lattis organization of these elements inside the crystalline structure, which form the slag inclusion, is the same. Thus the crystals that form the inclusion itself are the same and so a connection between the raw materials of the two different artefacts can be established.

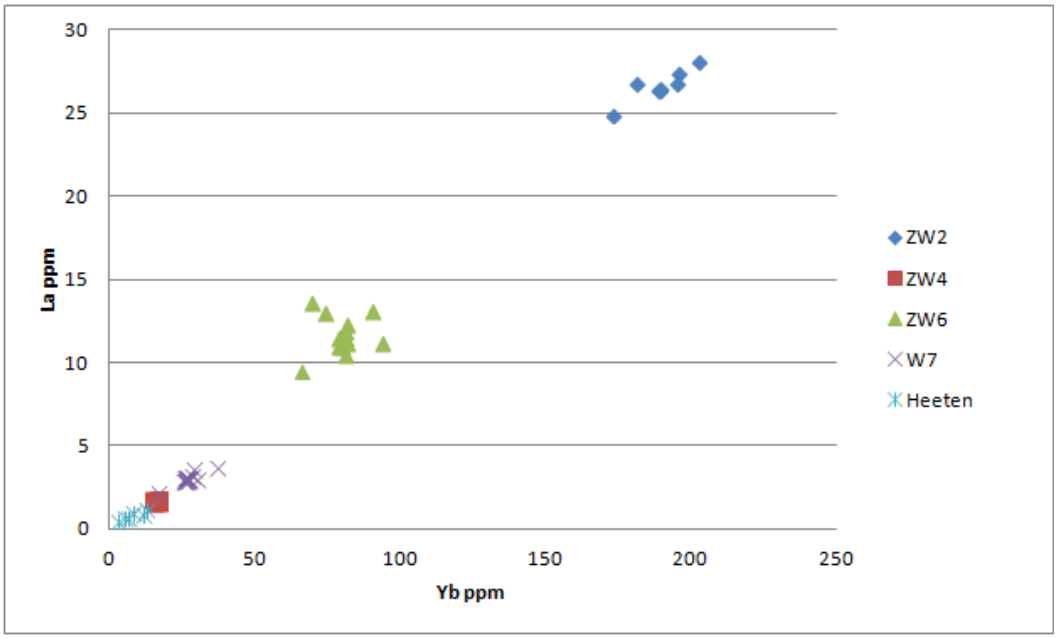

Figure 56: graph in which is plotted the ratio between Lanthanum and Ytterbium

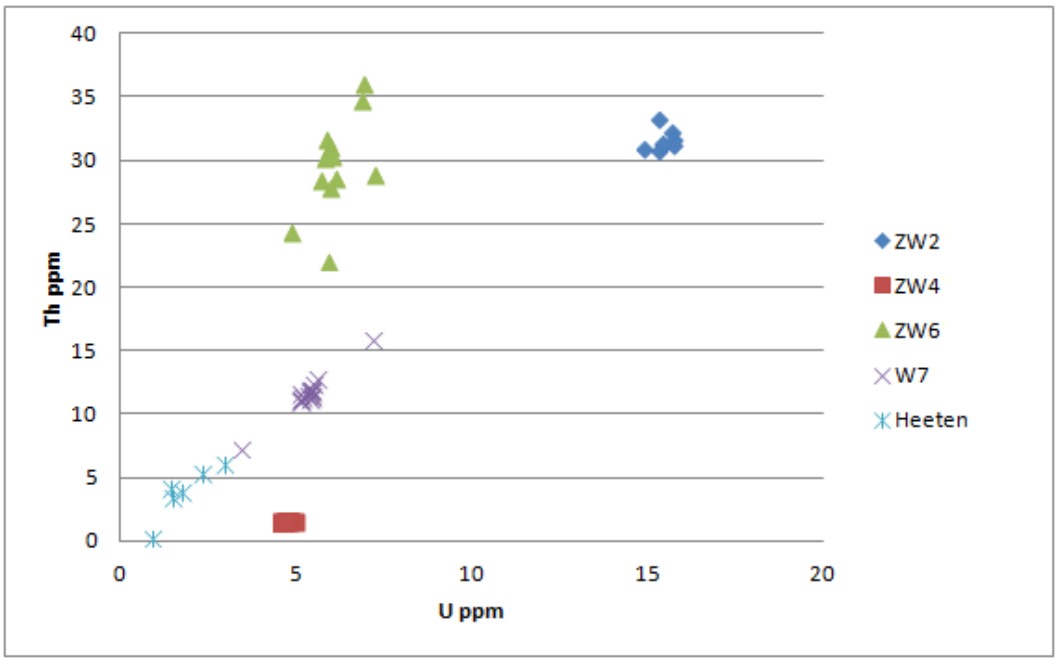

Figure 57: graph in which is plotted the ratio between Th/U

Inside this graph is clearly visible that there is a relation between the ship Woerden 7, Zwammerdam 2 and the reference sample of Heeten. The ships Zwammerdam 4 and 6 have a cloud of point that is very difficult to describe with only one line, and this line has

a different slope than the one that connect the ships Zwammerdam 2 and Woerden 7 with the samples from Heeten.

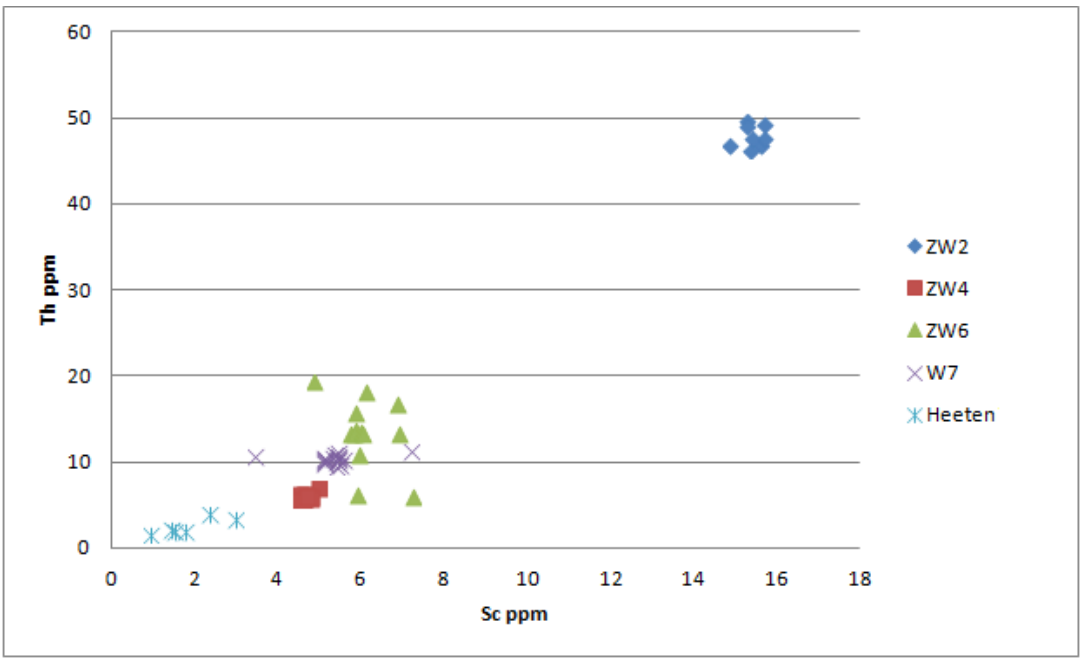

Figure 581: graph in which is plotted the ratio between Th/Sc

The last graph (fig. 58) shows a situation where is possible to create only a correlation between Heeten and the ship Zwammerdam 4. In the other cases are very difficult to create the mathematical lines to describe the trend of the data, because several lines with several slopes could describe the situation. The graphs above (fig. 56 and 57) describe a situation where there are similarities and differences. In conclusion it seems possible to create some correlations between the different ships, and in few cases also a relation to the iron production site of Heeten, but these similarities are not enough for a proof that the provenance of the iron used for build these ships is unique and that the iron came from the site of Heeten. To be really conclusive is necessary to create a standardization of the reference samples, the ones that have given more problems during the analyses. It is also necessary to collect a bigger amount of data, not only of the finished object but also of the bloom and of the raw material.

CONCLUSION:

The type of iron used to produce the nails is low carbon steel with a phosphorus concentration around 0,4-0,5 wt%, characterized by several layers of material. The crystallographic structure is made by ferrite grains with different ASTM sizes, from 2, in the inner part of the nail, to 8, in the external sides and in the tip. Structures of acicular ferrite, surrounded by zones of pearlite, are present in particular inside the nails taken from the Zwammerdam 4 and 6. The lower grain size is an indication that the head of the nail, the tip and the external sides of the stem were hammered. The hardness of the nails is in line with that of other objects produced in the same period all over the Roman Empire. The EDS analysis has shown that the principal composition is made up of silicon, aluminium, potassium, calcium and phosphorus. Some nails contain also manganese and magnesium, and other elements like titanium and barium, which were used to discriminate between ships. The composition of the slag inclusions of Zwammerdam 2 and Woerden 7 is comparable. It is possible to create a correlation between the nails ZW2-2, ZW4-6, ZW4-7, ZW6-9, ZW6-10 and W7-8 on the basis of the magnesium, and the ZW2-2, ZW6-7 and W7-8 on the base of manganese. All the others nails are put in another class related to the nails without these two elements.

The graphs of the LA-ICP-MS show, in certain cases, a correlation between some ships and the reference samples of Heeten. To be really conclusive is necessary to create a standardization of the reference samples, the ones that have given more problems during the analyses. It is also necessary to collect a bigger amount of data, not only of the finished object but also of the bloom and of the raw material. For the available data is possible to say that are presents some correlation between the iron production site of Heeten and the Zwammerdam and Woerden ships, but these correlation are not enough to validate the provenance, that for now have to be excluded.

FORWARD RESEARCH:

To be more conclusive about some of the analyzed characteristics, further research needs to be done. Several recommendations will be given in this section.

This research project started with the selection of samples from a precedent study (Mol 2012), focused on the archaeological aspects of these artefacts. In that work only the nails that belong to the type II were selected, the most common ones, for the characterization of the production and the use of the nails. In this thesis work, as a prosecution of the research, it was decided to focus on technical features of the implied alloy and on the provenance. For a real and deep study of the production techniques and for a better understanding of the technological level during that time, in the field of Roman ship archaeology, it is necessary to extend the research also on the others nail's types.

To study the quality of the metal and the components present inside the alloy, i.e. the carbon, phosphorus, etc (which elements?) content, it is suggested to use atomic absorption spectroscopy (AAS), Auger electron spectroscopy (AES) or electron probe micro analysis (EPMA). because... copy part from discussion above!

More literature research to find data about the (microstructural/elemental/?) characteristics of the ancient iron, the decarburization process and the creation of a specific phase diagram (I think you mean cct diagram) are recommended.

A lesser amount of averaging during the performing of the LA-ICP-MS test is recommended. The test requires the quantity of the elements inside the chosen standards and the quantity of a know elements for an internal calibration of the results. For the calibration of the spectra it was decided to use the average value of the silicon inside the slag inclusion achieved with the SEM-EDS analyses. Thus the use of the precise quantity of an element for a specific slag inclusion is recommended to obtain a more precise data.

The use of mirco X-ray Diffraction (XRD) to investigate the crystalline structure inside the slag inclusions to precise identify the crystal present is recommended.

BIBLIOGRAPHY:

Agricola, Georgius Herbert Clark and Lou Henry Hoover (editors and translation) 1950 [1556] *de re metallica*, Dover Publications Inc. , New York.

R.L. Smith & G.E. Sandland, 1922, *An Accurate Method of Determining the Hardness of Metals, with Particular Reference to Those of a High Degree of Hardness,* Proceedings of the Institution of Mechanical Engineers, Vol. I, p 623–641.

Ucelli Guido, 1950, *Le navi di Nemi*, la libreria dello stato, Roma, 147-180, 265-283.

Angus N. S./ Brow G. T./Cleere H. F. 1962 *The iron nails form the legionary fortress at Inchtuthil, Pertshire,* journal of the Iron and Steel Institute, November, 956-968.

Haalebos, J.K. 1977, *Zwammerdam Nigrum Pullum. Ein Auxiliarkastell am Niedergermanischen Limes.* Cingula 5. Amsterdam.

Peter Kresten 1984 *The mineralogical and chemistry of selected ancient iron slag from Dalarna, Sweden with contributions by Inga Serning,* Archeometallurgical Institute, University of Stockholm.

Hammer Friederike 1984 *Industry in north-west Roman Southwark*, London, English Heritage, molas monograph, 13-25 125-147.

Laures F.F., 1984 *Note and news. The evolution of antique ship construction in the Mediterranean: A hypothesis* in: IJNA 323-325.

T. Stambolov, 1985 *The corrosion and conservation of metallic antiquities and works of art,* Central Research Laboratory for Objects of Art and Science, CL Publication, Amsterdam, the Netherland.

Beunder, P.C., 1986*, Castella en havens, kapellen en hoven van Albaniana tot Laurum, via Bode(lo)Grave en Zwanenburg. Enkele notities over: de oudste geschiedenis, de Romeinse kei-zertijd, en de vroege Middeleeuwen in de Rijnstreek rond Alphen a/d Rijn, Zwammerdam, Bo-degraven en Woerden. 30 jaar snuffelen naar het verleden in Midden-Holland*. Bodegraven.

Weerd, M.D. de, 1988, *Schepen voor Zwammerdam*. Dissertatie Universiteit van Amsterdam.

Scott David A. 1991 *Metallography and Microstructure of ancient and historic metals*, Singapore The Getty Conservation Institute.

M. Boniardi, E. Gariboldi, M. Vedani, 1992, *Metallographic studies on an ancient roman nail,* metallurgical science and technology, Teksid Aluminium S.r.l., Carmagnola, Torino, Italy.

Beat Arnold, 1992 *Batallerie gallo-romaine sur le lac de Neuchatel*, tome 1. Saint-Blaise, Editors du ruau (Archeologie neuchateloise, 12) 62-70.

1995 *Soil archive classification of European excavation sites in terms of impact of conservability of archeological heritage,* Iserlohn, Germany.

Philips Electron Optics, 1996 *Environmental scanning electron microscope an introduction to esem,* Robert Johnson associates, Eindhoven, the Netherlands.

Koehler, L. 1997, *Kano en Kaar. De documentatie van twee boomstamkano's uit Zwammerdam*. Dissertatie Universiteit van Amsterdam.

Enrico Franceschi, Luisella Macció, Daniela Palazzi and Lucilla Rosa, 1998, *The corrosion of merallic artefacts within different enviroments archeological objects and*

laboratories simulations, proceeding of the international conference on metals conservation, 92-93, James & James, London, United Kingodom.

Godfrey Eveline, Van nie Matthjs, 2003, *A Germanic ultrahigh carbon steel punch of late Roman-Iron age* journal of Archelogical Science 31, 1117-1125.

Mike R. Notis and Aaron N. Shugar, 2003, *Roman shears: metallography, composition and historical approach to investigation,* international conference Archeometallurgy in Europe, proceedings vol. 1, 109-118, Milan, Italy.

William D. Callister jr, 2003 *material science and engineering an introduction sixth edition,* John Wiley & Sons Inc.

I. de Groot, H. A. Ankersmit, R. van Langh, W. Wei, 2004, *Corrosion layers on historic iron artefacts, cathodic protection of iron artefacts during cleaning in acid solution,* proceeding of the international conference on metals conservation, 307-313, national museum of Australia, Canberra, Australia.

L. Selwyn, 2004, *Overview of archeological iron: the corrosion problem, key factor affecting tratements, and gaps in current knowledge,* proceeding of the international conference on metals conservation, , national museum of Australia, Canberra, Australia. pag 294-303

Dimitrij Kmetic, Jana Horvat, Franc Vodopivec, 2004, *Metallographic examination of the roman republican weapons from the hoard of Grad near Smihe,* Archeoloski vestnik, 55, pag 291-312.

Joosten Ineke, 2004, *Technology of early historical iron production in the Netherlands,* Institute for Geo- and Bioarcheology, Vrije Universiteit, Amsterdam, the Netherlands.

Schrüfer-Kolb Irene, 2004, *Roman iron production in Britain, technological and socio-economic landscape development along the Jurassic Ridge,* Archeopress, publisher of British archeological reports, Oxford, United Kingdom.

Fulford Michael, Sim David, Doig Alistar, Painter Jon, 2005 *In defence of Rome: a metallographic investigation of Roman ferrous armour from Northern Britain,* Journal of Archeological Science 32 241-250.

E.G. Godfrey, 2007, *The technology of ancient and medieval directly reduced phosphoric iron,* PhD at the department of Archeological sciences, University of Bradford, United Kingdom.

Dillmann Philippe, L`Heritier Maxime, 2007, *Salg inclusion analyses for studying alloys employed in French medieval building: supply of materials and diffusion smelting process,* Journal of Archeological Science 34 1810-1823.

Groot, T. de & J.-M. A. W. Morel, 2007, *Het schip uit de Romeinse tijd De Meern 4 nabij boerderij de Balije, Leidsche Rijn, gemeente Utrecht. Waardestellend onderzoek naar de kwaliteit van het schip en het conserverend vermogen van het bodemmilieu*. RAM-rapport 147, Amersfoort, the Nederlands.

Jansma, E. & J.-M.A.W. Morel (red.) 2007, *Een Romeinse Rijnaak, gevonden in Utrecht-De Meern. Resultaten van het onderzoek naar de platbodem 'De Meern 1'*. RAM 144 (Banden A, B en Band met vouwbladen), Amersfoort, the Nederlands.

E. Blom, Y. Vorst & W. K. Vos, 2008, `18. De "Woerden 7": Een Romeinse platbodem'. In: E. Blom & W. K. Vos (red.), *Woerden-Hoochwoert. De opgravingen 2002-2004 in het Romeinse castellum Laurium, de vicus en van het schip de `Woerden 7'*. ADC Monografie 2, 349-401, Amersfoort/Leiden, the Nederlands.

C. Mapelli, W. Nicodemi, R. F. Riva, M. Verdani, E. Gariboldi, 2009, *Nails of the roman legionary at Inchtuthil,* La metallurgia italiana, Milano, Italy, 51-58.

Desaulty Anne-Marie, Dillmann Philippe, L`Heritier Maxime, Mariet Clarisse, Gratuze Bernard, Joron Jane-Louis, Fluzin Philippe, 2009, *Does it come from the Pays de Bray? Examination of an origin hypothesis for the ferrous reinforcements used in French*

medieval churches using major trace element analysis, Journal of Archeological Science 36, 2445-2462.

P. Dillman, P. Fluzin, L. Long, G. Pages, 2010, *A study of the Roman iron bars of Saint-Marie-de-la-Mer (Bouches-Du-Rhone France). A proposal for a comprehensive metallographic approach*, Journal of Archeological Science, 38, 1234 1252.

M. Berrranger, P. Fluzin, 2011, *From raw iron to semi-product: quality and circulation of material during the iron age in france*, Archaeometry, 1-21.

S. Leroy, R. Simon, L. Bertand, A. Williams, E. Foy and PH. Dillmann, 2011, *First examination of slag inclusion in medieval armours by confocal SR-µ-XRF and LA-ICP-MS,* Journal of Analytical Atomic Spectrometry, 26, 1078-1087, Cambridge, United Kingdom.

Ian Holton, 2012, *is energy-dispersive spectroscopy in the SEM a substitute for electron probe microanalysis?,* Microscopy and analysis, 54-57, John Wiley and Sons, Ltd. Chichester, United Kingdom.

Manar Bani-Hani, Ramadan Abd-Allah, Lamia El-Khouri, 2012, *Archeometallurgical finds from barsina northen Jordan: microstructural characterization and conservation treatement,* Journal of cultural Heritage, Elesvier Masson SAS, Issy les Moulineaux Cedex, Paris, France.